The Path of Light: An Investigation About Photon Trajectories in a Double-Slit Interferometer

Leonardo Assis Morais

Março de 2017

Universidade Federal de Minas Gerais

Instituto de Ciências Exatas — Departamento de Física

The Path of Light: An Investigation About Photon Trajectories in a Double-Slit Interferometer

Leonardo Assis Morais

Supervisor: Leonardo Teixeira Neves

"Dissertação apresentada ao Programa de Pós-Graduação do Departamento de Física do Instituto de Ciências Exatas da Universidade Federal de Minas Gerais como requisito parcial à obtenção do grau de Mestre em Física".

Agradecimentos

Primeiramente, gostaria de agradecer aos meus pais, Maria Aparecida e José das Graças, pelo apoio incondicional em todas as etapas da minha vida, seja no âmbito acadêmico, profissional ou pessoal. O suporte que eles deram desde o início foi fundamental para que todos os projetos que eu concretizei durante minha existência tenham sido realizados com êxito, sendo este apenas mais um deles.

Gostaria de agradecer também a Luciana, pelo amor, pelo cuidado e pela paciência ao longo desse período. A atenção e a compreensão que encontrei nela foram ímpares.

A toda minha familia, pela força, inspiração e por sempre acreditarem em mim, mesmo sem entender direito o que eu faço.

Um agradecimento especial ao Leo, que foi um orientador que promovia o debate, esclarecia dúvidas e estimulava a pesquisa independente. Agradeço-o não so pela orientação em si, mas também pelo exemplo de pesquisador e orientador que ele representou ao longo desses dois anos.

Agradeço ao Adalberto e ao Ronaldo, por terem aguentado minhas reclamações e bagunças durante todo esse tempo. Ao Mestre Mário e ao Brunoids, pela amizade e também pelo exemplo do pesquisador que um dia quero ser. A galera do Enlight, pelos seminários, encontrinhos e discussões prolíficas. Jamais esquecerei a importância do ambiente propício ao debate que lá encontrei. Ao Filó, Pumba, Betão, Erik e a galera da pós pelos cafés, pela conversa jogada fora, pelos momentos de pausa que todo mundo precisa. À Bad Company por serem the best company desde tempos imemoriais.

Aos servidores do departamento, em especial à Shirley, pela ajuda com a biblioteca, e à Juliana e à Ana Paula, pelo auxílio com todos os trâmites burocráticos.

E, por fim, ao CNPq pelo apoio financeiro e por ter tornado possível a realização desse projeto.

À todos vocês e à muitos outros que ajudaram de forma indireta nessa caminhada e que por ventura não foram explicitamente supracitados, o meu muito obrigado!

Para Tia Pequena.

Pela força.
Pelo carinho.
Pelo exemplo.

Contents

Abstract

In classical mechanics, we can define trajectory as the path followed by a body or a particle during its time evolution. If one knows the dynamics of a particle, the knowledge of the position and momentum in a given instant of time is sufficient to predict its entire trajectory. However, in quantum mechanics the trajectory of a single particle is an ill defined concept, since, as a consequence of the Heisenberg uncertainty relation, one is not able to simultaneously know its position and momentum. Nevertheless, Wiseman [New Journal of Physics **9**, 165 (2007)] proposed an operational way to define the average trajectory of an ensemble of quantum particles using the weak measurement protocol, which is a procedure developed by Aharonov, Albert and Vaidman [Physical Review Letters **60**, 1351 (1988)] with the purpose of performing a measurement barely changing the system state. Building on Wiseman's idea, Kocsis *et al.* [Science **332**, 1170 (2011)] have experimentally demonstrated the reconstruction of average trajectories of single photons in a double-slit interferometer. Their strategy consisted in making a weak measurement of the photon momentum followed by a post-selection in a given position. In this way, they were able to map the weak value of momentum as a function of position and, using this information, to reconstruct the average trajectories of a post-selected ensemble of photons. In this dissertation, we present a review of the weak measurement protocol and some of its most recent extensions, applications and interpretations. Within this framework, we reproduced the results obtained by Kocsis *et al.* and analyse some different scenarios through numerical simulations.

Resumo

Em mecânica clássica, podemos definir trajetória como o caminho percorrido por um corpo ou uma partícula durante sua evolução temporal. Uma vez que se saiba a dinâmica da partícula, o conhecimento da posição e do momento em um dado instante de tempo é suficiente para prever a trajetória completa. No entanto, em mecânica quântica a trajetória de uma partícula única é um conceito mal definido, já que, como consequência da relação de incerteza de Heisenberg, é impossível conhecer sua posição e momento simultaneamente. Não obstante, Wiseman [New Journal of Physics **9**, 165 (2007)] propôs uma maneira operacional de definir a trajetória média de um *ensemble* de partículas quânticas usando o protocolo de medição fraca, que é um procedimento desenvolvido por Aharonov, Albert e Vaidman [Physical Review Letters **60**, 1351 (1988)] com o propósito de realizar uma medição a qual praticamente não altera o estado do sistema. Trabalhando a ideia original de Wiseman, Kocsis *et al.* [Science **332**, 1170 (2011)] demonstraram experimentalmente a reconstrução de trajetórias médias usando fótons únicos em um interferômetro de fenda dupla. A estratégia usada por eles consiste em realizar uma medição fraca do momento do fóton seguido por uma pós-seleção numa certa posição. Dessa forma, eles conseguem mapear o valor fraco do momento como função da posição e, usando essa informação, reconstroem a trajetória média de um ensemble de fótons pós-selecionados. Nesta dissertação, apresentamos uma revisão do protocolo de medição fraca e algumas de suas mais recentes extensões, aplicações e interpretações. Dentro desse quadro, nós reproduzimos os resultados obtidos por Kocsis *et al.* e analisamos alguns cenários diferentes através de simulações numéricas.

Introduction

The problem of determining trajectories of bodies and particles is an old object of study in physics. Since early times, astronomers used ingenious calculations to predict future positions of planets and comets. Earthly questions were also addressed, for instance, the question about the fastest route a particle can take under the action of a uniform gravitational field, given fixed initial and final points — which was proven to be a curve called brachistochrone. As an example of an application, we may cite the operation of a mass spectrometer, which measures the radius of the circular trajectory of a charged particle in a homogeneous magnetic field in order to provide its charge-to-mass ratio. For instance, this technique can be used to determine the molecular composition of a sample, if one knows in advance the charge-to-mass ratio of its constituents.

With the advent of quantum theory, this scenario has changed. Developed in the beginning of the twentieth century as an attempt to explain the results observed in the atomic scale which could not be understood using classical physics, quantum mechanics abdicated the concept of trajectory of a single particle. One of the most basic and important results of this theory, the Heisenberg uncertainty relation, states that subsequent measurements of position and momentum irrevocably disturbs each other [1, 2]. As a consequence, one may never know simultaneously both quantities with full precision for a single quantum particle, being impossible to define its trajectory.

The problem of performing a measurement without appreciably disturbing the state of the system was addressed by Aharonov, Albert and Vaidman in 1988 [3]. Using elementary rules of quantum mechanics, they proposed a new measurement procedure whose goal was to extract information from a quantum system without perturbing its state. The procedure is called the weak measurement protocol and consists in weaken the interaction between the quantum system and the measurement apparatus in such a way that the disturbance caused by their interaction is minimal. This is followed by a post-selection in the quantum system, giving as a result the so-called weak value, which can be extracted from the measuring device after the protocol is over. Since the interaction between the systems is weak, in one run the measurement result is inconclusive and it is necessary to repeat the experiment many times in order to extract valuable information, which comes in the form of the weak value.

Using the weak measurement concept described above, in 2007 Wiseman [4] proposed

an operational definition for *average trajectories* in quantum mechanics. In 2011, Kocsis *et al.* [5] experimentally demonstrated these average trajectories using the suggestion given by Wiseman with some small modifications. Their idea was to make a weak measurement of the momentum of a quantum particle followed by a post-selection of position. As a consequence, one would have a map of the weak value of the momentum as a function of position and could use this information to reconstruct the average trajectories of an ensemble of particles which were post-selected in a given position. The work of Kocsis *et al.* consisted in reconstructing these average trajectories for single photons in a double-slit-like interferometer. It is important to note that, since determining the weak value requires one to repeat the experiment many times, the trajectories reconstructed using this method represent average trajectories of an ensemble of particles and respect the Heisenberg uncertainty relation.

In this dissertation, our main goals are to present an introduction to the weak measurement protocol, including extensions and applications, and to use the protocol to investigate the problem of reconstructing average trajectories of photons (one or more) in a double-slit interferometer. In order to do so, we start chapter 1 presenting a brief revision of the of the standard measurement theory in quantum mechanics. Next, we introduce the weak measurement protocol and compare both methods, stressing their differences. We highlight some interesting features of the weak value and present an example of how to calculate it. In chapter 2 we go deeper in the discussion about weak values, presenting some extensions of the idea, such as the joint weak value. Later, we present applications which brought a lot of attention to the weak measurement protocol recently, like the measurement of the spin Hall effect of light [6] and the direct measurement of a wavefunction [7]. Current interpretations of the weak value are quickly presented, giving special attention to the case where weak values can be interpreted as conditioned averages of an observable. Chapter 3 will be dedicated to the problem of trajectory reconstruction in quantum mechanics. We start the chapter discussing the procedure for reconstructing trajectories in classical and quantum mechanics. Then, we present our results for the average trajectories of single photons in a double-slit interferometer, obtained via numerical simulations. The results by Kocsis *et al.* [5] are reproduced and, in addition, we analyse different scenarios. Thereafter, their experiment is explained in order to show how the average trajectories are reconstructed in practice. Finally, we briefly discuss the possibilities of reconstructing the trajectories when a bi-photon is sent through the interferometer.

Chapter 1

Standard and Weak Measurements in Quantum Mechanics

The weak measurement protocol was presented in an article by Aharonov, Albert and Vaidman (hereafter referred to as AAV) as a measurement procedure hidden in the quantum formalism which could lead to fantastic results [3]. In their article, AAV argue that a weak measurement of an observable could return values outside the range of allowed eigenvalues. Although the previous affirmation seems to defy the postulates of quantum mechanics, AAV themselves urge to clarify that their result does not contradict the elementary rules of quantum physics [3, 8]. Nevertheless, how could a quantum mechanical measurement of an observable return a value which is not one of its eigenvalues? This chapter is dedicated to present the weak measurement protocol and the weak value, showing the necessary conditions and the procedure one must follow in order to obtain such unexpected results. Here we only discuss the basic ideas of the process, leaving more thorny issues, such as interpretations and applications, for the next chapter.

We begin in section 1.1 presenting a brief introduction about how projective measurements are performed in quantum mechanics, enunciating the postulates of quantum mechanics, and discussing how projective measurements are performed using the quantum mechanical formalism. In section 1.2, we present the weak measurement protocol itself, demonstrating that the result of this new measurement procedure is the weak value. We show the conditions where the weak approximation is valid and, in order to clarify the nature of the effect, compare the calculations with and without approximations. Once we have defined the weak value, it is easy to see that it is a complex quantity. Therefore, we need to establish how to measure its real and imaginary parts. This important question is addressed in section 1.3, in which we demonstrate its relation with the expected values of other physical observables that can be measured in the laboratory. Finally, in section 1.4 we present an optical apparatus in which is possible to implement weak measurements. This simple example will be useful to discuss some basic aspects of the protocol.

1.1 Measurements in Quantum Mechanics

In classical physics, it is commonly assumed that the act of measurement does not disturb the system under study. Or, being more rigorous, we could always assume that is possible to devise an experiment in which the disturbance caused by the measurement apparatus is so small that it may be neglected. In thermodynamics, for example, we could suppose the existence of a thermometer which has a small enough heat capacity, in such a way that it reaches the thermal equilibrium with the heat bath barely changing the temperature of the bath. In other branches of classical physics, such as classical mechanics and electromagnetism, similar ideas can also be applied.

Unlike the classical theories, in quantum physics the disturbance caused by the act of measurement cannot be neglected. The standard measurement procedure in quantum mechanics inevitably changes the state of the system being studied. In this section, we will use the quantum mechanical formalism to describe the measurement process.[1]

1.1.1 The Postulates of Quantum Mechanics

First of all, we present the postulates of quantum mechanics. Here, we follow closely the statements made in reference [11].

Postulate 1

The state of a closed physical system at each instant is represented by a ket $|\psi\rangle$ in the state space.

Postulate 2

To every physical quantity A of a physical system there is a correspondent Hermitian operator $\hat{A}$ which acts on the kets $|\psi\rangle$ used to describe the system. The only possible result of a measurement of this observable is one of the eigenvalues a_m of $\hat{A}$.

Postulate 3

The time evolution of the state of a quantum system is described by

$$|\psi(t)\rangle = \hat{U}(t, t_0)\,|\psi(t_0)\rangle\,, \tag{1.1}$$

where the unitary operator $\hat{U}$ is given by

$$\hat{U} = \exp\left(-\frac{i}{\hbar}\int \hat{\mathcal{H}} dt\right) \tag{1.2}$$

[1] Only projective measurements will be discussed in this section. The interested reader could find a brief introduction about generalised measurements in quantum mechanics in references [9, 10].

and preserves the normalisation of the ket $|\psi(t)\rangle$, with $\hat{\mathcal{H}}$ being the Hamiltonian operator of the system.

Postulate 4

When a measurement of an observable A is made on a generic state $|\psi\rangle$, the probability of obtaining an eigenvalue a_m is given by

$$P = |\langle a_m|\psi\rangle|^2, \tag{1.3}$$

where $|a_m\rangle$ is the eigenstate of A corresponding to the eigenvalue a_m. Immediately after the measurement, the state of the system will be the normalised eigenstate $|a_m\rangle$ of A.[2]

Note that Postulates 2 and 4 are directly related to measurements in quantum mechanics, therefore we will give special attention to them. According to Postulate 2, the eigenvalues a_m of the operator $\hat{A}$ are the only possible results of a strong measurement[3] of the observable A. Therefore, we can conclude that the lowest and highest possible results of such measurement are the minimum $a_{\min}$ and maximum $a_{\max}$ eigenvalues of $\hat{A}$. The Postulate 4 is responsible for making the connection between the abstract quantum state $|\psi\rangle$ to the results of measurements performed in quantum systems. Note that this Postulate gives only the probabilities of a given result to occur. Therefore, we need to measure an ensemble of identically prepared systems in order to check the predictions of equation (1.3).

It is also important to note that, according to Postulate 4, right after the measurement takes place, the state of the system changes from the $|\psi\rangle$ to the eigenstate $|a_m\rangle$ of the observable A associated with the result of the experiment a_m. This is the irrevocably change caused by the act of measurement in the quantum system which we have mentioned before. The only case where this abrupt change is not observed is when the state of the system before the measurement is already an eigenstate $|a_m\rangle$ of the observable A measured. In this case, we can predict with full certainty the measurement result, which will be the eigenvalue a_m, and after the measurement the system will be found in the same state. Nevertheless, in general, we can state that a strong measurement will change the state of the system in an unpredictable and unavoidable way.

[2] Unless we have a degenerate eigenvalue, i.e., an eigenvalue which is associated with more than one eigenvector. In these cases, the state of the system after the measurement will be a superposition of these eigenvectors.

[3] Along this dissertation we use the term 'strong measurement' to refer to standard measurements in quantum mechanics. We choose this term in opposition to 'weak measurements', the main theme treated here.

1.1.2 The Measurement Process

Now that we have discussed the basic aspects of the quantum theory we turn our attention to the measurement process itself. To perform a measurement we need to use a device (or apparatus) which is capable to probe the system under investigation. It is necessary to establish an interaction between them in such a way that we can correlate the changes observed in the device to the physical attribute of the system we are interested. To illustrate the idea, we use the example of the thermometer again. In this case one associates the mercury level inside the tube to the temperature of the body which the thermometer is put in contact with. It is known that both systems will exchange heat — the interaction — and, after a while, they will reach thermal equilibrium — a correlation between their temperatures. At this point the height of the mercury column inside the thermometer will allow the experimenter to infer the temperature of the body.

In classical mechanics, to model the interaction between the system under investigation $\mathcal{S}$ and the measuring apparatus $\mathcal{M}$, we may use the following Hamiltonian

$$H = g(t)PA, \tag{1.4}$$

where P is the momentum of $\mathcal{M}$ and A is the dynamical variable of $\mathcal{S}$ which we are interested to measure. The coupling parameter $g(t)$ represents the strength of the interaction between the two systems and is different from zero only during the time they interact ($t_i < t < t_f$). Using the Hamilton's equation of motion for X, we have [12]

$$\frac{dX}{dt} = \frac{\partial H}{\partial P} = g(t)A, \tag{1.5}$$

where we used (1.4) in the last step. If we integrate the above equation in the time interval from t_i to t_f, i.e., the time the interaction has lasted, we have

$$\Delta x = x_f - x_i = A \int_{t_i}^{t_f} g(t)dt, \tag{1.6}$$

where x_i and x_f are the positions of $\mathcal{M}$ before and after the interaction between both systems. Therefore, once the integral of $g(t)$ is known, one can infer the value of the observable A from the change in the position Δx of the measurement apparatus.

1.1.3 Describing a Measurement Using the Quantum Mechanical Formalism

Measurements in quantum systems follow the same idea presented in the previous section. To implement them we need to interact the measurement device $\mathcal{M}$ and the quantum system $\mathcal{S}$ in order to create a correlation between a macroscopic dynamical

variable of $\mathcal{M}$ and the observable of interest of $\mathcal{S}$. We now describe the measurement process using the quantum mechanical formalism. The argument presented here follows closely the one given in reference [13].

State Preparation

Imagine that we have a quantum system $\mathcal{S}$ prepared in an unknown state $|\psi_i\rangle$ from which we would like to know the value of the observable A. Firstly, we note that we may use the completeness relation [2]

$$\hat{I} = \sum_{n=1}^{N} |a_n\rangle\langle a_n|, \tag{1.7}$$

where $\hat{I}$ is the identity operator acting on an N-dimensional Hilbert space, to rewrite the initial state $|\psi_i\rangle$ in the basis formed by the eigenvectors $|a_n\rangle$ of the operator $\hat{A}$ as

$$|\psi_i\rangle = \sum_{n=1}^{N} \langle a_n|\psi_i\rangle\, |a_n\rangle. \tag{1.8}$$

An ideal measuring device $\mathcal{M}$ would have well defined initial and final value of position X from which we could read the value of the observable of interest A. Here we consider a typical situation, in which the initial state of the measuring device $|\phi_i\rangle$ is a Gaussian, centred at $x_i = 0$ with a spreading σ, such that[4]

$$|\phi_i\rangle = \int dx\, \langle x|\phi_i\rangle\, |x\rangle = \int dx \exp\left(\frac{-x^2}{(2\sigma)^2}\right) |x\rangle\,. \tag{1.9}$$

This state could represent the spatial state of a laser beam which has a Gaussian profile, for example. Remembering that the state in the momentum representation $\psi'(k)$, where $k = P/\hbar$, is proportional to the Fourier transform of the wavefunction $\mathcal{F}\{\psi(x)\}$ [1], namely,

$$\psi'(k) = \hbar^{-1/2}\mathcal{F}\{\psi(x)\} = (2\pi\hbar)^{-1/2} \int dx \exp(-ikx)\psi(x), \tag{1.10}$$

we can rewrite the initial state $|\phi_i\rangle$ of $\mathcal{M}$ in the basis of the momentum operator as

$$|\phi_i\rangle = \int dk\, \langle k|\phi_i\rangle\, |k\rangle = \hbar^{-1/2} \int dk \exp(-\sigma^2 k^2)\, |k\rangle\,. \tag{1.11}$$

Therefore, equations (1.8) and (1.11) describe the initial state of the global system, which is

$$|\Psi_i\rangle = |\psi_i\rangle \otimes |\phi_i\rangle\,. \tag{1.12}$$

[4]Here we used the completeness relation for continuous variables, which can be stated as $\hat{I} = \int dx\, |x\rangle\langle x|$.

The first part of the measurement process ends here, the system preparation.

Interaction

The next step is to establish an interaction between the systems $\mathcal{S}$ and $\mathcal{M}$. This interaction is described by the coupling Hamiltonian

$$\hat{\mathcal{H}} = g(t)\hat{P} \otimes \hat{A}, \tag{1.13}$$

as proposed by von Neumann in reference [14]. $\hat{P}$ is the operator associated to the macroscopic dynamical variable P of the measuring system $\mathcal{M}$, while $\hat{A}$ is the operator associated to the observable A of the system of interest $\mathcal{S}$. According to Postulate 3, the evolution of these systems will be described by the unitary operator $\hat{U}$ given by equation (1.2), namely,

$$\hat{U} = \exp\left(-\frac{i}{\hbar} \int g(t)\, dt\, \hat{P} \otimes \hat{A} \right), \tag{1.14}$$

where we used the Hamiltonian (1.13). We define the constant c, which will give the strength of the coupling interaction between the measurement apparatus and the quantum system, as

$$c = \int_{t_i}^{t_f} g(t)\, dt, \tag{1.15}$$

where t_i and t_f are the instants where the interaction started and finished, respectively. Using this definition together with equation (1.14), we have

$$\hat{U} = \exp(-ic\hat{k} \otimes \hat{A}), \tag{1.16}$$

where $\hat{k} = \hat{P}/\hbar$. Applying the evolution operator (1.16) in the initial state (1.12) and using equations (1.8) and (1.11), we conclude that after interaction the systems will be found in the state[5]

$$|\Psi\rangle = \hat{U}\,|\psi_i\rangle\,|\phi_i\rangle = \hbar^{-1/2} \sum_{n=1}^{N} \langle a_n|\psi_i\rangle \int dk \exp(-\sigma^2 k^2) \exp(ick a_n)\,|a_n\rangle\,|k\rangle. \tag{1.17}$$

Using again the fact that $\psi'(k)$ is proportional to the Fourier transform of $\psi(x)$, we can rewrite above equation in the basis of the $\hat{X}$ as

$$\begin{aligned} |\Psi\rangle &= \sum_{n=1}^{N} \langle a_n|\psi_i\rangle \int dx \exp\left(-\frac{(x - ca_n)^2}{(2\sigma)^2} \right) |a_n\rangle\,|x\rangle \\ &= \sum_{n=1}^{N} \langle a_n|\psi_i\rangle\,|a_n\rangle\,|\phi_n\rangle\,, \end{aligned} \tag{1.18}$$

[5]Henceforth, we will omit the tensor product sign $\otimes$, since its presence is clear from the context.

where $|\phi_n\rangle$ is defined as

$$|\phi_n\rangle = \int dx \exp\left(-\frac{(x - ca_n)^2}{(2\sigma)^2}\right) |x\rangle \,. \tag{1.19}$$

In the basis of the eigenstates $|x\rangle$ of the operator $\hat{X}$, the states $|\phi_n\rangle$'s (for $n = 1, \ldots, N$) of the measuring apparatus are Gaussians distributions centred at $x = ca_n$ with a dispersion σ, as shown in figure 1.1. Equation (1.18) describes the global state of the systems $\mathcal{S}$ and $\mathcal{M}$ after their interaction, which is an entangled state.[6] This interaction is the responsible for establishing the correlation between $\mathcal{S}$ and $\mathcal{M}$ needed to perform the measurement, as we will see next. This correlation is also illustrated in figure 1.1.

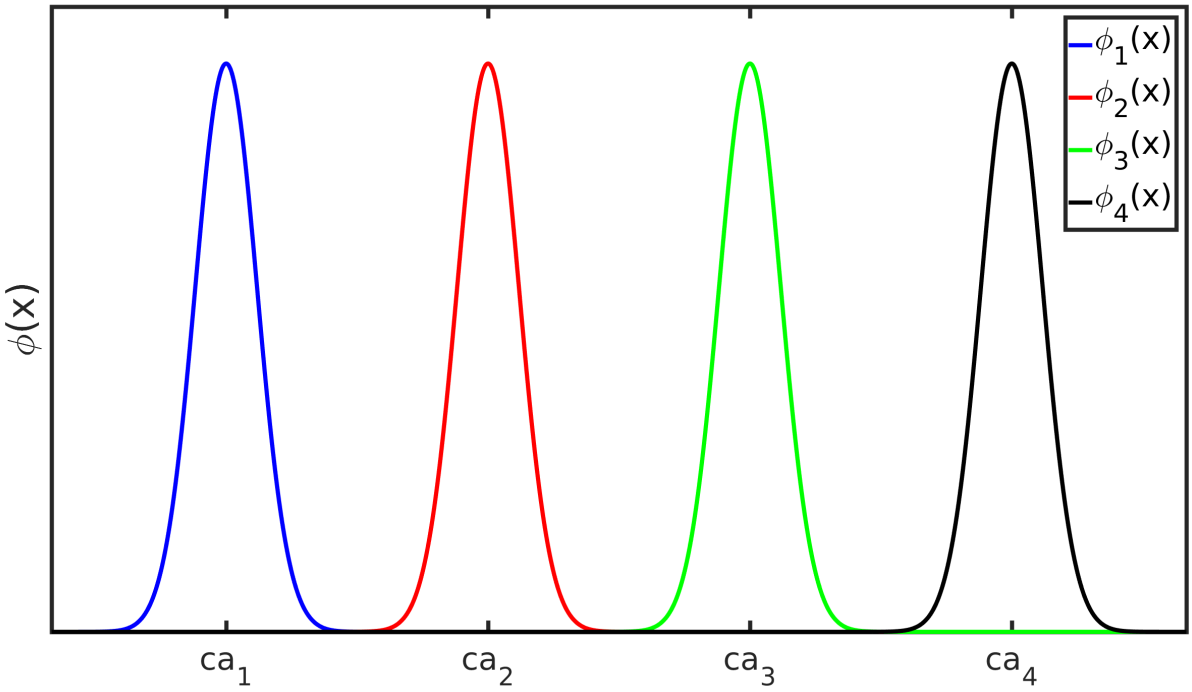

Figure 1.1: Graphical representation of the entangled state of equation (1.18) for $N = 4$. Each of the Gaussians $\phi_n(x)$ representing the state of the measuring apparatus $\mathcal{M}$ is centred at ca_n. Each of these states of $\mathcal{M}$ is associated to a state $|a_n\rangle$ of the system $\mathcal{S}$. In the limit of an ideal measurement, the overlap between these $\phi_n(x)$'s is negligible and we may determine unequivocally the state of the system $\mathcal{S}$ based on the result $x = ca_m$ read in the measurement device.

Reading of the Measurement Result

The third and last part of the process is the reading of the result in the measurement device. In the case of a standard measurement, the dispersion σ of the $\phi_n(x)$'s is much

[6] An entangled pure state is a pure state of a composite system which cannot be written as a tensor product of the states of its subsystems, i.e., $|\Psi_{12}\rangle \neq |\psi_1\rangle\,|\phi_2\rangle$. For instance, unless $\langle a_n|\psi_i\rangle = \delta_{in}$ (for any $n = 1, \ldots, N$) in (1.18), the global state of $\mathcal{S}$ and $\mathcal{M}$ will be entangled.

smaller than the distance between two peaks corresponding to consecutive eigenvalues a_n's, that is,

$$\sigma << c\,(a_{n+1} - a_n). \tag{1.20}$$

Thus the overlap between the Gaussians will be negligible. In this regime, assume that the reading of the measuring system $\mathcal{M}$ gives $x \simeq ca_m$, which corresponds to project $\mathcal{M}$ in the state $|ca_m\rangle$. Then, from equation (1.18), the state of $\mathcal{S}$ becomes

$$\begin{aligned} |\psi_f\rangle = \langle ca_m|\Psi\rangle &= \sum_{n=1}^{N} \langle a_n|\psi_i\rangle \int dx \exp\left(-\frac{(x-ca_n)^2}{(2\sigma)^2}\right) |a_n\rangle \langle ca_m|x\rangle \\ &= \sum_{n=1}^{N} \langle a_n|\psi_i\rangle \exp\left(-\frac{(ca_m - ca_n)^2}{(2\sigma)^2}\right) |a_n\rangle\,. \end{aligned} \tag{1.21}$$

Using the condition given in equation (1.20) we conclude that

$$\exp(-(ca_m - ca_n)^2/(2\sigma)^2) \simeq 0, \qquad \text{for any } a_n \neq a_m. \tag{1.22}$$

Finally, the final state of $\mathcal{S}$ after the measuring procedure will be

$$|\psi_f\rangle \propto \langle a_m|\psi_i\rangle\,|a_m\rangle\,. \tag{1.23}$$

We conclude that a given reading of the measuring device corresponds to a certain eigenvalue a_m of the quantum system, revealing the value of the observable A.

In summary, the measuring process in the quantum mechanical formalism can be divided in three steps:

1. *System preparation.* One needs to prepare the measuring device $\mathcal{M}$ in a known state $|\phi_i\rangle$. The observable used as meter, X for example, must have a definite and known value x_i in this initial state. The initial state $|\psi_i\rangle$ of the quantum system $\mathcal{S}$ does not need to be known at this stage.

2. *Interaction.* Systems $\mathcal{S}$ and $\mathcal{M}$ interact, through the Hamiltonian (1.13). Thus, a correlation between the eigenstates of the measured observable A and the eigenstates of the meter observable X is created, i.e., we say that these observables are entangled. This correlation allows one to know the state of $\mathcal{S}$ based on the result read in the measuring apparatus.

3. *Reading the result.* When one reads the result of the measurement x_f in the device, the state of the measuring system is projected in an eigenstate $|x_f\rangle$ associated to the observable X. Thus, due to the correlation existent between systems $\mathcal{S}$ and $\mathcal{M}$, the state of the quantum system will also be projected in an eigenstate of the measured observable A. The measurement result is given by the difference $x_f - x_i$.

We stress that all the characteristics of an ideal measurement were achieved in the process presented here:

1. The result of the measurement is always one of the eigenvalues a_m, as stated in Postulate 2.

2. The probability of getting the eigenvalue a_m as a result is given by $|\langle a_m|\psi\rangle|^2$, as stated in Postulate 4.

3. The system is left in the eigenstate $|a_m\rangle$ associated to the measured eigenvalue a_m, as stated in Postulate 4.

1.2 Weak Measurements and the Weak Value

1.2.1 The Weak Measurement

Strong vs Weak Measurements

In the previous section we discussed how to perform a strong measurement: one must associate unequivocally a state of the system $\mathcal{M}$ to an eigenstate of the measured observable A of the system $\mathcal{S}$, as shown by figure 1.1. As a result of the act of measurement, the state of $\mathcal{S}$ suddenly changes and becomes one of these eigenstates of A. Now, we would like to devise a different measurement strategy which causes the smallest possible perturbation over the measured system $\mathcal{S}$. In order to accomplish this goal, AAV suggested that one should weaken the interaction, i.e., reduce the coupling parameter c, between systems $\mathcal{S}$ and $\mathcal{M}$ during the act of measurement [3]. The procedure in this weak measurement is the same as presented in last section and, after the interaction, the global state of the system will also be given by equation (1.18). However, since we have weakened the interaction between the systems, condition (1.20) does not hold anymore. In fact, now we have

$$\sigma >> c\,(a_{n+1} - a_n), \tag{1.24}$$

which means that, in this case, the dispersion in the initial state $|\phi_i\rangle$ of $\mathcal{M}$, given by (1.9), is much bigger than the separation between two consecutive eigenvalues. In this type of low resolution measurement, in each run of the experiment the value registered in the measurement apparatus is related to many eigenstates of A, since the dispersion σ is much bigger than the distance between eigenvalues $c(a_n - a_m)$, as shown in figure 1.2. As a consequence, the perturbation caused by the act of measurement is reduced, since $\mathcal{S}$ is left in a superposition of these unresolved states.[7] Nevertheless, it is still possible to

[7] In this sense, in a weak measurement, systems $\mathcal{S}$ and $\mathcal{M}$ are less entangled than in the case of a strong measurement.

determine the average value of A in this limit of weak interaction. In order to do so, one must repeat the experiment many times in identically prepared systems.

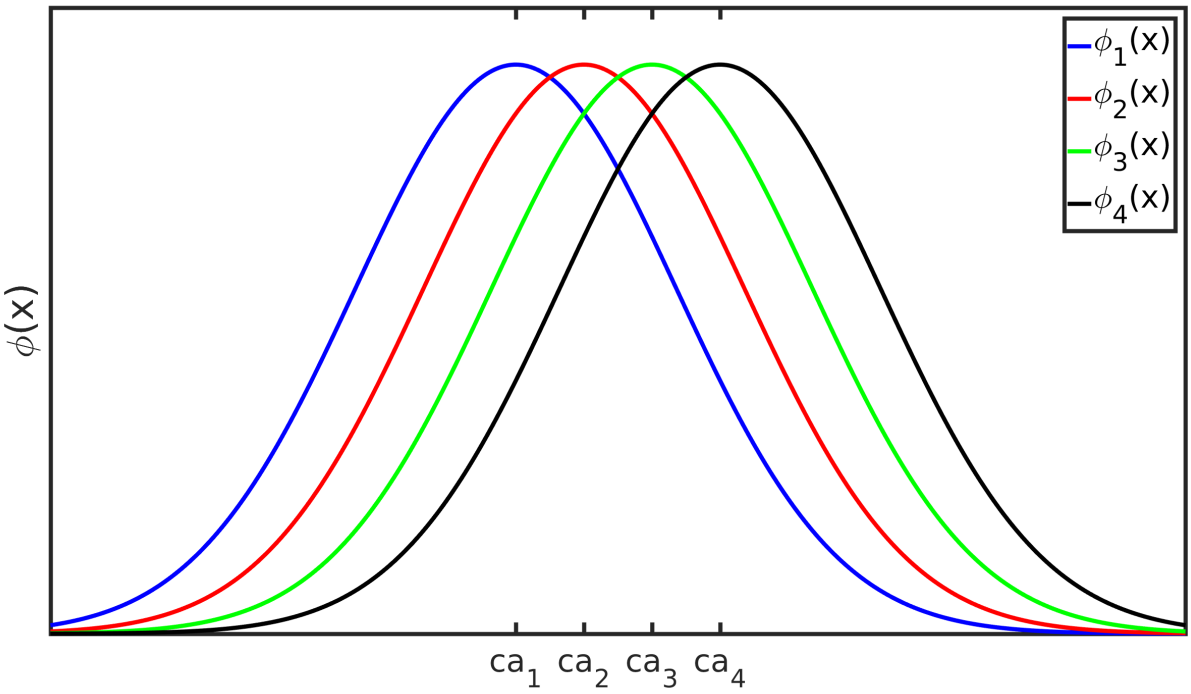

Figure 1.2: Graphical representation of the entangled state of equation (1.18) for $N = 4$ when the measurement performed is weak. Note that when one reads a given result $x = ca_n$ in the measuring device, there is a relevant probability of the measured system to be found in any of the states $|a_n\rangle$.

To clarify the concept, we use the measurement of the polarisation of a laser beam as an example to compare weak and strong measurements. In order to measure the polarisation, we use the transverse beam profile as a meter. To perform the experiment, one could send a laser beam through a birefringent material which separates the components with different polarisations by some distance a, as sketched in figure 1.3(a). In the case of a strong measurement, the distance a is much bigger than the beam waist w_0 and one can easily infer the polarisation of each component, as shown in figure 1.3(b). However, if the interaction between the laser and the birefringent material is weak, a will be smaller than w_0. As a consequence, one will not be able to resolve which is the polarisation of each beam component after it passes the birefringent material and we say that a weak measurement has been performed, as shown in figure 1.3(c).

The Weak Measurement Protocol

In their seminal work, AAV used the weak measurement idea to show an interesting effect: a measurement protocol in which the meter $\mathcal{M}$ registers a result which could lie

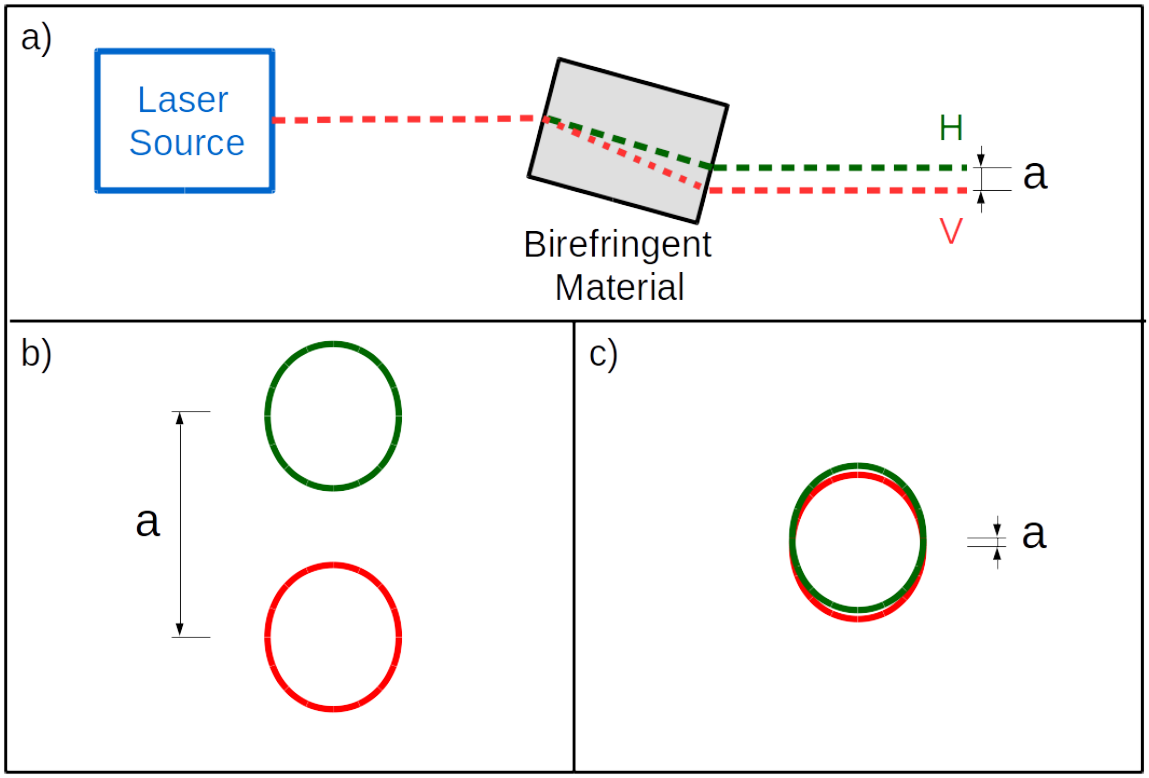

Figure 1.3: a) Schematic representation of a polarisation measurement of a laser beam. The birefringent material is used to separate the components of the beam with different polarisations. b) Transverse cut of the beam components after a strong measurement. The components are spatially separated and it is possible to identify the polarisation state of the beam by the position of the centre of the transverse profile. c) Transverse cut of beam components after a weak measurement. Note how the overlap between them is almost complete, making impossible to identify the polarisation of each component.

outside the range of allowed eigenvalues [3].[8] Below we present the four steps of the procedure proposed by AAV, whose result is called weak value.

1. *Pre-selection.* Systems $\mathcal{S}$ and $\mathcal{M}$ must be prepared in a known state. Since one prepares $\mathcal{S}$ in a known initial state $|\psi_i\rangle$, this step is called pre-selection.

2. *Weak interaction.*[9] $\mathcal{S}$ and $\mathcal{M}$ weakly interact with each other according to the coupling Hamiltonian, given by equation (1.13). Since the interaction between these systems is weak, after it takes place one is not able to resolve the eigenstates of $\mathcal{S}$.

3. *Post-selection.* Before reading the result in $\mathcal{M}$, we project $\mathcal{S}$ in a known state $|\psi_f\rangle$.

[8] This effect, also known as AAV effect, was presented by the first time by Aharonov *et al.* in reference [15]. Nevertheless, the definition of a weak value and the proposal of the weak measurement as a protocol are introduced by the first time in reference [3].

[9] In the literature, it is usual to refer to this part of the protocol as "weak measurement". In this dissertation, we make a clear distinction between "weak measurement" and "weak interaction" as exposed later on.

Only this post-selected part of the system of interest will be taken into account in the result of this measurement process.

4. *Weak value extraction.* Finally, we need to extract the information, i.e., read the result, in the measuring apparatus. In the case of a weak measurement, instead of showing an eigenvalue a_n associated to the measured observable A, $\mathcal{M}$ will show the weak value A_w, as defined by AAV.

Now we made an important distinction between three terms that will be extensively used throughout this text:

- **Weak Interaction:** Refers to the nature of the interaction between two systems, not necessarily related to an act of measurement. Is a necessary step to perform weak measurements and the weak measurement protocol.
- **Weak Measurement:** Refers to a measurement process, as described in section 1.1, with the difference that the interaction between systems $\mathcal{S}$ and $\mathcal{M}$ is weak.
- **Weak Measurement Protocol:** Refers to the new measurement procedure proposed by AAV [3] which consists in four steps: pre-selection, weak interaction, post-selection and extraction of the weak value.

Once the protocol was presented, we proceed to define the weak value A_w and show how this quantity appears in the context of the weak measurement protocol.

1.2.2 The Weak Value

We will demonstrate how the weak value, a number which is not restricted to be in the interval of the possible eigenvalues of the measured observable and could even be complex, is the value read in a measurement apparatus in the weak measurement protocol. Note that we will constantly refer to the section 1.1, highlighting the main differences and similarities between this protocol and the strong measurement process.

Again, the initial state of the global system is given by equation (1.12), where $|\psi_i\rangle$ and $|\phi_i\rangle$ describe the initial state of systems $\mathcal{S}$ and $\mathcal{M}$, respectively. Unlike the strong measurement described in the previous section, in which $|\psi_i\rangle$ does not need to be known *a priori*, in the case of the weak measurement protocol one must know $|\psi_i\rangle$, i.e., one must make a pre-selection in the system $\mathcal{S}$.

Following the pre-selection, a weak interaction between systems $\mathcal{S}$ and $\mathcal{M}$ described by the coupling Hamiltonian (1.13) takes place. Then, the system evolves according to the unitary operator $\hat{U}$, given by equation (1.16). However, due to the weakness of interaction, we may use a Taylor expansion to approximate $\hat{U}$ by

$$\hat{U} = \hat{I} - ic\hat{A}\hat{k} - c^2\hat{A}^2\hat{k}^2 + \mathcal{O}(c^3), \tag{1.25}$$

where c is a parameter related to the coupling strength and is given by (1.15). If we consider that only the term linear in c is a relevant correction, i.e., the interaction between the measuring apparatus and the system of interest is weak, we may approximate the global state after the interaction by

$$|\Psi\rangle \simeq |\psi_i\rangle\,|\phi_i\rangle - ic\hat{A}\,|\psi_i\rangle\,\hat{k}\,|\phi_i\rangle\,. \tag{1.26}$$

The next step in the weak measurement protocol is to make a post-selection in $\mathcal{S}$, i.e., project it in a specific state $|\psi_f\rangle$. After the post-selection, the state $|\phi\rangle$ of $\mathcal{M}$ will be given by

$$|\phi\rangle = \langle\psi_f|\Psi\rangle \simeq \langle\psi_f|\psi_i\rangle\,|\phi_i\rangle - ic\,\langle\psi_f|\,\hat{A}\,|\psi_i\rangle\,\hat{k}\,|\phi_i\rangle\,. \tag{1.27}$$

Finally, putting the term $\langle\psi_f|\psi_i\rangle$ in evidence, we get

$$|\phi\rangle \simeq \langle\psi_f|\psi_i\rangle\left(\,|\phi_i\rangle - ic\frac{\langle\psi_f|\,\hat{A}\,|\psi_i\rangle}{\langle\psi_f|\psi_i\rangle}\hat{k}\,|\phi_i\rangle\,\right). \tag{1.28}$$

The above equation describes the state of $\mathcal{M}$ after the post-selection. As the last step of the weak measurement protocol, we only need to read the value registered by the measurement apparatus from the state $|\phi\rangle$. At this point we make an assumption about the initial state $|\phi_i\rangle$ of $\mathcal{M}$: we assume it can be described by a distribution centred at $k = 0$, for convenience, with a width Δk. An example would be a Gaussian distribution.

In order to calculate the value read in the measurement device, we make another approximation. Remembering that we are working in the weak measurement regime, we approximate the linear term in the equation (1.28) by an exponential,

$$|\phi\rangle \simeq \langle\psi_f|\psi_i\rangle\exp\left(\,-ic\frac{\langle\psi_f|\,\hat{A}\,|\psi_i\rangle}{\langle\psi_f|\psi_i\rangle}\hat{k}\right)|\phi_i\rangle\,. \tag{1.29}$$

This approximation can be done as long as we guarantee that

$$\left|c\frac{\langle\psi_f|\,\hat{A}\,|\psi_i\rangle}{\langle\psi_f|\psi_i\rangle}\Delta k\right| >> \left|c^n\left(\frac{\langle\psi_f|\,\hat{A}^n\,|\psi_i\rangle}{\langle\psi_f|\psi_i\rangle}\right)(\Delta k)^n\right| \tag{1.30}$$

is satisfied for any $n \geqslant 2$, which means that the first term in the Taylor expansion is much bigger than higher order terms, and

$$\left|c\Delta k\frac{\langle\psi_f|\,\hat{A}\,|\psi_i\rangle}{\langle\psi_f|\psi_i\rangle}\right| << 1. \tag{1.31}$$

Such conditions are obeyed when the interaction between the quantum system and the measuring device is weak. Once we have done this approximation, we rewrite the state of

the measurement apparatus in the basis of $\hat{X}$, i.e.,

$$|\phi\rangle \simeq \langle\psi_f|\psi_i\rangle \int dx\, |x\rangle\langle x| \exp\left(-ic\frac{\langle\psi_f|\,\hat{A}\,|\psi_i\rangle}{\langle\psi_f|\psi_i\rangle}\hat{k}\right)|\phi_i\rangle\,. \tag{1.32}$$

Using the fact that the momentum $\hat{P} = \hbar\hat{k}$ is the generator of spatial translations [1]

$$\exp(-ic\hat{k})\,|x\rangle = |x + c\rangle\,, \tag{1.33}$$

we have that the final state of the measurement apparatus is

$$|\phi\rangle \simeq \langle\psi_f|\psi_i\rangle \int dx\, \phi_i\left(x - c\frac{\langle\psi_f|\,\hat{A}\,|\psi_i\rangle}{\langle\psi_f|\psi_i\rangle}\right)|x\rangle\,. \tag{1.34}$$

Defining the weak value as

$$A_w \equiv \frac{\langle\psi_f|\,\hat{A}\,|\psi_i\rangle}{\langle\psi_f|\psi_i\rangle}, \tag{1.35}$$

and, in the same fashion as in the case of the strong measurement, assuming that $\phi_i(x)$ is described by a Gaussian centred at $x = 0$ with dispersion σ, we have

$$|\phi\rangle \simeq (2\pi\sigma^2)^{-1/4}\,\langle\psi_f|\psi_i\rangle \int dx\, \exp\left(\frac{-\,(x - cA_w)^2}{(2\sigma)^2}\right)|x\rangle\,. \tag{1.36}$$

From equation (1.35) is evident that the weak value may be complex. Also, from equation (1.36), note that the displacement of the initial wavefunction ϕ_i will be proportional to the weak value A_w. Also, compare this result with (1.19). While there the Gaussian was centred in one of the eigenvalues a_n, here it is centred in the weak value A_w, in both cases multiplied by the constant c. The difference is that, in section 1.1 the dispersion σ was much smaller than the distance between two consecutive eigenvalues $c(a_{n+1} - a_n)$, which allowed one to resolve the state of $\mathcal{S}$ based on the measured result $x = ca_n$ of $\mathcal{M}$. Now σ is much bigger than $c\mathrm{Re}(A_w)$, a consequence of the weak interaction between the systems $\mathcal{S}$ and $\mathcal{M}$. Therefore, the uncertainty in one measurement is much bigger than the result read in the measuring apparatus. Nevertheless, if we repeat the experiment many times in identically prepared systems, we note that the average result will always converge to the same value $x = cA_w$ from which the weak value A_w could be extracted.

Since the value registered by the measurement apparatus after the weak measurement protocol, i.e., the displacement of the wavefunction $\phi(x)$, is a number proportional to A_w, AAV argue that this quantity represents the result of such measurement process [3]. From the definition (1.35) it is easy to understand why the weak value may assume values outside the range of allowed eigenvalues: if one chooses the pre- and post-selected states almost orthogonal, the denominator $\langle\psi_f|\psi_i\rangle$ will be close to zero and the weak value could be much bigger than the $\hat{A}$'s highest eigenvalue $a_{\max}$ or much smaller than its

lowest eigenvalue $a_{\min}$. However, in the approximation we have done from equation (1.28) to (1.29), we have assumed that the product $|cA_w\Delta k|$ was much smaller than 1. This imposes a limit in the maximum achievable weak value,

$$|A_w| << \frac{1}{c\Delta k}, \tag{1.37}$$

since if its value is too large our approximation breaks down.[10] Additionally, note there is a term $\langle\psi_f|\psi_i\rangle$ in the final wavefunction of the measurement apparatus, equation (1.36). This means that the probability of detection of the signal will be proportional to $|\langle\psi_f|\psi_i\rangle|^2$, also imposing a practical limit to the measurement of large weak values, since in this case $\langle\psi_f|\psi_i\rangle$ is approximately zero.

Another interesting point that equation (1.36) makes clear is the possibility of using anomalous weak values, which is the denomination for these weak values found outside the range of allowed eigenvalues, to amplify small signals. In this case, one is interested in determining the constant c related to the interaction between the systems $\mathcal{S}$ and $\mathcal{M}$. Sometimes, c is so small that experimenters have difficulties to measure it in the laboratory. Using the weak measurement protocol, one can devise an experiment in which the weak value A_w is large enough to the term cA_w to be measurable in the laboratory. Once one calculates A_w, this procedure allows one to measure the value of c. We will discuss this and other applications of the weak value in section 2.2.

As a final remark, it is important to note that the weak value is a complex quantity. When we measure it as the displacement of a wavefunction as described above, we are able to determine only its real part. This may be easily proven using equation (1.36) in order to calculate $|\phi(x)|^2$, namely

$$\begin{aligned} |\phi(x)|^2 &= |\,\langle x|\phi\rangle\,|^2 \\ &= \frac{|\,\langle\psi_f|\psi_i\rangle\,|^2}{\sqrt{2\pi}\sigma}\exp\left(\frac{-\,(x-cA_w^*)^2}{(2\sigma)^2}\right)\exp\left(\frac{-\,(x-cA_w)^2}{(2\sigma)^2}\right) \\ &= \frac{|\,\langle\psi_f|\psi_i\rangle\,|^2}{\sqrt{2\pi}\sigma}\exp\left(\frac{-\,[x-c\mathrm{Re}(A_w)]^2}{2\sigma^2}\right) \end{aligned} \tag{1.38}$$

Nevertheless, it is an easy task to devise a procedure to determine the imaginary part of the weak value. A strategy to measure $\mathrm{Im}(A_w)$ will be discussed in section 1.3.

1.2.3 The Exact Result of the Weak Measurement Protocol

A more curious reader may ask what would be the result of a weak measurement protocol if none of the approximations done above were considered. We analyse this situation now.

[10] In section 2.1.2 we will see how we can use an extension in the weak value definition to describe stronger interactions between systems $\mathcal{S}$ and $\mathcal{M}$.

Remember that the global state of the system after the interaction between systems $\mathcal{S}$ and $\mathcal{M}$ is given by

$$|\Psi\rangle = \hat{U}\,|\psi_i\rangle\,|\phi_i\rangle = \exp(-ic\hat{A}\hat{k})\,|\psi_i\rangle\,|\phi_i\rangle\,. \tag{1.39}$$

Rewriting $|\psi_i\rangle$ in the basis of the operator $\hat{A}$, we have

$$|\Psi\rangle = \sum_{n=1}^{N} \langle a_n|\psi_i\rangle \exp(-ica_n\hat{k})\,|a_n\rangle\,|\phi_i\rangle\,. \tag{1.40}$$

The next step in the weak measurement protocol is the post-selection of system $\mathcal{S}$ in the state $|\psi_f\rangle = \sum_m \langle a_m|\psi_f\rangle\,|a_m\rangle$. Then

$$\begin{aligned} |\phi\rangle = \langle\psi_f|\Psi\rangle &= \sum_{n=1}^{N}\sum_{m=1}^{M} \langle\psi_f|a_m\rangle\,\langle a_n|\psi_i\rangle \exp(-ica_n\hat{k})\,\langle a_m|a_n\rangle\,|\phi_i\rangle \\ &= \sum_{n=1}^{N} \langle\psi_f|a_n\rangle\,\langle a_n|\psi_i\rangle \exp(-ica_n\hat{k})\,|\phi_i\rangle\,. \end{aligned} \tag{1.41}$$

Following the same idea as in the previous demonstration, we write the state of $\mathcal{M}$ in the basis of $\hat{X}$. Thus,

$$|\phi\rangle = \sum_{n=1}^{N} \langle\psi_f|a_n\rangle\,\langle a_n|\psi_i\rangle \int dx\phi_i(x - ca_n)\,|x\rangle\,. \tag{1.42}$$

Note that the wavefunction $\phi(x) = \langle x|\phi\rangle$ of $\mathcal{M}$ in this case is in a superposition of $\phi_i(x)$'s, each of them centred in a value proportional to an eigenvalue a_n of $\hat{A}$. To compare these results with the one obtained previously, we assume $\phi_i(x)$ is given by

$$\phi_i(x) = (2\pi\sigma^2)^{-1/4} \exp\left(\frac{-x^2}{(2\sigma)^2}\right), \tag{1.43}$$

a Gaussian distribution with centre at $x = 0$ and dispersion σ. Therefore, the state $|\phi\rangle$ of the system $\mathcal{M}$ will be

$$|\phi\rangle = (2\pi\sigma^2)^{-1/4} \sum_{n=1}^{N} \langle\psi_f|a_n\rangle\,\langle a_n|\psi_i\rangle \int dx \exp\left(\frac{-(x - ca_n)^2}{(2\sigma)^2}\right)|x\rangle\,, \tag{1.44}$$

which, in position representation, is a superposition of N Gaussians, each of which centred at $x = ca_n$ with dispersion σ and complex coefficients given by $\langle\psi_f|a_n\rangle\,\langle a_n|\psi_i\rangle$.

Compare the results of equations (1.36) and (1.44). Both describe the state of the measuring device after the post-selection, the last step in the weak measurement protocol before reading the result. According to the exact result (1.44), this state is described by a

superposition of N broad Gaussians centred at $x = ca_n$, proportional to the eigenvalues of the measured observable A. Note that the coefficients of this sum are not strictly positive and it is possible that the terms cancel out each other. In the limit of a weak interaction, the cancellation is almost complete and we are left, approximately, with a small Gaussian centred in $x = cA_w$, as stated in equation (1.36).

1.3 Measuring the Weak Value

In the last section we have seen how the weak value appears as a result of a weak measurement protocol. It was demonstrated that we can measure its real part based on the displacement of the wavefunction describing the measuring system. However, as its definition in equation (1.35) makes clear, the weak value is a complex quantity. Therefore, it is mandatory to design an experiment in which we are able to measure the imaginary part of the weak value.

We start this section using a different method to show the proportionality between the expectation value $\langle \hat{X} \rangle$ of the measuring device position operator and the real part of the weak value A_w. Then, we use a similar strategy to show how to measure the imaginary part of A_w.

1.3.1 Measuring the Real Part of the Weak Value

To relate the real part of the weak value to a measurable quantity one may calculate the expectation value $\langle \hat{X} \rangle$ of the position operator of the system $\mathcal{M}$ in the state $|\phi\rangle$, right after the post-selection is made in system $\mathcal{S}$, which is given by equation (1.28). The arguments applied here follow closely the ideas presented by Lundeen and Resch [16].

We assume that the initial state $\phi_i(x)$ of the measuring apparatus in position representation is given by equation (1.43). We shall calculate the expectation value $\langle X \rangle$ in the state

$$|\phi\rangle = |\phi_i\rangle - icA_w \hat{k} |\phi_i\rangle \,. \tag{1.45}$$

Since, in quantum mechanics, the expectation value $\langle \hat{A} \rangle$ of an operator in a certain state $|\chi\rangle$ is given by

$$\langle \hat{A} \rangle = \langle \chi | \hat{A} | \chi \rangle \,, \tag{1.46}$$

we have

$$\begin{aligned} \langle \hat{X} \rangle &= \langle \phi | \hat{X} | \phi \rangle \\ &= \langle \phi_i | \hat{X} | \phi_i \rangle - icA_w \langle \phi_i | \hat{X}\hat{k} | \phi_i \rangle + icA_w^* \langle \phi_i | \hat{k}\hat{X} | \phi_i \rangle + \mathcal{O}(c^2) \\ &\approx \langle \phi_i | \hat{X} | \phi_i \rangle - ic\mathrm{Re}(A_w) \langle \phi_i | [\hat{X}, \hat{k}] | \phi_i \rangle + c\mathrm{Im}(A_w) \langle \phi_i | \{\hat{X}, \hat{k}\} | \phi_i \rangle \,, \end{aligned} \tag{1.47}$$

where we considered only linear terms in c. In the result above, we have used the defini-

tions of the commutator

$$[\hat{A}, \hat{B}] = \hat{A}\hat{B} - \hat{B}\hat{A} \tag{1.48}$$

and the anti-commutator

$$\{\hat{A}, \hat{B}\} = \hat{A}\hat{B} + \hat{B}\hat{A} \tag{1.49}$$

between two operators. We will carefully analyse each of the three terms in the right side of equation (1.47).

The first term is the expectation value of position in the initial state $|\phi_i\rangle$, as one may see from the definition (1.46). Since the initial wavefunction is a Gaussian distribution centred at $x = 0$, we note that it is an even function of x. Therefore, by symmetry arguments, it is easy to prove that

$$\langle\phi_i|\, \hat{X}\, |\phi_i\rangle = 0. \tag{1.50}$$

To verify the contribution of the other two terms we must calculate the commutator and anti-commutator of $\hat{X}$ and $\hat{k}$ in the state $|\phi_i\rangle$ of system $\mathcal{M}$. Remember that, in position representation, the operators $\hat{X}$ and $\hat{k}$ act in a wavefunction $\psi(x)$ as follows [1,2]

$$\hat{X}\psi(x) = x\psi(x) \quad \text{and} \quad \hat{k}\psi(x) = -i\frac{\partial\psi(x)}{\partial x}. \tag{1.51}$$

Using the above relations, we calculate the expectation values of the products between $\hat{X}$ and $\hat{k}$,

$$\langle\phi_i|\, \hat{X}\hat{k}\, |\phi_i\rangle = \frac{1}{\sqrt{2\pi}}\frac{i}{2\sigma^3}\int_{-\infty}^{\infty} dx\, x^2 \exp\left(\frac{-x^2}{2\sigma^2}\right) \tag{1.52}$$

and

$$\langle\phi_i|\, \hat{k}\hat{X}\, |\phi_i\rangle = \frac{i}{\sqrt{2\pi}\sigma}\left[\frac{1}{2\sigma^2}\int_{-\infty}^{\infty} dx\, x^2 \exp\left(\frac{-x^2}{2\sigma^2}\right) - \int_{-\infty}^{\infty} dx \exp\left(\frac{-x^2}{2\sigma^2}\right)\right]. \tag{1.53}$$

These Gaussian integrals are easily calculated and it is possible to show that

$$\langle\phi_i|\, \hat{X}\hat{k}\, |\phi_i\rangle = \frac{i}{2} \quad \text{and} \quad \langle\phi_i|\, \hat{k}\hat{X}\, |\phi_i\rangle = -\frac{i}{2}. \tag{1.54}$$

Hence, the expectation value of the anti-commutator is

$$\langle\phi_i|\, \{\hat{X}, \hat{k}\}\, |\phi_i\rangle = 0, \tag{1.55}$$

and of the commutator is

$$\langle\phi_i|\, [\hat{X}, \hat{k}]\, |\phi_i\rangle = i, \tag{1.56}$$

as we expected, since this commutator is one of the most famous relationships in quantum mechanics and can be found in any decent book about the subject [1,2]. As one may see,

the term proportional to the commutator between $\hat{X}$ and $\hat{k}$ is the only non-zero term in equation (1.47). Consequently, using the results obtained in equations (1.50), (1.55) and (1.56), we conclude that

$$\langle\phi|\,\hat{X}\,|\phi\rangle \simeq c\mathrm{Re}(A_w). \tag{1.57}$$

The above equation proves that the real part of the weak value A_w is proportional to the expectation value $\langle\hat{X}\rangle$ of the position operator of system $\mathcal{M}$ in the state $|\phi\rangle$. Now, we move on to prove, in a similar fashion, how to measure the imaginary part of the weak value.

1.3.2 Measuring the Imaginary Part of the Weak Value

The strategy applied here is closely related to the previous demonstration. Instead of calculating the expectation value $\langle\hat{X}\rangle$ of the position operator, this time we will calculate the expectation value of its canonically conjugated observable, the momentum $\hat{k}$, in the same state $|\phi\rangle$. Then, using equation (1.45) and considering only linear terms in c, we have

$$\langle\phi|\,\hat{k}\,|\phi\rangle \simeq \langle\phi_i|\,\hat{k}\,|\phi_i\rangle - ic\mathrm{Re}(A_w)\,\langle\phi_i|\,(\hat{k}^2-\hat{k}^2)\,|\phi_i\rangle + c\mathrm{Im}(A_w)\,\langle\phi_i|\,(\hat{k}^2+\hat{k}^2)\,|\phi_i\rangle\,. \tag{1.58}$$

From the above equation it is obvious that the term proportional to the real part of the weak value is zero. In position representation, the first term could be written as

$$\langle\phi_i|\,\hat{k}\,|\phi_i\rangle = \frac{1}{\sqrt{2\pi}}\frac{i}{2\sigma^3}\int_{-\infty}^{\infty} dx\, x\exp\left(\frac{-x^2}{2\sigma^2}\right). \tag{1.59}$$

Since we are integrating an odd function in x over an interval centred at $x=0$, by symmetry arguments, it is clear that the result of this integral is 0. Therefore,

$$\langle\phi|\,\hat{k}\,|\phi\rangle \simeq 2c\mathrm{Im}(A_w)\,\langle\phi_i|\,\hat{k}^2\,|\phi_i\rangle\,, \tag{1.60}$$

showing that the expectation value of $\hat{k}$ is directly proportional to the imaginary part of the weak value. Since $\langle x|\phi_i\rangle$ is given by equation (1.43), we have

$$\langle\phi_i|\,\hat{k}^2\,|\phi_i\rangle = \frac{1}{\sqrt{2\pi}}\frac{1}{2\sigma^3}\left[\int_{-\infty}^{\infty} dx\exp\left(\frac{-x^2}{2\sigma^2}\right) - \frac{1}{(2\sigma)^2}\int_{-\infty}^{\infty} dx\, x^2\exp\left(\frac{-x^2}{2\sigma^2}\right)\right]. \tag{1.61}$$

Solving the integrals, we are left with

$$\langle\phi_i|\,\hat{k}^2\,|\phi_i\rangle = \frac{1}{2\sigma^2} - \frac{1}{4\sigma^2} = \frac{1}{4\sigma^2}. \tag{1.62}$$

Finally,

$$\langle\phi|\,\hat{k}\,|\phi\rangle \simeq \frac{c}{2\sigma^2}\mathrm{Im}(A_w). \tag{1.63}$$

Therefore, in order to measure the imaginary part of the weak value A_w all we need is to measure the expectation value $\langle\phi|\,\hat{k}\,|\phi\rangle$ of the momentum of the measuring apparatus in the state $|\phi\rangle$. We stress that different observables of the measuring system could have been used in this demonstration, the important property here being the fact they are canonically conjugated with each other [16]. For instance, we could have obtained similar results using different components of the polarisation, as we will see in chapter 3.

The purpose of this demonstration is to show that, although the weak value is a complex variable, it can be written in terms of expectation values of common quantum observables, like position and momentum. It also allows one to measure both parts of the weak value in the laboratory in a straightforward way. Once we have established the weak measurement idea in solid grounds, we proceed to describe a simple experimental setup in which the weak measurement protocol can be implemented.

1.4 An Optical Example

1.4.1 The Experimental Setup

In order to illustrate the weak measurement protocol, we will describe how a simple optical apparatus may be used to measure the weak value S_w of the polarisation of a laser beam[11], with the operator $\hat{S}$ defined as

$$\hat{S} = |H\rangle\langle H| - |V\rangle\langle V|\,, \tag{1.64}$$

where $|H\rangle$ and $|V\rangle$ represent the states with horizontal and vertical polarisations, respectively. In this case, the transverse profile of the beam will play the role of the measuring device. The setup presented here is similar to the one proposed by Duck *et al.* [13]. Although this experiment may also be understood as the superposition of classical electromagnetic waves [20], it is a useful example to discuss some of the basic aspects of the weak measurement formalism.

Pre-selection

The experimental setup is schematically shown in figure 1.4. The laser beam is collimated and propagates in the z direction in the paraxial regime. It is prepared in a Gaussian mode with a beam waist w_0. To prepare the polarisation initial state $|\psi_i\rangle$, one uses a half wave plate (HWP) and a quarter wave plate (QWP). Once knowing the polarisation of the laser beam, we may use this configuration of plates to prepare any desired

[11] The first experimental tests of the weak measurement protocol were made in optical systems and were concerned in measuring the weak value of polarisation of a laser beam [17, 18] following the suggestions of references [13, 19].

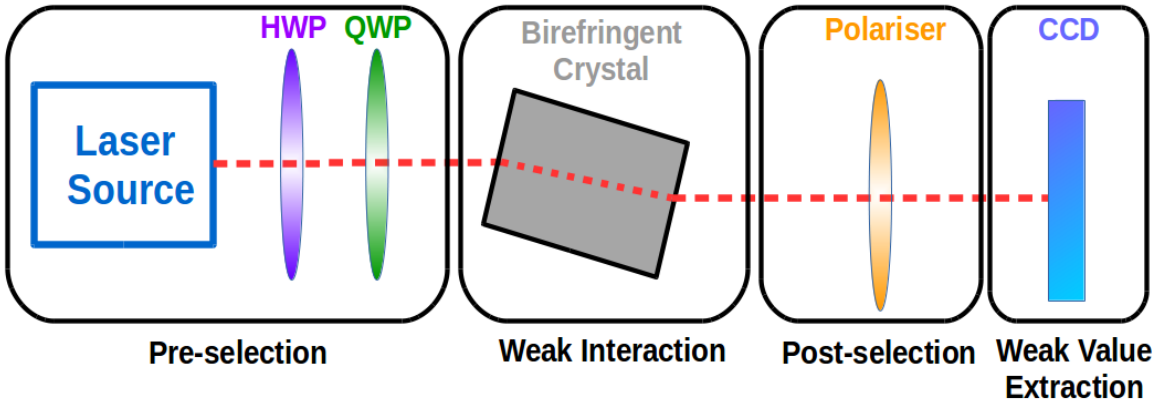

Figure 1.4: Scheme representing the experimental optical setup to measure the real part of the weak value $\mathrm{Re}(S_w)$. The imaginary part $\mathrm{Im}(S_w)$ could be measured including a lens between the crystal and the polariser in order to project the far field of the crystal in the CCD sensor.

polarisation state. Thus,

$$|\psi_i\rangle = \cos\alpha\,|H\rangle + e^{i\theta}\sin\alpha\,|V\rangle\,, \tag{1.65}$$

where α is twice the angle between the polarisation of incoming light and the fast axis of the HWP and θ is the angle between the polarisation of incoming light and the fast axis of the QWP.

Weak Interaction

The weak interaction is implemented using a slab of a birefringent material, such as quartz or calcite. Such materials have the interesting property of having different refraction indices for different polarisations of light [21]. Therefore, as the beam passes through the material, different components of polarisation, $|H\rangle$ and $|V\rangle$ for example, will be displaced by different amounts. Since the interaction between the laser beam and the birefringent crystal is weak, the distance between the centre of the transverse profile of the displaced beams a will be much smaller than the beam waist w_0. Therefore, although there is a correlation between the transverse profile and the polarisation of the beam, it is not strong enough to identify the beam polarisation based on the position of the centre of the transverse profile [see figure 1.3(c)].

Post-Selection

After the laser interacts with the birefringent material, one uses a polariser to post-select its polarisation state. The polariser is placed making an angle β with the horizontal

axis, such that the post-selected state $|\psi_f\rangle$ is written in the H-V basis as

$$|\psi_f\rangle = \cos\beta\,|H\rangle + \sin\beta\,|V\rangle\,. \tag{1.66}$$

Reading out the Weak Value

To read the weak value, one measures the intensity profile of the beam, using a charge coupled device (CCD) sensor. As we have seen previously, it is possible to measure the real part of the weak value based on the displacement of the wavefunction, or of the beam transverse intensity profile in the present case, due to the weak interaction.

First, one must measure the profile of the post-selected beam without the presence of the birefringent crystal. Then, the weak measurement protocol is implemented following the previous three steps and finally recording the beam intensity at the CCD. Using both recorded intensities, one may calculate the difference between their peaks, which should be equal to $a\mathrm{Re}(S_w)$. In this setup, the constant a is the distance between the transverse profile centre of the two beam components. To determinate its value, one chooses a specific set of pre- and post-selected states and calculates the weak value S_w from the definition in equation (1.35). Then, from the measured displacement of the intensity profile, one may calculate the value of the constant a. Once a is determined, it is possible to read the real part of the weak value from the measured displacement of the intensity profile.

In order to measure the imaginary part of the weak value $\mathrm{Im}(S_w)$, one may use a lens to image the Fourier plane of the crystal in the CCD, in such a way that each pixel will correspond to a post-selection in momentum [22]. Using this apparatus, we may easily measure the expectation value of $\langle\hat{k}\rangle$ and from it, as shown in the previous section, calculate $\mathrm{Im}(S_w)$.

1.4.2 Calculating Weak Values

Firstly, we prove a general property of weak values A_w. If one pre-selects the system in an eigenstate of the observable A, the weak value will be equal to the eigenvalue associated to that eigenstate. The demonstration is straightforward,

$$A_w = \frac{\langle\psi_f|\,\hat{A}\,|a_i\rangle}{\langle\psi_f|a_i\rangle} = a_i\frac{\langle\psi_f|a_i\rangle}{\langle\psi_f|a_i\rangle} = a_i. \tag{1.67}$$

Note that the same occurs when one post-selects the system in an eigenstate of A.

Now, we would like to analyse the weak values of the laser beam polarisation. Using equation (1.64) and the pre- and post-selected states of equations (1.65) and (1.66), we may calculate the weak value dependence with the angles α, β and θ, using the definition

(1.35). Therefore,

$$S_w(\alpha,\beta,\theta) = \frac{\langle\psi_f|\,\hat{S}\,|\psi_i\rangle}{\langle\psi_f|\psi_i\rangle} = \frac{\cos\beta\cos\alpha - e^{i\theta}\sin\beta\sin\alpha}{\cos\beta\cos\alpha + e^{i\theta}\sin\beta\sin\alpha}. \tag{1.68}$$

Equation (1.68) gives the weak value for any pair of pre- and post-selected states we choose to measure. Therefore, if we fix the pre-selected state, i.e., the angles α and θ, we may plot the weak value S_w as a function of the angle β, which determines the post-selected state.

The data presented in the following graphs were generated considering four different initial states: the eigenstates of operator $\hat{S}$, $|H\rangle$ and $|V\rangle$; the diagonal state, $|D\rangle = (|H\rangle + |V\rangle)\sqrt{2}$; and the right-circular polarisation state, $|R\rangle = (|H\rangle + i\,|V\rangle)\sqrt{2}$. As proved in the beginning of this section, once the initial states are eigenstates of the observable of interest, the weak values will be the eigenvalues associated to these eigenstates, independent of the post-selection we choose to make, as shown in figure 1.5. Observe that there is a region where S_w assume anomalous values, i.e., they are bigger (or smaller) than the allowed eigenvalues. For the pre-selected state $|D\rangle$, note that the weak value diverges as β approaches $3\pi/4$, which represents the state anti-diagonal $|A\rangle$, orthogonal to $|D\rangle$, where S_w is not well defined. The other initial state considered, $|R\rangle$, is interesting because in this case $\mathrm{Im}(S_w)$ is different from 0, as clearly shown in figure 1.6, leaving no doubts about the complex nature of S_w. Although, as pointed out in the last section, note that this presents no menace to the weak value definition, since it is possible to measure this imaginary part with the appropriate apparatus.

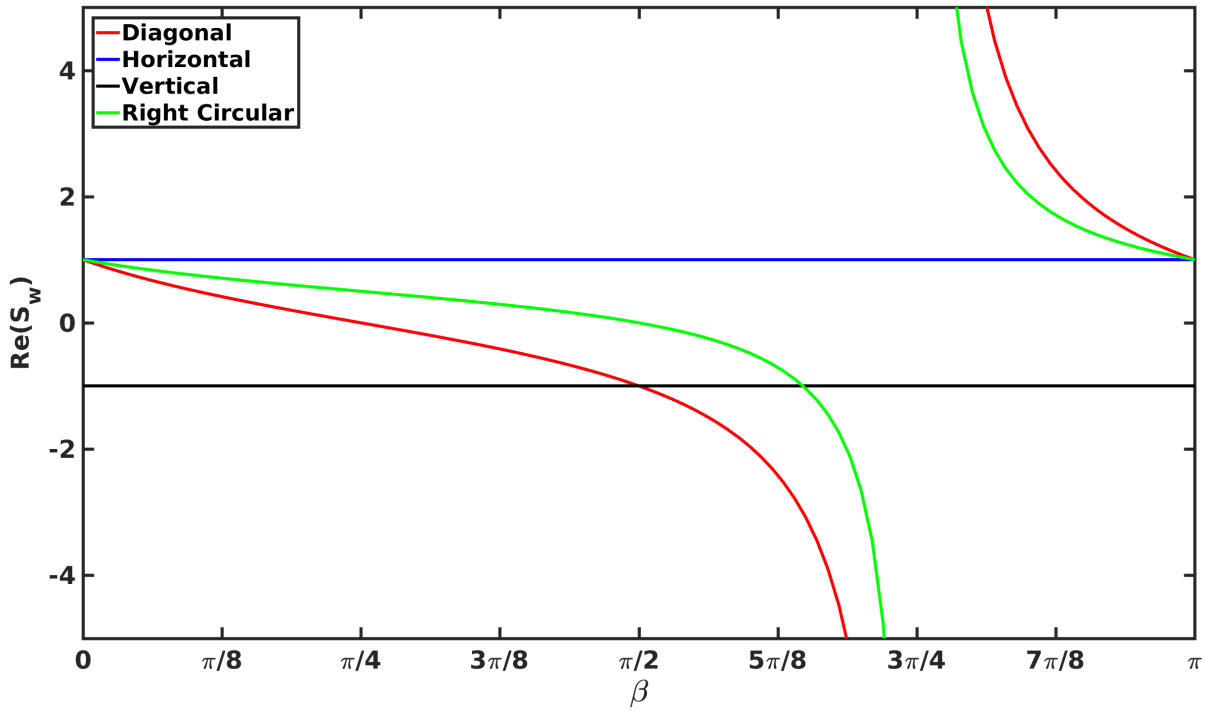

Figure 1.5: Real part of the weak value $\mathrm{Re}(S_w)$ as a function of the post-selection angle β for four different initial states: $|H\rangle$, $|V\rangle$, $|D\rangle = (|H\rangle + |V\rangle)\sqrt{2}$ and $|R\rangle = (|H\rangle + i\,|V\rangle)\sqrt{2}$. Note the region where the $\mathrm{Re}(S_w)$ assumes anomalous values, being bigger (or smaller) than the possible eigenvalues $+1$ and -1. When the initial states are the eigenstates of S the weak value S_w is always the associated eigenvalue, independent of β.

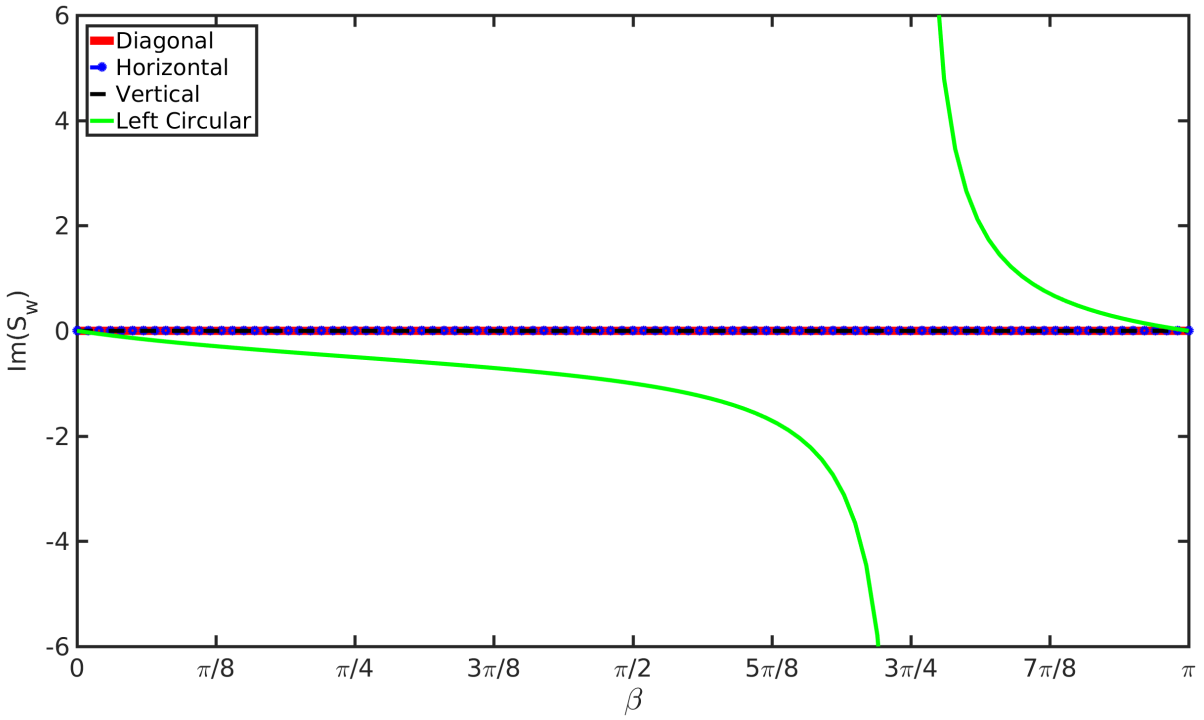

Figure 1.6: Imaginary part of the weak value $\mathrm{Im}(S_w)$ as a function of the angle β for four different initial states: $|H\rangle$, $|V\rangle$, $|D\rangle$ and $|R\rangle$. Note that only for $|\psi_i\rangle = |L\rangle$ the $\mathrm{Im}(S_w)$ is different from zero.

Chapter 2

Weak Values: Extensions, Applications, and Interpretations

Once we have established the idea of the weak measurement protocol in solid grounds, as done in chapter 1, we are now able to tackle more subtle questions about weak measurements and the weak value. Since its very beginning, the history of the weak value has been filled with discussions about the validity of the idea and its interpretations [3,8,13,23–25]. Duck *et al.* [13] explicitly showed that the weak value is a well defined quantum variable and, later, Ritchie *et al.* [17] measured a weak value in the laboratory for the first time.

Although these works put the existence of the weak value beyond doubt, there were still many questions about its meaning and usefulness. Since then many applications proved that the weak values could be used as a valuable resource in the laboratory [6,7,26–29]. It is interesting to note that some of these applications used extensions of this quantity, such as the joint weak values [29–32]. Nevertheless, the discussions about what the weak value of an observable means have never ceased and no consensus was achieved until now [33–36]. This chapter is devoted to present useful extensions of the weak value, some of the most interesting applications using this concept and briefly discuss some currently interpretations of this new quantum variable.

In section 2.1, we present two extensions of the weak value concept: the joint weak value, which is an extension aimed to calculate the weak value of two or more variables jointly, and the weak value of n^{th} order, which can be used to describe interactions of any strength. Then, in section 2.2, we move on to present some interesting applications of the weak value. We can use its exquisite properties — such as being a complex valued measurable quantity and not being restricted to lie between the interval of possible eigenvalues — to perform useful tasks in laboratory, like amplifying a small signal. In section 2.3 we briefly present two opposing views about the meaning of the weak value, a topic which has not achieved a consensus until now. To finish the chapter, in section 2.4 we discuss how the weak value can be seen as a conditioned average of an observable, a notion which will be essential for the discussions on chapter 3.

2.1 Extensions of the Weak Value

2.1.1 Joint Weak Measurements

Joint Measurements

Joint measurements are a necessary experimental tool to implement many quantum information protocols, such as quantum teleportation [37,38], entanglement swapping [39], dense coding [40], among others. They also may be used to test fundamental concepts in quantum mechanics [41–43] and to characterise the entanglement of a quantum mechanical state [44, 45].

Despite its usefulness, the direct measurement of a joint observable $C = AB$ is a challenging experimental task. To measure C directly, one needs a coupling interaction between the measuring apparatus $\mathcal{M}$ and and the quantum system $\mathcal{S}$, here assumed to be composed by two particles, a and b. This interaction is described by

$$\hat{\mathcal{H}} = g\hat{C}\hat{P} = g\hat{A}\hat{B}\hat{P}, \tag{2.1}$$

where $\hat{P}$ is the momentum operator of the system $\mathcal{M}$ and g is a coupling parameter, which we assumed to be constant during the time of interaction between $\mathcal{S}$ and $\mathcal{M}$. Note that in this case there is only one degree of freedom of the measurement device to account for two different observables related to particles a and b. As a consequence, to carry out the joint measurement directly one would need to establish an interaction between the particles and to know how this interaction works. This could be a problem in a system where the particles do not interact with each other, like in the case of two photons, or when more than two particles are involved, which could lead to more complicated interactions. To circumvent this problem, one may adopt a different strategy which consists in measuring each observable A and B separately and then computing their correlations to measure C. In this new procedure, the Hamiltonian is given by

$$\hat{\mathcal{H}} = g_A\hat{A}\hat{P}_x + g_B\hat{B}\hat{P}_y, \tag{2.2}$$

where $\hat{P}_x$ and $\hat{P}_y$ are the momentum operators conjugated to two position operators $\hat{X}$ and $\hat{Y}$ of the measuring systems $\mathcal{M}_A$ and $\mathcal{M}_B$, respectively.

We know that this procedure is feasible: it reduces to the problem of making two single measurements, which we have seen how to implement in chapter 1, and compute their correlations, which is a trivial task.[1] Therefore, the value of C is determined by the calculation of the observed correlations in the results obtained from local measurements of A and B. To measure joint observables in quantum optics experiments, for example,

[1] Note that this procedure may be easily extended for a joint observable C composed by N observables $A_1, ..., A_N$. The interested reader could find a complete analysis of this case in the references [16, 46].

one utilises a single-photon counter to measure the desired observable of each photon and a coincidence logic circuit to measure the correlations between the single measurements.

Measuring Joint Weak Values

Since we have established a strategy to perform joint measurements, now we would like to devise a similar procedure to perform joint weak measurements. Here we derive a relationship between the result of a joint weak measurement, the joint weak value C_w, to the single weak values A_w and B_w. The derivation showed here is based in the arguments used in reference [47].[2]

As in the case of joint measurements, the Hamiltonian which describes the interaction between the system of interest $\mathcal{S}$ and the measuring apparatus $\mathcal{M}$ is given by equation (2.2). The initial state of the global system is given by

$$|\Psi_i\rangle = |\psi_i\rangle\,|\Phi_i\rangle\,, \tag{2.3}$$

where $\mathcal{S}$ is composed by two particles prepared in the known state $|\psi_i\rangle$ and the state $|\Phi_i\rangle$ of the measuring devices $\mathcal{M}$ is given by

$$|\Phi_i\rangle = |\phi_x\rangle\,|\phi_y\rangle = \frac{1}{\sqrt{2\pi\sigma_x\sigma_y}}\int dy\int dx\exp\left(\frac{-x^2}{(2\sigma_x)^2}\right)\exp\left(\frac{-y^2}{(2\sigma_y)^2}\right)|x\rangle\,|y\rangle\,. \tag{2.4}$$

According to Postulate 3 of section 1.1, after interaction between the systems $\mathcal{S}$ and $\mathcal{M}$, the global state will evolve according to

$$|\Psi\rangle = \hat{U}\,|\Psi_i\rangle\,, \tag{2.5}$$

where

$$\hat{U} = \exp\left(\frac{-igt}{\hbar}\hat{\mathcal{H}}\right), \tag{2.6}$$

for a time-independent Hamiltonian. Then, following the weak measurement protocol, we project $\mathcal{S}$ in the state $|\psi_f\rangle$ and the state of $\mathcal{M}$ will be given by

$$|\Phi\rangle = \frac{\langle\psi_f|\Psi\rangle}{\langle\psi_f|\psi_i\rangle} = \frac{\langle\psi_f|\,\hat{U}\,|\Psi_i\rangle}{\langle\psi_f|\psi_i\rangle}, \tag{2.7}$$

where $\langle\psi_f|\psi_i\rangle$ is a renormalisation factor. In the same spirit of section 1.3, in order to calculate the real part of the joint weak value $(AB)_w$, we will calculate the expectation value of joint operator $\hat{X}\hat{Y}$ in the state $|\Phi\rangle$, which describes the state of $\mathcal{M}$ after the

[2] In fact, there is a proposal to perform joint weak measurements in a strong interacting system using trapped ions [48]. Nevertheless, there is no experimental work exploring this idea.

post-selection in $\mathcal{S}$. Then,

$$\langle\Phi|\,\hat{X}\hat{Y}\,|\Phi\rangle = \frac{\langle\Psi_i|\,\hat{U}^\dagger\,|\psi_f\rangle\langle\psi_f|\,\hat{X}\hat{Y}\hat{U}\,|\Psi_i\rangle}{|\,\langle\psi_f|\psi_i\rangle\,|^2}, \tag{2.8}$$

where we used equation (2.7). For convenience in the long calculation that awaits us, we define

$$\langle\Phi|\,\hat{X}\hat{Y}\,|\Phi\rangle_{\rm UN} = \langle\Phi|\,\hat{X}\hat{Y}\,|\Phi\rangle\,|\,\langle\psi_f|\psi_i\rangle\,|^2, \tag{2.9}$$

to eliminate the term in denominator in equation (2.8). Defining operator $\hat{O}_{xy}$ as

$$\hat{O}_{xy} = |\psi_f\rangle\langle\psi_f|\,\hat{X}\hat{Y} \tag{2.10}$$

and using equations (2.6) and (2.8), we can rewrite the expectation value (2.9) as

$$\langle\Phi|\,\hat{X}\hat{Y}\,|\Phi\rangle_{\rm UN} = \langle\Psi_i|\exp\left(\frac{igt}{\hbar}\hat{\mathcal{H}}\right)\hat{O}_{xy}\exp\left(-\frac{igt}{\hbar}\hat{\mathcal{H}}\right)|\Psi_i\rangle\,. \tag{2.11}$$

Applying the the Baker–Hausdorff lemma [2]

$$\begin{aligned}\exp(\lambda\hat{D})\hat{E}\exp(-\lambda\hat{D}) = \hat{E} + \lambda[\hat{D},\hat{E}] + \frac{\lambda^2}{2!}[\hat{D},[\hat{D},\hat{E}]] + \ldots \\ + \frac{\lambda^n}{n!}[\hat{D},[\hat{D},[\hat{D},\ldots[\hat{D},\hat{E}]]]] + \ldots\end{aligned} \tag{2.12}$$

we may approximate equation (2.11) by

$$\langle\Phi|\,\hat{X}\hat{Y}\,|\Phi\rangle_{\rm UN} \simeq \langle\Psi_i|\,\hat{O}_{xy} - \frac{it}{\hbar}[\hat{\mathcal{H}},\hat{O}_{xy}] - \frac{1}{2}\left(\frac{t}{\hbar}\right)^2[\hat{\mathcal{H}},[\hat{\mathcal{H}},\hat{O}_{xy}]]\,|\Psi_i\rangle\,, \tag{2.13}$$

where we considered terms only until $(t/\hbar)^2$ due to the fact that we are working in the limit of weak interactions. Now we need to analyse each term in the right side of above equation. The first term, which corresponds to the expected value of operator $\hat{O}_{xy}$ in the initial state $|\Psi_i\rangle$, is given by

$$\begin{aligned}\langle\Psi_i|\,\hat{O}_{xy}\,|\Psi_i\rangle &= \langle\psi_i|\,\langle\Phi_i|\,\hat{O}_{xy}\,|\Phi_i\rangle\,|\psi_i\rangle \\ &= |\,\langle\psi_f|\psi_i\rangle\,|^2\,\langle\phi_x|\,\hat{X}\,|\phi_x\rangle\,\langle\phi_y|\,\hat{Y}\,|\phi_y\rangle\,,\end{aligned} \tag{2.14}$$

where we used the definition (2.10) and equations (2.3) and (2.4) which describe the initial state of the global and measuring systems. Here we note that

$$\langle\phi_x|\,\hat{X}\,|\phi_x\rangle = 0 \quad \text{and} \quad \langle\phi_y|\,\hat{Y}\,|\phi_y\rangle = 0, \tag{2.15}$$

since the initial wavefunctions $\phi_x(x) = \langle x|\phi_x\rangle$ and $\phi_y(y) = \langle y|\phi_y\rangle$ given in equation (2.4) are even functions and, by symmetry arguments, it is easy to see that the expectation

values of position evaluated in these states are zero. Thus,

$$\langle\Psi_i|\,\hat{O}_{xy}\,|\Psi_i\rangle = 0. \tag{2.16}$$

The results expressed in equation (2.15) will be very important to simplify many of the following calculations. Now, we move on to calculate the expectation value of the commutator

$$\langle\Psi_i|\,[\hat{\mathcal{H}},\hat{O}_{xy}]\,|\Psi_i\rangle = \langle\Psi_i|\,\hat{\mathcal{H}}\hat{O}_{xy}\,|\Psi_i\rangle - \langle\Psi_i|\,\hat{O}_{xy}\hat{\mathcal{H}}\,|\Psi_i\rangle\,. \tag{2.17}$$

Using equations (2.2) and (2.10), we can show that

$$\begin{aligned}\hat{\mathcal{H}}\hat{O}_{xy} &= (g_A\hat{A}\hat{P}_x + g_B\hat{B}\hat{P}_y)\,|\psi_f\rangle\langle\psi_f|\,\hat{X}\hat{Y}\\ &= g_A\hat{A}\,|\psi_f\rangle\langle\psi_f|\,\hat{P}_x\hat{X}\hat{Y} + g_B\hat{B}\,|\psi_f\rangle\langle\psi_f|\,\hat{X}\hat{P}_y\hat{Y},\end{aligned} \tag{2.18}$$

and

$$\hat{O}_{xy}\hat{\mathcal{H}} = g_A\,|\psi_f\rangle\langle\psi_f|\,\hat{A}\hat{X}\hat{P}_x\hat{Y} + g_B\,|\psi_f\rangle\langle\psi_f|\,\hat{B}\hat{X}\hat{Y}\hat{P}_y. \tag{2.19}$$

When we calculate the expectation value, all terms will be proportional to $\langle\phi_x|\,\hat{X}\,|\phi_x\rangle$ or $\langle\phi_y|\,\hat{Y}\,|\phi_y\rangle$, which are both zero as shown in equation (2.15). Thus,

$$\langle\Psi_i|\,[\hat{\mathcal{H}},\hat{O}_{xy}]\,|\Psi_i\rangle = 0. \tag{2.20}$$

Now we have to deal with the commutator

$$[\hat{\mathcal{H}},[\hat{\mathcal{H}},\hat{O}_{xy}]] = \hat{\mathcal{H}}\hat{\mathcal{H}}\hat{O}_{xy} + \hat{O}_{xy}\hat{\mathcal{H}}\hat{\mathcal{H}} - 2\hat{\mathcal{H}}\hat{O}_{xy}\hat{\mathcal{H}}. \tag{2.21}$$

Using the Hamiltonian (2.2) and the definition (2.10), we may show that

$$\begin{aligned}[\hat{\mathcal{H}},[\hat{\mathcal{H}},\hat{O}_{xy}]] = {}& g_A^2\,(\,\hat{A}^2\,|\psi_f\rangle\langle\psi_f|\,\hat{P}_x^2\hat{X} + |\psi_f\rangle\langle\psi_f|\,\hat{A}^2\hat{X}\hat{P}_x^2 - 2\hat{A}\,|\psi_f\rangle\langle\psi_f|\,\hat{A}\hat{P}_x\hat{X}\hat{P}_x\,)\hat{Y}\\ &+ g_B^2\,(\,\hat{B}^2\,|\psi_f\rangle\langle\psi_f|\,\hat{P}_y^2\hat{Y} + |\psi_f\rangle\langle\psi_f|\,\hat{B}^2\hat{Y}\hat{P}_y^2 - 2\hat{B}\,|\psi_f\rangle\langle\psi_f|\,\hat{B}\hat{P}_y\hat{Y}\hat{P}_y\,)\hat{X}\\ &+ g_Ag_B[\,\{\hat{A},\hat{B}\}\,|\psi_f\rangle\langle\psi_f|\,\hat{P}_x\hat{X}\hat{P}_y\hat{Y} + |\psi_f\rangle\langle\psi_f|\,\{\hat{A},\hat{B}\}\hat{X}\hat{P}_x\hat{Y}\hat{P}_y\\ &- 2\,(\,\hat{A}\,|\psi_f\rangle\langle\psi_f|\,\hat{B}\hat{P}_x\hat{X}\hat{Y}\hat{P}_y + \hat{B}\,|\psi_f\rangle\langle\psi_f|\,\hat{A}\hat{X}\hat{P}_x\hat{P}_y\hat{Y}\,)\,],\end{aligned} \tag{2.22}$$

where we used the definition (1.49) of the anti-commutator. From the above equation, we note that the terms proportional to g_A^2 and g_B^2 are also proportional to the operators $\hat{Y}$ and $\hat{X}$, respectively. Therefore, when we calculate the expectation value of these terms in the state $|\Psi_i\rangle$ they will be zero, as a consequence of equation (2.15). Then, the expectation

value of the commutator $[\hat{\mathcal{H}},[\hat{\mathcal{H}},\hat{O}_{xy}]]$ simplifies to

$$\begin{aligned}\langle\Psi_i|\,[\hat{\mathcal{H}},[\hat{\mathcal{H}},\hat{O}_{xy}]]\,|\Psi_i\rangle = g_A g_B\,\langle\Psi_i|\,[\,\{\hat{A},\hat{B}\}\,|\psi_f\rangle\langle\psi_f|\,\hat{P}_x\hat{X}\hat{P}_y\hat{Y}\\ +|\psi_f\rangle\langle\psi_f|\,\{\hat{A},\hat{B}\}\hat{X}\hat{P}_x\hat{Y}\hat{P}_y - 2\,(\,\hat{A}\,|\psi_f\rangle\langle\psi_f|\,\hat{B}\hat{P}_x\hat{X}\hat{Y}\hat{P}_y\\ +\hat{B}\,|\psi_f\rangle\langle\psi_f|\,\hat{A}\hat{X}\hat{P}_x\hat{P}_y\hat{Y}\,)\,]\,|\Psi_i\rangle\,.\end{aligned} \tag{2.23}$$

We may simplify further this result, by calculating the expectation of the products of $\hat{X},\hat{P}_x,\hat{Y}$, and $\hat{P}_y$. For Gaussian distributions, as is the the case of $\phi_x(x)$ and $\phi_y(y)$, we have already performed these calculations in section 1.3.1, which reads

$$\langle\phi_x|\,\hat{X}\hat{P}_x\,|\phi_x\rangle = \langle\phi_y|\,\hat{Y}\hat{P}_y\,|\phi_y\rangle = \frac{i\hbar}{2}, \tag{2.24}$$

and

$$\langle\phi_x|\,\hat{P}_x\hat{X}\,|\phi_x\rangle = \langle\phi_y|\,\hat{P}_y\hat{Y}\,|\phi_y\rangle = -\frac{i\hbar}{2}. \tag{2.25}$$

Using these results in equation (2.23), we have

$$\begin{aligned}\langle\Psi_i|\,[\hat{\mathcal{H}},[\hat{\mathcal{H}},\hat{O}_{xy}]]\,|\Psi_i\rangle = -\frac{\hbar^2}{4}g_A g_B[\,\langle\psi_i|\,\{\hat{A},\hat{B}\}\,|\psi_f\rangle\,\langle\psi_f|\psi_i\rangle + \langle\psi_i|\psi_f\rangle\,\langle\psi_f|\,\{\hat{A},\hat{B}\}\,|\psi_i\rangle\\ +2\,(\,\langle\psi_i|\,\hat{A}\,|\psi_f\rangle\langle\psi_f|\,\hat{B}\,|\psi_i\rangle + \langle\psi_i|\,\hat{B}\,|\psi_f\rangle\langle\psi_f|\,\hat{A}\,|\psi_i\rangle\,)].\end{aligned} \tag{2.26}$$

Applying the results obtained in equations (2.16), (2.20) and (2.26), in the equation (2.13), we obtain

$$\begin{aligned}\langle\Phi|\,\hat{X}\hat{Y}\,|\Phi\rangle_{\mathrm{UN}} \simeq \frac{c_A c_B}{8}[\,\langle\psi_i|\,\{\hat{A},\hat{B}\}\,|\psi_f\rangle\,\langle\psi_f|\psi_i\rangle + \langle\psi_i|\psi_f\rangle\,\langle\psi_f|\,\{\hat{A},\hat{B}\}\,|\psi_i\rangle\,+\\ +2\,(\,\langle\psi_i|\,\hat{A}\,|\psi_f\rangle\langle\psi_f|\,\hat{B}\,|\psi_i\rangle + \langle\psi_i|\,\hat{B}\,|\psi_f\rangle\langle\psi_f|\,\hat{A}\,|\psi_i\rangle\,)],\end{aligned} \tag{2.27}$$

where $c_j = g_j t$ for $j = A$ or B. Then, using equation (2.9) we obtain

$$\begin{aligned}\langle\Phi|\,\hat{X}\hat{Y}\,|\Phi\rangle \simeq \frac{c_A c_B}{8}\Bigg[\frac{\langle\psi_i|\,\{\hat{A},\hat{B}\}\,|\psi_f\rangle}{\langle\psi_i|\psi_f\rangle} + \frac{\langle\psi_f|\,\{\hat{A},\hat{B}\}\,|\psi_i\rangle}{\langle\psi_f|\psi_i\rangle}\\ +2\left(\frac{\langle\psi_i|\,\hat{A}\,|\psi_f\rangle}{\langle\psi_i|\psi_f\rangle}\frac{\langle\psi_f|\,\hat{B}\,|\psi_i\rangle}{\langle\psi_f|\psi_i\rangle} + \frac{\langle\psi_i|\,\hat{B}\,|\psi_f\rangle}{\langle\psi_i|\psi_f\rangle}\frac{\langle\psi_f|\,\hat{A}\,|\psi_i\rangle}{\langle\psi_f|\psi_i\rangle}\right)\Bigg].\end{aligned} \tag{2.28}$$

Using the definition of the weak value (1.35) and noting that we have two sums of terms which are the complex conjugates of each other, we have

$$\langle\Phi|\,\hat{X}\hat{Y}\,|\Phi\rangle \simeq \frac{c_A c_B}{2}\left[\mathrm{Re}\left(\frac{1}{2}\frac{\langle\psi_f|\,\{\hat{A},\hat{B}\}\,|\psi_i\rangle}{\langle\psi_f|\psi_i\rangle} + A_w^* B_w\right)\right]. \tag{2.29}$$

Since $\hat{A}$ and $\hat{B}$ are operators acting in two different particles and therefore commute, we

have

$$\mathrm{Re}(AB)_w \equiv \mathrm{Re}\left(\frac{\langle\psi_f|\,\hat{A}\hat{B}\,|\psi_i\rangle}{\langle\psi_f|\psi_i\rangle}\right) = \frac{2\,\langle\Phi|\,\hat{X}\hat{Y}\,|\Phi\rangle}{c_A c_B} - \mathrm{Re}(A_w^* B_w), \tag{2.30}$$

finally showing how to measure the real part of the joint weak value $(AB)_w$. Note that we need to make a joint measurement of the position of both measurement devices and also measure the single weak values A_w and B_w. We call attention for the fact that

$$\mathrm{Re}(A_w^* B_w) = \mathrm{Re}(A_w)\mathrm{Re}(B_w) + \mathrm{Im}(A_w)\mathrm{Im}(B_w), \tag{2.31}$$

therefore in order to measure the joint weak value of a pair of observables we need to measure both the real and imaginary parts of single weak values.

We may proceed in a similar manner to derive an expression for the imaginary part of the joint weak value $(AB)_w$. The main difference is that instead of calculating the expectation value $\langle\hat{X}\hat{Y}\rangle$, we need to calculate $\langle\hat{X}\hat{P}_y\rangle$. The calculation is made following exactly the same steps as the ones presented here. In this case, one will obtain

$$\mathrm{Im}(AB)_w = \frac{4\sigma_y^2}{\hbar}\frac{\langle\Phi|\,\hat{X}\hat{P}_y\,|\Phi\rangle}{c_A c_B} - \mathrm{Im}(A_w^* B_w), \tag{2.32}$$

completing the proof that it is possible to measure joint weak values using only local measurements and computing their correlations. The joint weak values have been employed in attempts to solve quantum paradoxes, such as the Hardy's Paradox [31, 32, 49], and also to direct measure the density matrix of a system [29, 50]. In the next section, we will discuss some interesting applications of the weak value.

2.1.2 Weak Value of Order n

In chapter 1 we have seen that the weak value, defined in equation (1.35), is a quantity extracted from a pre- and post-selected states of a system when, between these projections, a weak interaction with a measuring device disturbs the system. In this section, our aim is to analyse a different and more general situation, in which we do not make any restrictions about the strength of the intermediate interaction which takes place between the pre- and post-selection.

To start our analysis, we propose the study of a simple quantum mechanical experiment in which we prepare a system in an initial state $|i\rangle$ and try to detect it in a final state $|f\rangle$. According to the postulate 4 of quantum mechanics presented in section 1.1, we have that the probability of a successful detection P in this case is

$$P = |\,\langle f|i\rangle\,|^2. \tag{2.33}$$

Another way of describing this situation is to say that the system was pre-selected in the

state $|i\rangle$ and post-selected in the state $|f\rangle$. The probability of a successful post-selection to occur is given by equation (2.33).

Assume that, before post-selection, the system interacts with another system changing its initial state. Consequently, the probability of a successful post-selection also changes and the new probability P' will be given by

$$P' = |\langle f|\hat{U}(\epsilon)|i\rangle|^2, \tag{2.34}$$

where $\hat{U}(\epsilon)$ is the unitary operator that describes this interaction and ϵ is a parameter related to the interaction strength. Now we are interested in calculating the effect of this intermediate perturbation, which could be of arbitrary strength, in the change of the probability of a successful post-selection. In order to compare the situations with and without an intermediate interaction we will calculate the ratio P'/P. First, we must determine P', so we need to know the form of the unitary operator $\hat{U}(\epsilon)$, which in the present case we assume to be

$$\hat{U}(\epsilon) = \exp(-i\epsilon\hat{B}), \tag{2.35}$$

where $\hat{B}$ is some Hermitian operator. Using the Taylor expansion of the exponential, we may rewrite $\hat{U}$ as

$$\hat{U}(\epsilon) = \sum_{n=0}^{\infty} \frac{(-i\epsilon)^n}{n!}\hat{B}^n. \tag{2.36}$$

Thus, the probability P' will be given by

$$P' = \left|\sum_{n=0}^{\infty} \frac{(-i\epsilon)^n}{n!}\langle f|\hat{B}^n|i\rangle\right|^2, \tag{2.37}$$

where we used the result of equation (2.36) in (2.34). Dividing the result above by P given in equation (2.33), we have

$$\frac{P'}{P} = \left|\sum_{n=0}^{\infty} \frac{(-i\epsilon)^n}{n!}\frac{\langle f|\hat{B}^n|i\rangle}{\langle f|i\rangle}\right|^2. \tag{2.38}$$

From the above equation we define a new quantity, which is an extension of the weak value: the weak value of order n, namely,

$$B_w^n = \frac{\langle f|\hat{B}^n|i\rangle}{\langle f|i\rangle}. \tag{2.39}$$

Note that the weak value of first order correspond to the definition of the weak value, given in equation (1.35). Using this new quantity, we are able to rewrite the ratio P'/P

as

$$\begin{aligned}\frac{P'}{P} &= \left|\sum_{n=0}^{\infty}\frac{(-i\epsilon)^n}{n!}B_w^n\right|^2. \\ &= \sum_{n=0}^{\infty}\frac{(-1)^n\epsilon^{2n}}{n!^2}|B_w^n|^2 + \sum_{n=0}^{\infty}\sum_{\substack{m=0\\m\neq n}}^{\infty}\frac{(-1)^n\, i^{n+m}\,\epsilon^{n+m}}{n!m!}B_w^n(B_w^m)^*,\end{aligned} \tag{2.40}$$

where $(B_w^m)^*$ is the complex conjugated of B_w^m. By computing the ratio P'/P one is capable to observe the effects of the intermediate interaction over the system of interest. In equation (2.40) we showed that these effects may be described only in terms of the weak value of n^{th} order. The important fact here is that we did not make any assumptions about the strength of the interaction in this case, showing the power of this generalisation of the weak value concept. In the case which the interaction is weak, we can neglect terms of order ϵ^2 or higher to obtain

$$\frac{P'}{P} \simeq 1 + 2\epsilon\text{Im}(B_w), \tag{2.41}$$

showing that the imaginary part of weak value B_w is a function of the ratio of the measured probabilities. Note that in order to keep the demonstration above simpler, we assumed that the unitary operator $\hat{U}$ which describes the interaction between the systems was given by (2.35) instead of (1.16), which explicit contains the respective operators of each system. Then, if we assume

$$\hat{B} = \hat{A}\hat{k}, \tag{2.42}$$

both operators will have exactly the same form. Here, as in chapter 1, A is the measured observable in the system of interest and k is the momentum in the measuring system divided by $\hbar$. Note that in this case B will be a joint observable and equation (2.41) gives the imaginary part of the joint weak value B_w. Using the above definition in equation (2.41), we obtain

$$\frac{P'}{P} \simeq 1 + 2\epsilon(\text{Re}(A_w)\text{Im}(k_w) + \text{Im}(A_w)\text{Re}(k_w)). \tag{2.43}$$

As shown in reference [22], we can choose the pre- and post-selected states in such a way that k_w will be purely real or imaginary, leaving the ratio between the detected probabilities as a function exclusively of the imaginary or real parts of the weak value A_w, respectively.

If one would like to consider stronger interactions, it is easy to show that

$$\frac{P'}{P} \simeq 1 + 2\epsilon\text{Im}(B_w) + \epsilon^2[\text{Re}(B_w^2) - |B_w|^2], \tag{2.44}$$

where we took into account terms until second order in ϵ. For even stronger interactions, all we need to do is consider higher order terms in the expansion given in equation (2.40). Observe that the result (2.40) is general, showing that the suggested generalisation of the weak value concept given in equation (2.39) is a useful tool to describe intermediate interactions of any strength between the pre- and post-selection of the states of a given system.

2.2 Some Applications of the Weak Value

Weak values present some unique features which allow them to be utilised as a useful tool in laboratory. For instance, we mention the use of the weak measurement protocol in high precision measurements [26], in the debate about which mechanism forces complementarity in a double-slit experiment [51], in experimental tests of the Bell inequalities [52] and in the reconstruction of average trajectories of post-selected photons in a double-slit interferometer [5], which is the main theme of the next chapter.

In this section, we discuss some applications of the weak measurement protocol, showing that, more than a curiosity hidden in the quantum mechanical formalism, this procedure is a powerful experimental technique. Each application presented was meticulously chosen to highlight an important feature of the weak value. We begin the section discussing its usefulness as a signal amplifier, an application which took advantage of the fact that the weak value can be much bigger than the eigenvalues of the measured observable. Then we move on to discuss the direct measurement of a quantum state, which uses the complex nature of the weak value, whose both real and imaginary parts can be measured. Besides, this technique exploits the fact that a weak measurement barely changes the state of the measured system before post-selection is made. In the last part, we discuss the use of the weak measurement protocol in the context of a gekanden experiment proposed by Hardy, which is one of the first experimental realisations of a joint weak measurement [31, 32] and will pave the way for the discussion about the interpretations of the weak value in the next section.

2.2.1 Weak Value as a Signal Amplifier

In their seminal paper [3], AAV proposed the first application of the recent procedure developed by them: use the weak value as a signal amplifier [3]. This application exploits the unique characteristic of the weak values of not being restricted to lie between the allowed eigenvalues of the measured observable A. As an example, we can imagine a Stern-Gerlach experiment in which the objective is to measure the gradient of the magnetic field in z-direction, $\partial B_z/\partial z$, in which spin-1/2 particles went through. Remember that in this case the eigenvalues of $\hat{\sigma}_z$, operator corresponding to the z-component of the intrinsic

angular momentum, are given by $\hbar/2$ and $-\hbar/2$. Thus, the separation Δz between the centre of the beams induced by the magnetic field gradient is given by

$$\Delta z = z_+ - z_- = \frac{\partial B_z}{\partial z}\left[\frac{\hbar}{2} - \left(\frac{-\hbar}{2}\right)\right] = \hbar\frac{\partial B_z}{\partial z}, \tag{2.45}$$

where $\partial B_z/\partial z$ plays the role of the coupling parameter c. Therefore, if the gradient $\partial B_z/\partial z$ is large enough, the separation between the components of the beam corresponding to different eigenvalues could be resolved by the measurement apparatus. Once one measures the separation Δz between the centres of these beams, one uses equation (2.45) to determine $\partial B_z/\partial z$. However, imagine a situation in which the gradient is so small that one is not able to clearly separate the two beams, i.e., a case in which the interaction between the particles and the field is weak. Since the overlap between the beams is almost complete, it is hard to measure the separation between their centres, making impossible the determination of the field gradient. In such cases, one can make a post-selection and measure the weak value of $\hat{\sigma}_z$. Making a clever choice of the pre- and post-selected states, $|\psi_i\rangle$ and $|\psi_f\rangle$, $\mathrm{Re}[(\sigma_z)_w]$ may be much larger than the eigenvalues of $\hat{\sigma}_z$. Then, the measured displacement $\Delta z'$ of the wavefunction $\psi(z)$ after the weak measurement protocol is given by

$$\Delta z' = \frac{\partial B_z}{\partial z}\mathrm{Re}[(\sigma_z)_w], \tag{2.46}$$

as shown in section 1.2. This strategy makes possible to measure $\Delta z'$ using the measurement apparatus at disposal and, ultimately, to determine the magnetic field gradient.

One interesting aspect of this application is, since the weak value A_w is used only as a multiplicative constant, there is no need in attaching a meaning to it, which makes this type of procedure completely independent of the interpretation one gives to A_w. We must note that one does not get this amplification for free: larger amplification factors mean that the overlap between pre- and post-selected states is smaller — remember that the weak value is inversely proportional to this overlap, as one may see in its definition (1.35). Consequently, the detection probability, which is proportional to $|\langle\psi_f|\psi_i\rangle|^2$, decreases as the amplification increases. We also have to note that we are working in the weak interaction regime, therefore the conditions (1.30) and (1.31) need to hold, also imposing a limit for the amplification provided by this technique.

In the following, we briefly discuss two milestone experiments which explored this idea. The interested reader may found an extensive list of experiments where the weak value was used as an signal amplifier in section IV.A of reference [22] and in section 2.7 of reference [53].

The First Realisation of a Weak Measurement

Duck *et al.* [13] were the first to suggest the use of an optical analogue of the Stern-Gerlach experiment as a feasible setup to implement the weak measurement protocol. Few years later, Ritchie *et al.* [17] were the responsible for carrying out the experiment, measuring the weak value for the first time and confirming the idea that it could be used as a signal amplifier.[3] A simplified version of their experimental setup, which consists in using a birefringent crystal to implement a weak interaction between the polarisation and the transverse profile of a laser beam, was presented in section 1.4 (see figure 1.4). They showed that, in the region where the weak approximation is valid, the value registered by the measuring apparatus could be almost 20 times larger than the actual separation between the centre of two components with orthogonal polarisations of the laser beam. As a consequence of this amplification, the intensity peak registered by them after the weak measurement protocol was 10^{-5} times smaller than the peak in the case which no post-selection was done.

The Spin Hall Effect of Light

In an outstanding work, Hosten and Kwiat used the weak measurement protocol to amplify the tiny displacement of photons caused by the spin Hall effect of light (SHEL) [6,55]. This effect was predicted by Onoda *et al.* [56] and occurs when linearly polarised light passes through an interface between two media with different refractive indexes. During the transition, each component of circularly polarised light is displaced by a small amount in opposite directions, which are perpendicularly oriented in relation to the propagation direction as shown in figure 2.1, hence the name of spin Hall effect of light. The experimental confirmation of this prediction was hard to achieve due to the displacement magnitude, which is in the order of nanometers. Since the displacement caused by the SHEL is smaller than the wavelength of the laser beam used, we observe that the effect occurs in the weak interaction regime and, hence, we may interpret the phenomenon as a weak measurement of the circular polarisation of the beam using its transverse profile as the meter. Using polarisers to make the pre- and post-selection required in a weak measurement protocol, the authors choose the states $|\psi_i\rangle$ and $|\psi_f\rangle$ in such a way that the weak value is purely imaginary. As shown in section 1.3, the imaginary part of the weak value is proportional to the expected value of the momentum of the measuring system, since we are using the position of the measuring system as the meter. Therefore, the imaginary weak value causes a change in the propagation direction, or angle, of the light, instead of its position. Hosten and Kwiat used this fact to achieve amplification factors of the order of 10^4, making possible to measure the tiny displacements induced by SHEL.

[3] The effect observed in this experiment can also be explained within the framework of classical electromagnetic theory. Only years later, the measurement of the weak value of photon polarisation was done in the quantum domain [54].

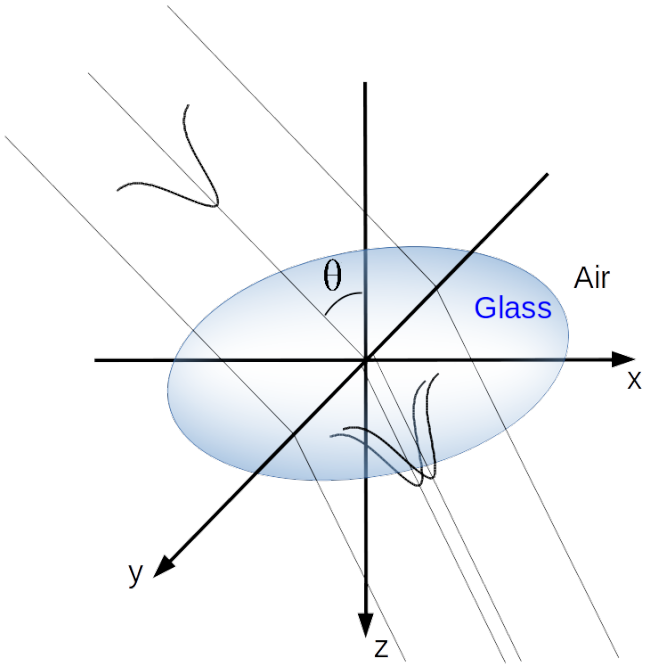

Figure 2.1: Scheme representing the spin Hall effect of light. The incoming linearly polarised laser beam is divided in two components circularly polarised in the glass-air interface. Since the displacement occurs in a direction perpendicular to the propagation direction and the separation depends on the circularly polarised components of polarisation, this effect was called the spin Hall effect of light.

2.2.2 Direct Measurement of the Wavefunction

One of the remarkable characteristics of weak values is the fact that it is a measurable complex quantity, as shown in section 1.3. We may use this feature to determine other complex entities which appear in quantum theory, such as the quantum state. The usual method of determining a quantum state is performing a quantum tomography, which consists in making many projections of identically prepared systems in different basis and use these results to reconstruct their state [57]. This procedure demands a high computational power to reconstruct the states using all the information gathered in the projective measurements and, for systems of high dimensionality, this could make the process impossible to realise. The weak measurement protocol presents an alternative method of experimentally determining a quantum state.

In classical mechanics, one may determine the state of a system by measuring its position and momentum in a given instant. In quantum mechanics, the problem is not so simple, since standard measurements in position perturb subsequent measurements in momentum and vice versa, as stated in the Heisenberg uncertainty relation [1, 2]. In an interesting work, Lundeen *et al.* [7] proposed that if one implements the weak measurement protocol by weakly measuring the position and making a post-selection in momentum, one would be able to determine directly the wavefunction of the system. The measurement

is said to be 'direct' in the sense that its outcome, i.e., the weak value, in a given point x is proportional to the wavefunction $\psi(x)$ on that point, which is only possible due to the complex nature of the weak value. Also, one must note that the core idea of the new method is essentially different from the tomography: now one is able to perform local measurements and determine the wavefunction point by point based on their results.

Here we prove the relation between weak values and the wavefunction $\psi_i(x)$. The idea is to measure the weak value of the position operator $\hat{X} = |x\rangle\langle x|$. Assuming that the pre- and post-selected states are $|\psi_i\rangle$ and $|p\rangle$, respectively, and using the definition (1.35), we have

$$X_w = \frac{\langle p|x\rangle \langle x|\psi_i\rangle}{\langle p|\psi_i\rangle}. \tag{2.47}$$

Remembering that [1]

$$\langle p|x\rangle = \frac{e^{ipx/\hbar}}{\sqrt{2\pi\hbar}} \qquad \text{and} \qquad \langle p|\psi\rangle = \frac{\Phi(p)}{\sqrt{\hbar}}, \tag{2.48}$$

we obtain

$$X_w = \frac{e^{ipx/\hbar}}{\sqrt{2\pi}} \frac{\psi_i(x)}{\Phi(p)}. \tag{2.49}$$

Finally, making the post-selection in the state with $p = 0$, we prove

$$X_w = \frac{1}{\sqrt{2\pi}} \frac{\psi_i(x)}{\Phi(0)}. \tag{2.50}$$

From the above equation we note that $\psi_i(x)$ is directly proportional to the weak value X_w in each point. Using this relation, Lundeen *et al.* measured the photon spatial mode [7]. In fact, the method developed by them may be used to determine quantum pure states in general and has been used with success to directly measure the polarisation state of photons [27] and their orbital angular momentum states in 27 dimensions [28]. More recently, theoretical proposals were made in the sense of using joint weak values to extend the procedure presented here to directly measure general quantum states, pure or mixed [30, 58]. Last year, the first experimental realisation of these proposals was reported [29, 50].

2.2.3 The Hardy Paradox

The gedanken experiment proposed by Hardy is an example of how the use of retrodiction[4] could lead to paradoxes in quantum mechanics [59]. Its setup consists in two Mach-Zehnder interferometers arranged in such a way that their inner arms overlap each other, as shown in figure 2.2. These interferometers, when taken separately, are aligned

[4]Retrodiction is the act of inferring a past event based on a present information. In our context, retrodiction refers to the act of inferring the path of the particle inside the interferometer based on the position it was detected.

in a configuration that every detection occurs in the same port, namely, B. An electron is sent in one of them and a positron in the other. Therefore, if both of them travel by the inner arms of the interferometers, they will be annihilated in region Y. The state of both particles after passing the first beam splitters $\mathrm{BS1}^+$ and $\mathrm{BS1}^-$ is given by

$$|I\rangle = \frac{1}{2}(i\,|\mathrm{in}^+\rangle + |\mathrm{out}^+\rangle)(i\,|\mathrm{in}^-\rangle + |\mathrm{out}^-\rangle), \tag{2.51}$$

where $|\mathrm{in}\rangle$ and $|\mathrm{out}\rangle$ represent the states of the particles in the inner and outer arms of the interferometer respectively, while the "+" signal indicates the positron and the "−" the electron. After they pass the annihilation region Y, their state is

$$|I\rangle_{\mathrm{Y}} = \frac{1}{2}(-\,|\gamma\rangle + i\,|\mathrm{in}^+\rangle\,|\mathrm{out}^-\rangle + i\,|\mathrm{out}^+\rangle\,|\mathrm{in}^-\rangle + |\mathrm{out}^+\rangle\,|\mathrm{out}^-\rangle), \tag{2.52}$$

where we used $|\gamma\rangle = |\mathrm{in}^+\rangle\,|\mathrm{in}^-\rangle$ to represent the annihilation of the pair. Using the figure 2.2, we note that the action of $\mathrm{BS2}^+$ and $\mathrm{BS2}^-$ is

$$|\mathrm{in}^k\rangle \longrightarrow |b^k\rangle + i\,|d^k\rangle \tag{2.53}$$

and

$$|\mathrm{out}^k\rangle \longrightarrow i\,|b^k\rangle + |d^k\rangle\,, \tag{2.54}$$

for $k = \pm$, where $|b^k\rangle$ and $|d^k\rangle$ denotes the states detected in the ports B^k and D^k, respectively. Therefore, using the above relations and the state (2.52), we have that the state of the system after the particles go through $\mathrm{BS2}^+$ and $\mathrm{BS2}^-$ will be

$$|F\rangle = \frac{1}{4}(-2\,|\gamma\rangle - 3\,|b^+\rangle\,|b^-\rangle + i\,|b^+\rangle\,|d^-\rangle + i\,|d^+\rangle\,|b^-\rangle - |d^+\rangle\,|d^-\rangle). \tag{2.55}$$

From the above equation we perceive that, due to the interaction between the electron and the positron, now it is possible to any of them to reach the respective detector D. In fact, there is a probability for both of them reach the detectors D^+ and D^-, which is the case we will analyse more carefully. The question we would like to answer is, for these cases where we have both particles arriving at the detectors D, which was their path inside the interferometer?

- Since the electron reached the detector D^-, one concludes that the positron has travelled in the inner arm in^+ and interfered with the electron. Otherwise the electron would have arrived in detector B^-.
- Additionally, since the positron was also detected in D^+, we may use the same reasoning above to conclude that the electron was in the inner arm in^-.
- However, both positron and electron could not have been in the inner arm at the

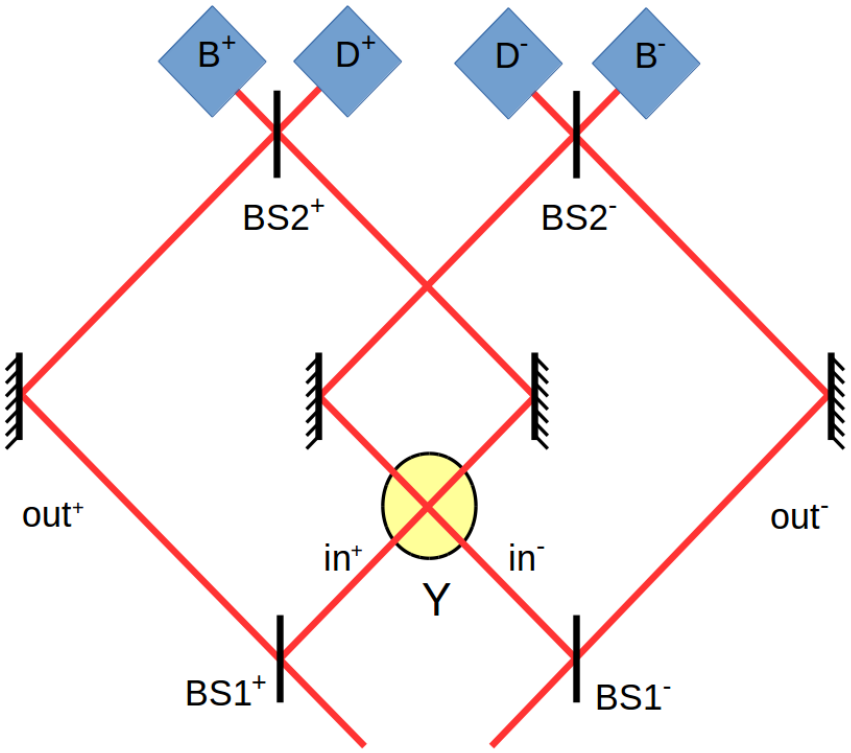

Figure 2.2: Setup of the gedanken experiment proposed by Hardy. One sends an electron in the right side of the double Mach-Zehnder interferometer and a positron in the left side. There is an overlap between their inner arms, in such a way that if both particles travels in these arms they will be annihilated in region Y. When took separately, each interferometer is aligned in such a way that the particles always exit in the bright ports, B^+ and B^-. The paradox arises when one tries to infer the path followed by the particles inside the interferometer when both particles arrive at dark ports, D^+ and D^-.

same time, since in this case they would have been annihilated. Hence, we have the paradox.

Usually, this paradox is dismissed with the argument that we are making conjectures about the electron and the positron positions without carrying out the respective measurements [49]. On the other hand, if one actually makes these measurements, one disturbs the system and this perturbation, caused by the interaction with the measuring system, is enough to explain a detection in the D ports. Then, the paradox only exists when we talk about an experiment that we have not done, which is not a situation that a physicist should worry about.

However, this scenario has changed with the weak measurement protocol. Now, we are able to perform a measurement in the system barely disturbing it: we can measure the weak values of the occupation numbers in each interferometer arm in a system which the final state is post-selected in $|d^-\rangle\,|d^+\rangle$, corresponding to the detection in the dark ports. Aharonov *et al.* [49] proposed the calculation of the single and joint weak values of the occupation numbers of the arms as a way to investigate the path the particles have taken

inside the interferometer. The pre-selected state in this case is given by equation (2.52) and the post-selected state is

$$\left|d^{+}\right\rangle \left|d^{-}\right\rangle = \frac{1}{2}(\left|\text{out}^{+}\right\rangle - \left|\text{in}^{+}\right\rangle)(\left|\text{out}^{-}\right\rangle - \left|\text{in}^{-}\right\rangle). \tag{2.56}$$

In its turn, the occupation number operator $\hat{N}$ in each arm is given by

$$\hat{N}_j^k = |j_k\rangle\langle j_k|\,, \tag{2.57}$$

where $k = \pm$ and $j = i, o$ indicate the particle and the arm of the interferometer, respectively. The joint operators are given by the products $\hat{N}_j^k \hat{N}_l^m$. Using the pre- and post-selected states given by equations (2.52) and (2.56) and the definitions of the occupation number (2.57) and the weak value (1.35), we are able to calculate the single weak values of interest, namely

$$\begin{aligned} &\text{a) } (N_o^+)_w = 0, && \text{b) } (N_o^-)_w = 0, \\ &\text{c) } (N_i^+)_w = 1, && \text{d) } (N_i^-)_w = 1. \end{aligned} \tag{2.58}$$

Using the definition of joint weak values in the left side of equation (2.30), we compute the following results for the joint observables

$$\begin{aligned} &\text{e) } (N_i^+ N_i^-)_w = 0, && \text{f) } (N_o^+ N_i^-)_w = 1, \\ &\text{g) } (N_i^+ N_o^-)_w = 1, && \text{h) } (N_o^+ N_o^-)_w = -1. \end{aligned} \tag{2.59}$$

These results were later experimentally confirmed by two independent research groups in photonic versions of Hardy's proposal [31, 32]. Nevertheless, there is not a consensus about their interpretation. Aharonov *et al.* advocate that these weak values solve the paradox in a strange, but consistent manner. Before presenting their interpretation of these results, we remember the result obtained in the beginning of section 1.4: when the state chosen to pre- or post-select the system is an eigenstate of the measured observable, the weak value will be equal to the respective eigenvalue. Note that most of the weak values calculated above are eigenvalues of the measured observables, therefore, according to the interpretation given by Aharonov *et al.*, the results c) and d) indicate that both positron and electron were in the inner arm of the interferometer. Nevertheless, they are not in the inner arm at the same time, since their joint weak value is zero, as read in result e). On the other hand, there is an electron in the inner arm and a positron in the outer arm, as stated in f), and vice versa, according to g)! Although, we had only a pair in the beginning of the experiment, how can it be two of them now? According to Aharonov *et al.* there is not, since there is -1 pair in the outer arms, as given in h)! In this sense, the solution of the paradox confirms all the statements made before: the electron is in

the inner arm of the interferometer, just like the positron. However, both of them are not there together, therefore they are not annihilated.

Many readers may feel uneasy with the interpretation given in the last paragraph. The interpretation of the weak value is a thorny issue and still generates intense debates [20, 33–36, 60]. An alternative interpretation is offered here, once one remembers that weak values are numbers registered by a measurement apparatus. In order to perform the weak measurement protocol, one needs to insert some device capable of interacting with the particles in the arms of the interferometer. This interaction has to be weak in order to not disturb the system and to not spoil the interference effect. In this case, we could think in some detector which is able to detect the charge of the particle, for instance, small positive test charges. Then, the electron will attract the test charge and the positron will repel it. When we measure a negative weak value it means that one of the test charges moved in the opposite direction from which it was expected to move by the interaction between it and the measured system. Researchers with this point of view believe that the weak value does not reveal an intrinsic characteristic of the system. Instead they argue that it characterises the interaction between measuring and measured systems. According to them, the weak values do not solve the Hardy paradox because there is no paradox at first place, since the single and joint weak values in equations (2.58) and (2.59) cannot be interpreted as indicators of the particle's presence in a given arm of the interferometer.

2.3 Interpretations of the Weak Value

Although the weak measurement protocol has proven to be a useful laboratory tool, the discussion about the meaning of the weak value has never ceased [8, 13, 23, 24]. Now we move on to briefly present two opposing interpretations of the weak value.

A Property of the System Between Two Measurements

The first point of view we present is the one shared by Aharonov and collaborators, who argue that the weak value is a real property of the quantum system during the intermediate time between the pre- and post-selection [25]. Although they admit that the effects predicted by them could be explained by the standard interpretation of quantum theory, they argue that these explanations are unnecessarily complicated [25, 33]. According to them, the strange predictions associated with the weak value are a hint that we should reinterpret quantum mechanics in a different, more suitable way. They propose an alternative formulation of the theory, called the two-state vector formalism, which, as the name suggests, uses two states to describe a quantum system: one that evolves from the past towards the future, and another one that evolves from the future towards the past [25, 33, 35]. Although this time symmetric formulation radically changes the way one

thinks about the time evolution of a quantum system, it makes the same predictions as other interpretations of quantum theory [33].

A Quantum Interference Effect

Many critics [34] of the Aharonov and collaborators ideas believe that the weak values are simply a result of quantum interference [13, 20, 36]. This argument is based on the comparison between the exact (1.42) and approximated (1.36) states of the measuring device after the weak measurement protocol is over. In these equations it is possible to note that the exact result is a superposition of Gaussians centred in different eigenvalues with complex magnitudes that, when one considers the limit of weak interaction, interfere destructively leaving as a result a unique Gaussian with its centre at the weak value. According to these authors, the weak value could not be viewed as a property of the system, which avoids the appearance of many paradoxes, such as the Hardy's [49] and the Cheshire cat[5] [61] paradoxes. Unlike Aharonov and collaborators, they argue that, once one can understand the protocol and its results using the standard interpretation of quantum mechanics, alternative reformulations of the theory are not necessary.

2.4 Weak Value as a Conditioned Average

In this section we discuss how the real part of the weak value may be related to a conditioned average of a given observable, as proposed in reference [62]. This notion will be useful in the discussions of the next chapter. In order to do so, we will use the example of the photon polarisation S, following the same lines of the idea presented in reference [22]. The scenario is similar to the one presented in section 1.4, with the setup shown in figure 1.4: we prepare an ensemble of photons in a known initial state, which goes through a birefringent crystal, responsible to create the correlation between polarisation and spatial degrees of freedom; a post-selection in a given polarisation state is performed and we detect their transverse positions with a camera. The initial state of the photons is given by

$$|\Psi_i\rangle = |i\rangle\,|\psi_i\rangle\,, \tag{2.60}$$

where $|i\rangle$ is the initial polarisation state and $|\psi_i\rangle$ is the initial spatial state given by

$$\langle x|\psi_i\rangle = (2\pi\sigma)^{-1/4}\exp\left(-\frac{x^2}{(2\sigma)^2}\right). \tag{2.61}$$

[5]The Cheshire Cat paradox is a proposal of Aharonov *et al.* [61] in which they argue that a particle and one of its properties could be found in different places. In the bibliography, the interested reader can find an experiment in which the authors claim to have demonstrated this effect [60] and an alternative explanation considering the effect as a result of quantum interference [36].

The evolution operator $\hat{U}(\epsilon)$ which describes the interaction of the photons with the birefringent crystal is

$$\hat{U}(\epsilon) = \exp(-i\epsilon\hat{S}\hat{k}), \tag{2.62}$$

where ϵ is the parameter that defines the strength of the interaction, $\hat{k}$ is the momentum operator of the measuring system and $\hat{S}$ is the polarisation operator given by equation (1.64). After this interaction, the probability $P_\epsilon(x, f)$ for the camera to register a photon in the position x with polarisation f is

$$P_\epsilon(x, f) = |\langle f|\langle x|\hat{U}(\epsilon)|i\rangle|\psi_i\rangle|^2, \tag{2.63}$$

as given in equation (2.34). Now imagine a scenario in which no post-selection is made. In this case, the probability $P_\epsilon(x)$ for the camera to register the arrival of a photon at the position x can be calculated by summing over all the complementary polarisations, namely,

$$P_\epsilon(x) = \sum_f |\langle f|\langle x|\hat{U}(\epsilon)|i\rangle|\psi_i\rangle|^2. \tag{2.64}$$

In the H-V basis, we have to sum over the states $|H\rangle$ and $|V\rangle$. Using this fact and equation (2.62), we have

$$P_\epsilon(x) = |\langle H|\langle x|\exp(-i\epsilon\hat{S}\hat{k})|i\rangle|\psi_i\rangle|^2 + |\langle V|\langle x|\exp(-i\epsilon\hat{S}\hat{k})|i\rangle|\psi_i\rangle|^2. \tag{2.65}$$

Writing the polarisation state $|i\rangle$ in the H-V basis, i.e.,

$$|i\rangle = \langle H|i\rangle|H\rangle + \langle V|i\rangle|V\rangle, \tag{2.66}$$

we can show that

$$P_\epsilon(x) = |\langle x|\exp(-i\epsilon\hat{k})|\psi_i\rangle|^2|\langle H|i\rangle|^2 + |\langle x|\exp(i\epsilon\hat{k})|\psi_i\rangle|^2|\langle i|V\rangle|^2. \tag{2.67}$$

Applying the generator of spatial translations, we finally arrive to

$$P_\epsilon(x) = \langle i|\left(|\langle x-\epsilon|\psi_i\rangle|^2|H\rangle\langle H| + |\langle x+\epsilon|\psi_i\rangle|^2|V\rangle\langle V|\right)|i\rangle. \tag{2.68}$$

From the above equation, we can define the probability operator $\hat{\Pi}_x$ as

$$\hat{\Pi}_x = |\langle x-\epsilon|\psi_i\rangle|^2|H\rangle\langle H| + |\langle x+\epsilon|\psi_i\rangle|^2|V\rangle\langle V|, \tag{2.69}$$

whose expectation value in a certain polarisation state $|i\rangle$ gives the probability of a photon to be detected in the position x of the camera.

Just for the sake of the argument, assume that we assign a value (x/ϵ) to each position

x of the camera.[6] In the following, we will prove that it is possible to measure the average polarisation $\langle \hat{S} \rangle$ using this parameterization. First, we calculate the weighted average of the factor (x/ϵ) over the area of the camera. Since the probability of detection in each point is given by $P_\epsilon(x)$, this average will be given by

$$\int \frac{x}{\epsilon} P_\epsilon(x) dx = \langle i | \left(\int \frac{x}{\epsilon} \hat{\Pi}_x dx \right) | i \rangle , \tag{2.70}$$

where we used equations (2.68) and (2.69). Using the definition of $\hat{\Pi}_x$, equation (2.69), and remembering that the initial spatial state of the photon is given by equation (2.61), we have

$$\begin{aligned} \int \frac{x}{\epsilon} \hat{\Pi}_x \, dx = \frac{1}{(2\pi)^{1/2}\sigma\epsilon} \Bigg[& \int dx \, x \exp\left(\frac{-(x-\epsilon)^2}{2\sigma^2} \right) |H\rangle\langle H| \\ & + \int dx \, x \exp\left(\frac{-(x+\epsilon)^2}{2\sigma^2} \right) |V\rangle\langle V| \Bigg]. \end{aligned} \tag{2.71}$$

Assuming that the camera sensor is much greater than the Gaussian dispersion σ, we have

$$\frac{1}{(2\pi)^{1/2}\sigma\epsilon} \int dx \, x \exp\left(\frac{-(x \pm \epsilon)^2}{2\sigma^2} \right) = \mp 1. \tag{2.72}$$

Thus, we arrive at the following identity between the probability operator $\hat{\Pi}_x$ and the polarisation operator $\hat{S}$

$$\int \frac{x}{\epsilon} \hat{\Pi}_x \, dx = \hat{S}. \tag{2.73}$$

Therefore, we may use $\hat{\Pi}_x$ to determine the expectation value of $\hat{S}$, i.e.,

$$\langle i | \left(\int \frac{x}{\epsilon} \hat{\Pi}_x \, dx \right) | i \rangle = \langle i | \, \hat{S} \, | i \rangle , \tag{2.74}$$

which, using the above equation and (2.70), can be written as

$$\langle i | \, \hat{S} \, | i \rangle = \int \frac{x}{\epsilon} P_\epsilon(x) dx. \tag{2.75}$$

Therefore, using the parameterization suggested (x/ϵ) and the probabilities of detection $P_\epsilon(x)$ — which could be measured — we are able to determinate the expectation value of polarisation. Addressing such values to the positions in the camera allows us to measure $\langle \hat{S} \rangle$ even when the interaction between the birefringent crystal and the photons is weak. The equation (2.73) is an important identity because it shows that this procedure is

[6] For a strong measurement, the components of polarisation after the calcite are well separated and detecting a photon in the positive or negative part of the x-axis is enough to identify its polarisation. For weaker measurements, the correlation is not strong enough to guarantee this condition. The factor (x/ϵ) takes this uncertainty existent in weaker measurements into account and, as we will see, is able to give the correct value for the average of polarisation. One may see it as a correction or calibration factor.

independent of the initial states $|i\rangle$. Also, the parametrization factor (x/ϵ) is not unique and can be conveniently chosen [22].

Now, we analyse a different situation in which post-selection is made before the photon is detected. What we would like to measure is the conditioned average of polarisation in this case. We have just proven that the expectation value of polarisation can be measured using the strategy that leads to equation (2.75). In order to measure the conditioned average of this observable, we use the same strategy, only changing the unconditioned probability of detection $P_\epsilon(x)$ by the conditioned probability of detection $P_\epsilon(x|f)$, to take into account the post-selection performed. This conditioned probability is defined as

$$P_\epsilon(x|f) = \frac{P_\epsilon(x,f)}{\int P_\epsilon(x,f)dx}\,. \tag{2.76}$$

Therefore, in this situation we will calculate a form of conditioned average of polarisation, which, similarly to (2.75), will be given by

$$\langle \hat{S} \rangle_{\text{cond}} = \int \frac{x}{\epsilon} P_\epsilon(x|f)dx. \tag{2.77}$$

Now, we proceed to prove that, in the limit of weak interaction between the birefringent crystal and the photons, the conditioned average of the polarisation given in equation (2.77) is approximately the real part of the weak value of S. Firstly, we remember the result obtained in equation (2.43) of section 2.1, namely

$$P_\epsilon(x,f) \simeq P(x)\,\{1 + 2\epsilon[\text{Re}(S_w)\text{Im}(k_w) + \text{Im}(S_w)\text{Re}(k_w)]\,\}, \tag{2.78}$$

where, in our case, the observable A is replaced by the polarisation S. By its turn, $P(x)$ is the probability of detection in the case where no crystal is placed between the state preparation and the post-selection and will be given by

$$P(x) = |\,\langle x|\psi_i\rangle\,|^2, \tag{2.79}$$

where we used equation (2.33). Note that we have already taken into account that the correlation between polarisation and spatial states is weak to derive equation (2.78). The weak value of momentum k_w is given by

$$k_w = \frac{\langle x|\,\hat{k}\,|\psi_i\rangle}{\langle x|\psi_i\rangle} = -\frac{i}{\psi_i(x)}\frac{d\psi_i(x)}{dx}\,. \tag{2.80}$$

Remembering that $\psi_i(x)$ is given by equation (2.61), we have

$$k_w = i\frac{x}{2\sigma^2}. \tag{2.81}$$

Using this result we may simplify equation (2.78) to

$$P_\epsilon(x,f) \simeq P(x)\left[1+\frac{\epsilon x}{\sigma^2}\mathrm{Re}(S_w)\right]. \tag{2.82}$$

Therefore, the integral in the denominator of equation (2.76), will be given by

$$\int P_\epsilon(x,f)dx \simeq \int dx\, P(x)\left[1+\frac{\epsilon x}{\sigma^2}\mathrm{Re}(S_w)\right]. \tag{2.83}$$

Using equation (2.79), we have

$$\int P_\epsilon(x,f)dx \simeq 1+\frac{\epsilon}{\sigma^2}\mathrm{Re}(S_w)\int dx\,|\psi_i(x)|^2 x. \tag{2.84}$$

Remembering that $\psi_i(x)$ is a Gaussian centred at zero, we note that the result of the integral in the left side of the above equation in zero. Therefore,

$$\int P_\epsilon(x,f)\,dx \simeq 1. \tag{2.85}$$

Thus, using this result with equation (2.76) and substituting them in (2.77), we have

$$\langle\hat{S}\rangle_{\mathrm{cond}} \simeq \int \frac{x}{\epsilon}P_\epsilon(x,f)\,dx. \tag{2.86}$$

Again, we will use equation (2.82) to solve this integral. Then,

$$\begin{aligned}\int \frac{x}{\epsilon}P_\epsilon(x,f)\,dx &\simeq \int \frac{x}{\epsilon}P(x)\left[1+\frac{\epsilon x}{\sigma^2}\mathrm{Re}(S_w)\right]dx \\ &= \int \frac{x}{\epsilon}\,|\psi_i(x)|^2\,dx + \mathrm{Re}(S_w)\int \frac{x^2}{\sigma^2}\,|\psi_i(x)|^2 dx.\end{aligned} \tag{2.87}$$

As mentioned before, the result of the first integral is zero and since

$$\int x^2|\psi_i(x)|^2\,dx = \sigma^2, \tag{2.88}$$

we have

$$\int \frac{x}{\epsilon}P_\epsilon(x,f)\,dx \simeq \mathrm{Re}(S_w). \tag{2.89}$$

Then, using this result in equation (2.86), we finally arrive to

$$\begin{aligned}\langle\hat{S}\rangle_{\mathrm{cond}} &= \int \frac{x}{\epsilon}P_\epsilon(x|f)dx \\ &\simeq \mathrm{Re}(S_w).\end{aligned} \tag{2.90}$$

From the above equation, we conclude that, in the limit where the interaction between

systems is weak, the conditioned average of polarisation can be described by the real part of its weak value in a well defined operational way. This result will be essential in chapter 3, when we will discuss a method to reconstruct the average trajectories of a post-selected ensemble of photons.

Chapter 3

Average Photons Trajectories In a Double-Slit Interferometer

The weak measurement protocol allowed one to extract information of a system barely changing its quantum state. Taking advantage of this powerful characteristic of weak values, Wiseman [4] proposed the utilisation of this protocol in order to reconstruct the average trajectory of an ensemble of quantum particles in 2007. Four years later, Kocsis *et al.* [5] used a modified version of Wiseman's original proposal in order to experimentally demonstrate this reconstruction process. Interpreting the real part of the weak value of the momentum as a conditioned average of this observable, they use this information to reconstruct the average trajectories of single photons inside a double-slit-like interferometer. Based on the method of Kocsis *et al.,* we made numeric simulations in order to investigate the average trajectories of photons in a double-slit interferometer.

We start this chapter discussing the procedure of trajectory reconstruction in section 3.1. In order to keep things simple, first we discuss how to reconstruct the trajectory of a particle in classical mechanics. Once the basic principles are established, we move on to discuss the quantum limit, where the trajectory of a single particle cannot be determined, as a consequence of the Heisenberg uncertainty relation. Nevertheless, we argue that, although we cannot determine the trajectory of a single particle, using the weak measurement protocol we are able to reconstruct the average trajectories of an ensemble of particles. In section 3.2 we present the methods we used and the results of our simulations. We reproduced the results of [5] and also tested some others initial states. In section 3.3 we describe both theoretical and experimental parts of the experiment performed by Kocsis *et al.* [5], also showing the results obtained by them. In section 3.4 we propose a possible extension of their experiment, considering a pair of photons in the interferometer instead of only one. Our main interest in this case is to evaluate the effects of the entanglement in the reconstructed average trajectories of photons.

3.1 Reconstructing Trajectories of Particles

The method developed by Kocsis *et al.* [5] consists in mapping the weak value of the momentum of single photons in an interferometer and, based on this mapping, to reconstruct the average trajectories followed by them. In this section we will discuss how the process of trajectory reconstruction of a particle works, firstly examining this problem in the context of classical mechanics, which is simpler and allows us to discuss the basic aspects of the procedure. Once this method is presented, we move on to discuss the difficulties that arise in the quantum mechanical case and how to circumvent them.

3.1.1 The Classical Case

Before tackling the problem of reconstructing trajectories in the context of quantum mechanics, we will discuss how this reconstruction process works in classical mechanics. In order to perform such a task, one must know how to answer two questions: "Where is the particle?" and "Where is the particle going?". The process is simple and straightforward: once one knows the actual location of a particle $\mathbf{x}_1$,[1] one can use the information about where it is heading for — its momentum $\mathbf{p}(\mathbf{x}_1)$ — to predict its location in the next instant, $\mathbf{x}_2$, provided that the time interval $t_2 - t_1$ is sufficiently small. If one knows the momentum of the particle at the point $\mathbf{x}_2$, it is possible to use the same strategy to predict its next position $\mathbf{x}_3$. This process can be iterated to reconstruct its whole trajectory, which in this case will be given by the set of points $\mathbf{x}_n$. Note that to reconstruct any trajectory all information required is:

1. A starting point $\mathbf{x}_1$.
2. A mapping of the momentum as a function of position, $\mathbf{p}(\mathbf{x}_n)$, in the region of interest.

We can summarise these ideas in the following equation[2]

$$\mathbf{x}_{n+1} = \mathbf{x}_n + \frac{1}{m}\mathbf{p}(\mathbf{x}_n)\Delta t, \qquad n \in \mathbb{N}, \tag{3.1}$$

where m is the particle's mass and $\Delta t = t_{n+1} - t_n$ is a sufficiently small time interval. Before finishing this section, we analyse a specific and useful case in which the motion of the particle is restricted to the x-z plane. We assume that its momentum in z-direction, p_z, is constant; hence the method described above simplifies to calculate the position in x-direction in N equally spaced and sufficiently close z planes, as shown in figure 3.1. In

[1] This is a short notation for $\mathbf{x}(t_1)$, i.e., the position of a particle at the instant t_1.

[2] Problems of this nature are commonly found in the studies of non-linear dynamics. In particular, chaotic systems are an interesting object of study, since the trajectories followed by particles in these systems are extremely dependent on their starting points [63].

this case, equation (3.1) simplifies to

$$\begin{aligned} x_{n+1} &= x_n + \frac{1}{m} p_x(x_n, z_n)\Delta t, \qquad n = 1, \dots, N, \\ z_{n+1} &= z_0 + n\Delta z, \end{aligned} \tag{3.2}$$

where

$$\Delta z = \frac{p_z}{m}\Delta t. \tag{3.3}$$

We can use the above relation to eliminate the explicit dependence with time in the equation for the position in x-direction, namely,

$$x_{n+1} = x_n + \frac{\Delta z}{p_z} p_x(x_n, z_n), \qquad n = 1, \dots, N. \tag{3.4}$$

Assuming that $p_z >> p_x$, we can make the approximation $p_z \simeq |p|$ in the last equation. Thus,

$$x_{n+1} = x_n + \frac{\Delta z}{|p|} p_x(x_n, z_n), \qquad n = 1, \dots, N. \tag{3.5}$$

This example will be particularly useful in the next sections.

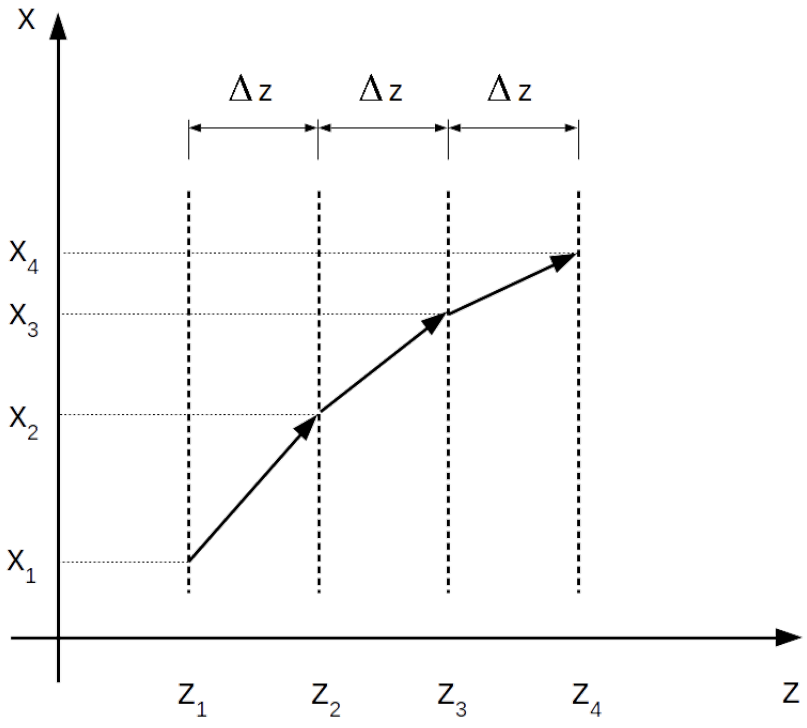

Figure 3.1: Example of how the procedure of trajectory reconstruction works in classical mechanics. In this case, we are showing a particle moving in the x-z plane with a constant momentum in z-direction, p_z.

3.1.2 The Quantum Case

In quantum mechanics, things are far more complicated. As a consequence of the Heisenberg uncertainty relation, a precise measurement of position will alter the momentum of the particle in an unpredictable way. In the same fashion, a precise measurement of momentum will also change the position of the system in an uncontrollable form. When we acquire precise information about one of these variables, we lose all the information previously gathered about the other. Therefore, the concept of trajectory of a single particle is lost in quantum mechanics, since we are not able to measure its position and momentum simultaneously.

Average Trajectories

Using the weak measurement protocol presented in chapter 1, it is possible to define in an operational way the average trajectory of a post-selected ensemble of quantum particles, as first suggested by Wiseman [4].[3] Kocsis *et al.* [5] implemented a modified version of Wiseman's proposal and we will apply their idea here. The experimental procedure to reconstruct the average trajectories of quantum particles could be divided in the following steps:

1. Prepare the measuring system and the spatial degree of freedom of the particles in a known state. The measuring system could be, for instance, another degree of freedom of the particles, such as their polarisation or spin.

2. Establish a weak interaction between the particle and the measuring device, which should be weak enough to gain some information about the momentum of the particle causing only a minimal disturbance in the system state.[4]

3. Make a post-selection of the particles in an eigenstate of position $|x_f\rangle$, which will allow us to map the weak value of momentum k_w as a function of the position x_f where the post-selection is performed.

4. Extract k_w from the measuring system.

Once we described the whole process, we need to highlight some of its important features. First of all, remember that to measure k_w one must repeat the experiment many times in an ensemble of identically prepared particles, thus it is only possible to reconstruct average trajectories. The essence of the idea is that we are making a low resolution

[3] Wiseman's proposal consisted in performing a weak measurement of position followed immediately by a strong measurement in a position x_f in order to determine the velocity of a quantum particle. Once this velocity is determined, one would be able to reconstruct the average trajectories for these particles.

[4] For instance, in the case of the double-slit interferometer that will be discussed later, the weak measurement should not disturb the interference pattern observed.

measurement of momentum in order to keep a good resolution in position, always working within the limits established by the Heisenberg uncertainty relation, namely,

$$\Delta P_x \Delta x \geqslant \frac{\hbar}{2}. \tag{3.6}$$

Another point worth stressing is that with this method we are not mapping the eigenvalues nor the expectation value of the momentum, but its weak value. Therefore, an important question to make is that if it is valid to use this quantity in order to reconstruct the average trajectories of the particles. As shown in section 2.4, in the limit of weak interactions, the real part of the weak value is a good approximation of the conditioned average of an observable. That is exactly the case here: the real part of the momentum weak value represents the conditioned average of the momentum of the particles, where we take into account only the ones that form the post-selected ensemble that arrived at the position x_f.[5] Therefore, once the mapping of the momentum weak value is done, we can use it to reconstruct the average trajectories of a post-selected ensemble of particles in a similar way to what was done in the classical case for a single particle. In our numerical simulations, we use the following definition to calculate the weak value

$$k_w = \frac{\langle x|\,\hat{k}\,|\psi\rangle}{\langle x|\psi\rangle}, \tag{3.7}$$

where $|\psi\rangle$ represents the initial spatial state of the system. In our case, our interest is to simulate the average trajectories of photons in a double-slit interferometer. Based on the conditions of the experiment performed by Kocsis *et al.* [5], we considered their propagation only in the x-z plane and that their momentum in z-direction, k_z, is much bigger than k_x, in such a way that $k_z \simeq k$. To reconstruct the average trajectories, we map the real part of the weak value of the transverse momentum, $\mathrm{Re}[(k_x)_w]$, in all the transverse positions of a given plane z. This process is repeated for N equally and closely spaced planes in the region where we would like to reconstruct the trajectories. Once this mapping is over, we use an adapted version of equation (3.5) to reconstruct the average trajectories of an ensemble of photons that arrived in a given transverse position x_f, namely,

$$x_{n+1} = x_n + \frac{\Delta z}{k}\mathrm{Re}[(k_x)_w]_n, \qquad n = 1, \ldots, N. \tag{3.8}$$

As the equation makes clear, by using the transverse position and momentum weak value in a plane z_n we can determine the position of the particle in the next plane z_{n+1}. Repeating this process until we reach the last z plane allows us to reconstruct the whole trajectory in the region of interest. In section 3.3 we will discuss the details of how to

[5] As Kocsis *et al.* [5] put it, "(...) These trajectories [reconstructed by this method] represent the average behaviour of the ensemble of photons when the weakly measured momentum in each plane is recorded contingent upon the final position at which a photon is observed."

measure this weak value in practice. For now, it is sufficient to know how to calculate it using (3.7).

3.2 Simulating the Reconstruction

In the first part of this section, we describe the methods employed in our simulations, also presenting a brief review about gaussian beams. In the second part, our results are presented and discussed. All the simulations were done using MATLAB.

3.2.1 Methods

In order to simulate the conditions of the experiment of Kocsis *et al.* [5], we considered that the spatial degree of freedom of the photons could be described by two Gaussians wave packets with origin in each slit. Before proceeding, we present a brief revision of Gaussian beams in the context of classical optics.

Gaussian Beams

The paraxial approximation is an important tool in classical optics used to analyse beams which have small divergence near to their propagation axis. For a monochromatic light beam which electric field is $E(\mathbf{x})$, the Helmholtz equation is[6]

$$\nabla^2 E(\mathbf{x}) - k^2 E(\mathbf{x}) = 0. \tag{3.9}$$

When we consider the paraxial approximation, the electric field should vary smoothly as a function of the propagation direction, which we assume here to be z. In this case, one may show that the Helmholtz equation simplifies to

$$\nabla_T^2 A(\mathbf{x}) - 2ik\frac{\partial A(\mathbf{x})}{\partial z} = 0, \tag{3.10}$$

where ∇_T^2 is the transverse Laplacian operator and we used

$$E(\mathbf{x}) = A(\mathbf{x})\exp(-ikz). \tag{3.11}$$

The Gaussian beam is a solution for equation (3.10) and is often used to describe laser beams [64]. Using the solution of equation (3.10) in equation (3.11), one may show that the propagation of a Gaussian beam is given by

$$E(\mathbf{x}) = A_P\frac{w_0}{w(z)}\exp\left(\frac{-\rho^2}{w^2(z)}\right)\exp\left[-i\left(kz + \frac{kz\rho^2}{2(z^2+z_R^2)} + \varphi(z)\right)\right]. \tag{3.12}$$

[6]The interested reader could find a comprehensive treatment of the paraxial approximation and Gaussian beams in chapters 2 and 3 of the reference [64].

In the equation above, $|A_P|$ is the peak amplitude, $\rho^2 = x^2 + y^2$, z_R is the Rayleigh length, φ is the Gouy phase and $w(z)$ is the waist of the beam, which behaviour is shown in figure 3.2, where we present the longitudinal profile of the beam in the x-z plane. As one may see, w_0 is the waist of the beam in its narrowest point. For a Gaussian beam, 86% of the beam power is concentrated within its waist. The waist radius $w(z)$ is given by

$$w(z) = w_0\sqrt{1 + \left(\frac{2z}{kw_0}\right)^2}, \tag{3.13}$$

while the Rayleigh length may be calculated using

$$z_R = \frac{kw_0}{2}, \tag{3.14}$$

and corrresponds to the distance along the direction of propagation between the point where the waist is minimum and the point where the intensity falls by 1/2. It is also shown in figure 3.2.

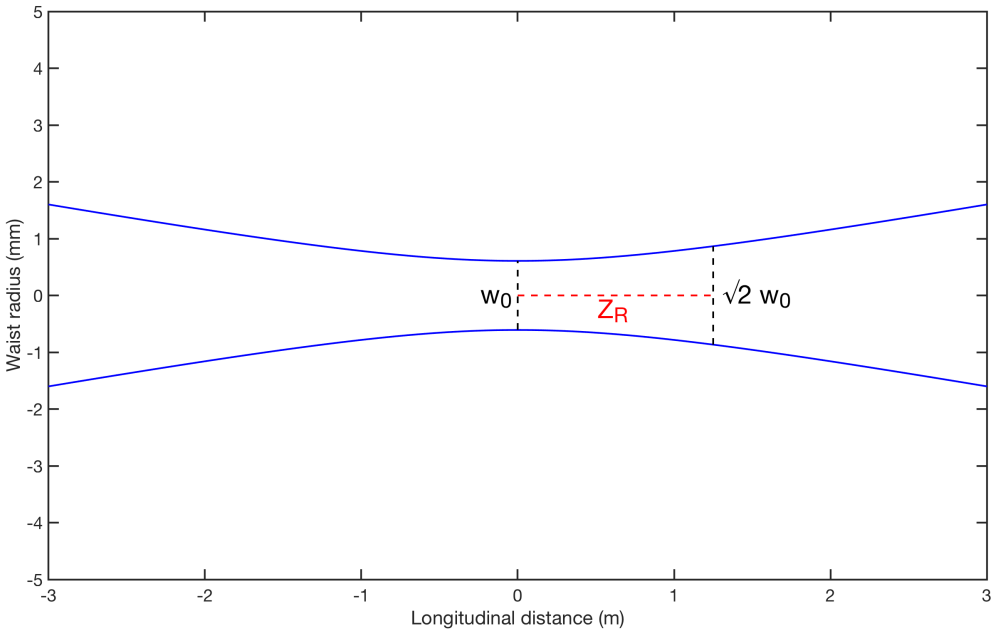

Figure 3.2: Profile of a Gaussian beam in the x-z plane. As shown, the waist radius w_0 is the radius of the beam in its narrowest point and the Rayleigh range z_R is the distance between this point and the point where the area of the beam is doubled.

Initial States

In our simulations, we considered that the spatial state of the photons would be Gaussian in order to reproduce the conditions of the Kocsis *et al.* [5] experiment. Therefore, using equation (3.12) and considering only the x-z plane, the spatial state of the photons

in each slit was given by

$$|i\rangle = \iint dxdz \frac{w_0}{w(z)} \exp\left(\frac{-x_i^2}{w^2(z)}\right) \exp\left[-i\left(kz + \frac{kzx_i^2}{2(z^2+z_R^2)} + \varphi(z)\right)\right] |x,z\rangle \quad (3.15)$$

where the index $i = 1, 2$ represents the slits and x_i is the transversal distance between the point x and the slit i,

$$x_1 = x + \frac{d}{2}, \quad x_2 = x - \frac{d}{2}, \quad (3.16)$$

where d is the distance between the slits. The parameters used in our simulations were $\lambda = 943$ nm, $d = 4.69$ mm and $w_0 = 0.608$ mm, reproducing the conditions of [5]. Our analysis was carried out considering four different initial states, namely,

$$\begin{aligned} |\psi_1\rangle &= \frac{1}{\sqrt{2}}(|1\rangle + |2\rangle), \\ |\psi_2\rangle &= \frac{1}{\sqrt{2}}(|1\rangle + i\,|2\rangle), \\ |\psi_3\rangle &= \frac{1}{\sqrt{2}}(|1\rangle - |2\rangle), \\ |\psi_4\rangle &= \sqrt{0.9}\,|1\rangle + \sqrt{0.1}\,|2\rangle\,, \end{aligned} \quad (3.17)$$

where $|\psi_1\rangle$ corresponds to the state used by Kocsis *et al.* [5] in their work. The phases added in states $|\psi_2\rangle$ and $|\psi_3\rangle$ related to $|\psi_1\rangle$ displaces the interference pattern and we would like to see how these changes would affect the average photon trajectories. By its turn, $|\psi_4\rangle$ forms an interference pattern with low visibility due to the difference of amplitudes between the states of each slit and we would like to analyse how we can visualise this effect using the trajectory reconstruction method.

Reconstructing Average Trajectories

In order to reconstruct the average trajectories of the photons in the double-slit interferometer, we follow the steps given below:

1. Using equation (3.7), calculate the weak value of the transverse momentum, $(k_x)_w$, in the whole region of interest.

2. Choose a starting plane $z = z_0$. All the trajectories will start from this plane.

3. Choose an initial transverse position $x = x_n$ on the plane z_0. In order to choose a starting point x_n, we used the following criteria:

   (a) No trajectory could start in a transverse point x_n whose intensity of the wavefunction, $|\psi_n(x_n, z_0)|^2$, in the starting plane $z = z_0$ was smaller than $0,1\%$ of the maximum value for the intensity on this plane.

(b) The distances between two adjacent starting points were inversely proportional to the intensities of the wavefunction on these points.

4. Use the real part of the weak value of transverse momentum in this position, $\mathrm{Re}[(k_x)_w(x_n, z_0)]$, to predict, using equation (3.8), the transverse position x_{n+1} of the photon in the next adjacent plane $z = z_1$.

5. In the plane z_1, repeat the previous step to determine the transverse position of the photon in plane $z = z_2$. Repeat this process until the photon reaches the last plane considered, $z = z_f$. The distance between two adjacent planes Δz is kept constant during the whole process.

6. Once this process in finished, choose another initial transverse position x_m (step 3) and repeat the entire process to reconstruct another trajectory.

3.2.2 Results

Now, we move on to present the results obtained in our numerical simulations. First of all, we present in figure 3.3 the real part of the weak value of transverse momentum, $\mathrm{Re}[(k_x)_w]$, divided by the photon wavenumber k, as a function of the transverse distance x in four selected z planes. From top to bottom, each row displays the results of the states given in equation (3.17) from $|\psi_1\rangle$ to $|\psi_4\rangle$. These planes were chosen to demonstrate how $\mathrm{Re}[(k_x)_w]$ evolves from the near-field to the far-field region. For states $|\psi_1\rangle$ and $|\psi_3\rangle$ we observe the appearance of anti-symmetric peaks. The distance between them increases as the propagation distance z increases. Although they also appear in the results for $|\psi_2\rangle$, they are not symmetric in this case. For $|\psi_3\rangle$ we also observe that the $\mathrm{Re}[(k_x)_w]$ diverges at $z = 0$. In the case of $|\psi_4\rangle$, we observe a pronounced peak for $x < 0$, with smaller peaks in other regions. In order to investigate the origin and meaning of these peaks, we analyse the intensity pattern of these states.

These patterns are shown in the left column of figure 3.4, where we plotted $|\psi_n(x)|$ instead of $|\psi_n(x)|^2$ to obtain a higher contrast between the regions of constructive and destructive interference. In the same figure, we depicted the real and imaginary parts of the transverse momentum weak value over the region of interest, represented in the centre and right column, respectively. We included the results for the imaginary part of $(k_x)_w$ only for completeness, since they are not required to reconstruct the average trajectories. Nevertheless, we believe it was a good opportunity to show the complex nature of the weak value.

Comparing the $|\psi_n(x)|$ pattern with the mapping of $\mathrm{Re}[(k_x)_w]$ we note that the regions where the weak value achieve its highest values — the peaks observed in figure 3.3 — coincide with the ones of destructive interference. On the other hand, in the places where constructive interference occurs, $\mathrm{Re}[(k_x)_w]$ is close to zero. Remembering that the real

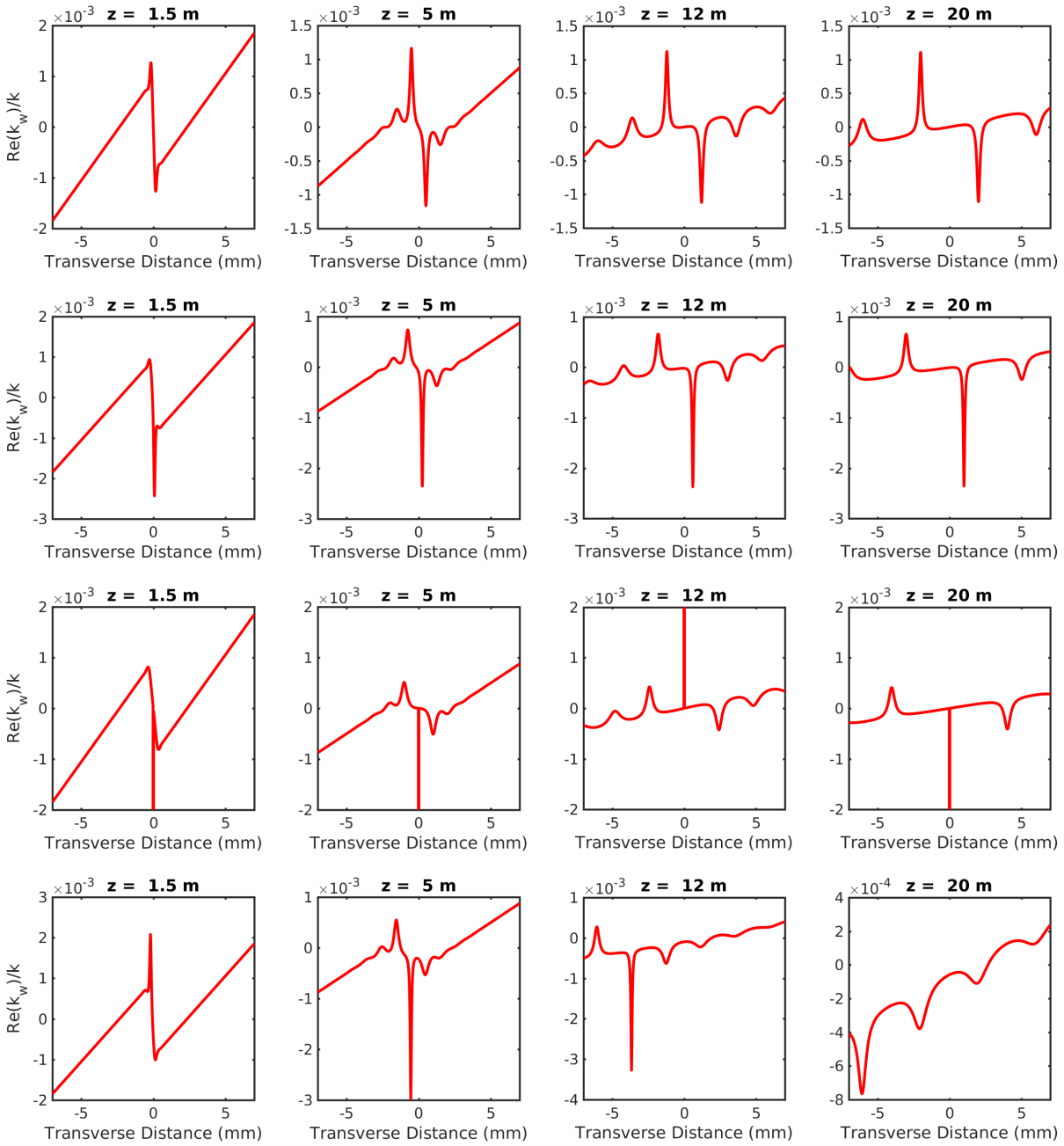

Figure 3.3: Real part of the weak value as a function of the transverse position x in four selected z planes. From top to bottom, results for states $|\psi_1\rangle$, $|\psi_2\rangle$, $|\psi_3\rangle$ and $|\psi_4\rangle$ are presented.

part of the weak value of the photon transverse momentum in a given position could be viewed as the conditioned average of this observable, we conclude that, in average, the ensemble of photons found in regions of destructive interference have a bigger transverse momentum then the ones found in regions of constructive interference. This is the behaviour one would expect: if the photons have a high transverse momentum in the regions of destructive interference, they will move transversely on to other locations while they propagate, leaving a dark spot in the former place. The same reasoning is valid for regions

where constructive interference occurs: there the transverse momentum is low, and, in average, the photons will remain in these transverse positions while they propagate along z direction, accumulating and, as a consequence, generating the bright spots we observe.

We also note the different scales for the cases of the $\mathrm{Re}[(k_x)_w]$ for the states $|\psi_3\rangle$ and $|\psi_4\rangle$. In the first case, we have to choose this scale due to the divergence of $\mathrm{Re}[(k_x)_w]$ when $x = 0$, which can be seen as a thin line precisely at this position. Without the scaling, it would be impossible to see the contrast we observe in the figure. For the case of $|\psi_4\rangle$ we also had a contrast problem, however the cause here was the low visibility of the interference pattern, due to the great difference between the amplitudes of $\langle x, z|1\rangle$ and $\langle x, z|2\rangle$.

From figures (3.5) to (3.8) we present our results for the average trajectories of a post-selected ensemble of single photons in the double-slit interferometer. We present the results for the four states of equation (3.17), with two figures for each state. In the top figure we always plot fewer trajectories in order to clearly show the behaviour of each displayed trajectory. In the bottom panel, we plot many more trajectories, usually the double, in order to observe how the intensity pattern of that state will look like. We plot trajectories from 0.5 m to 19.5 m, with a distance between adjacent planes of 0.05 m, for states $|\psi_1\rangle, |\psi_2\rangle$ and $|\psi_3\rangle$, and 0.025 mm for the state $|\psi_4\rangle$. For the three former states there are 65 trajectories in the top panel, while in the bottom panel we traced 130. For the latter, there are 46 and 93 trajectories in the top and bottom panels, respectively.

In figure 3.5, we present the average trajectories of the state $|\psi_1\rangle$. In both panels it is easy to note how the paths avoid certain regions, the ones where destructive interference occurs. On the other hand, the concentration of lines in the regions of constructive interference is also observed, with the region close to $x = 0$ being the local where this concentration is higher, as expected. The similarities between the graph in the bottom and the grey scale of $|\psi_n(x)|$ are a strong indicator of the success of the method. It is interesting to note that in this case none of the trajectories cross the symmetry line $x = 0$ and also that, for all the states presented, two trajectories never cross each other.

In figure 3.6 we present the average trajectories for the state $|\psi_2\rangle$. We observe that in this case the region with more concentration of lines were displaced a little bit into the negative side of x. Since our states are Gaussians, the $|\psi_2(x)|^2$ is not symmetric with relation to x, as we can see in the bottom panel of the figure. Note that in this case the paths coming from the slit 2 cross the $x = 0$ line.

The results presented in figure 3.7 corresponds to the state $|\psi_3\rangle$. In this case, we see that there is a small region around $x = 0$ where there are no trajectories. This can be seen as a consequence of the divergence of $\mathrm{Re}[(k_x)_w]$ in this transverse point. As in all previous cases, the figure with many traced average trajectories reproduces the observed $|\psi_n(x)|$ pattern.

The results of the last state $|\psi_4\rangle$ are displayed in figure 3.8. Since the criteria we

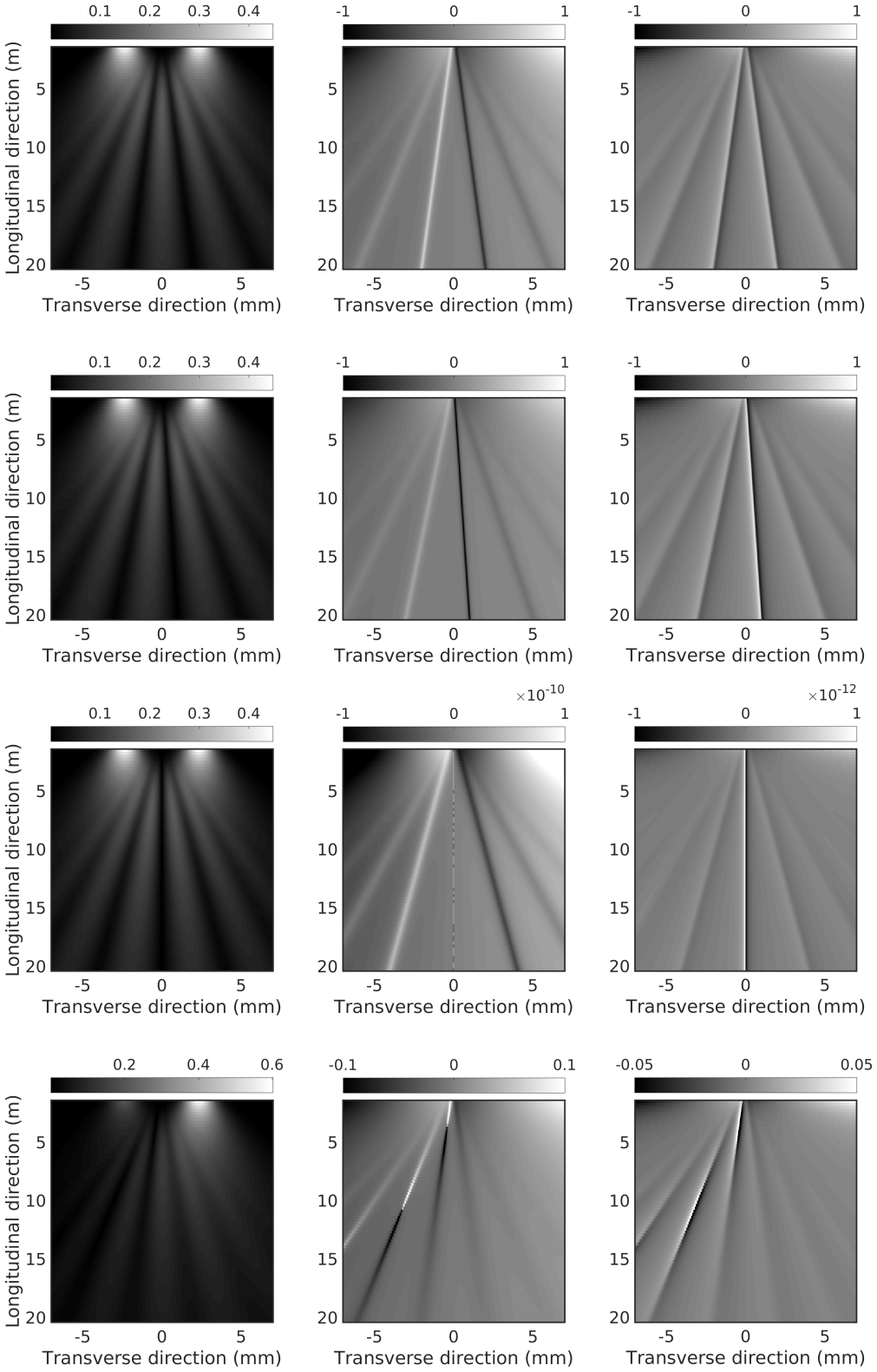

Figure 3.4: Grey scale of $|\psi|$ in the first column, $\mathrm{Re}[(k_x)_w]$ in the second column and $\mathrm{Im}[(k_x)_w]$ in the third column. From top to bottom, the results of states $|\psi_1\rangle$ to $|\psi_4\rangle$ are presented, just like in the previous figure.

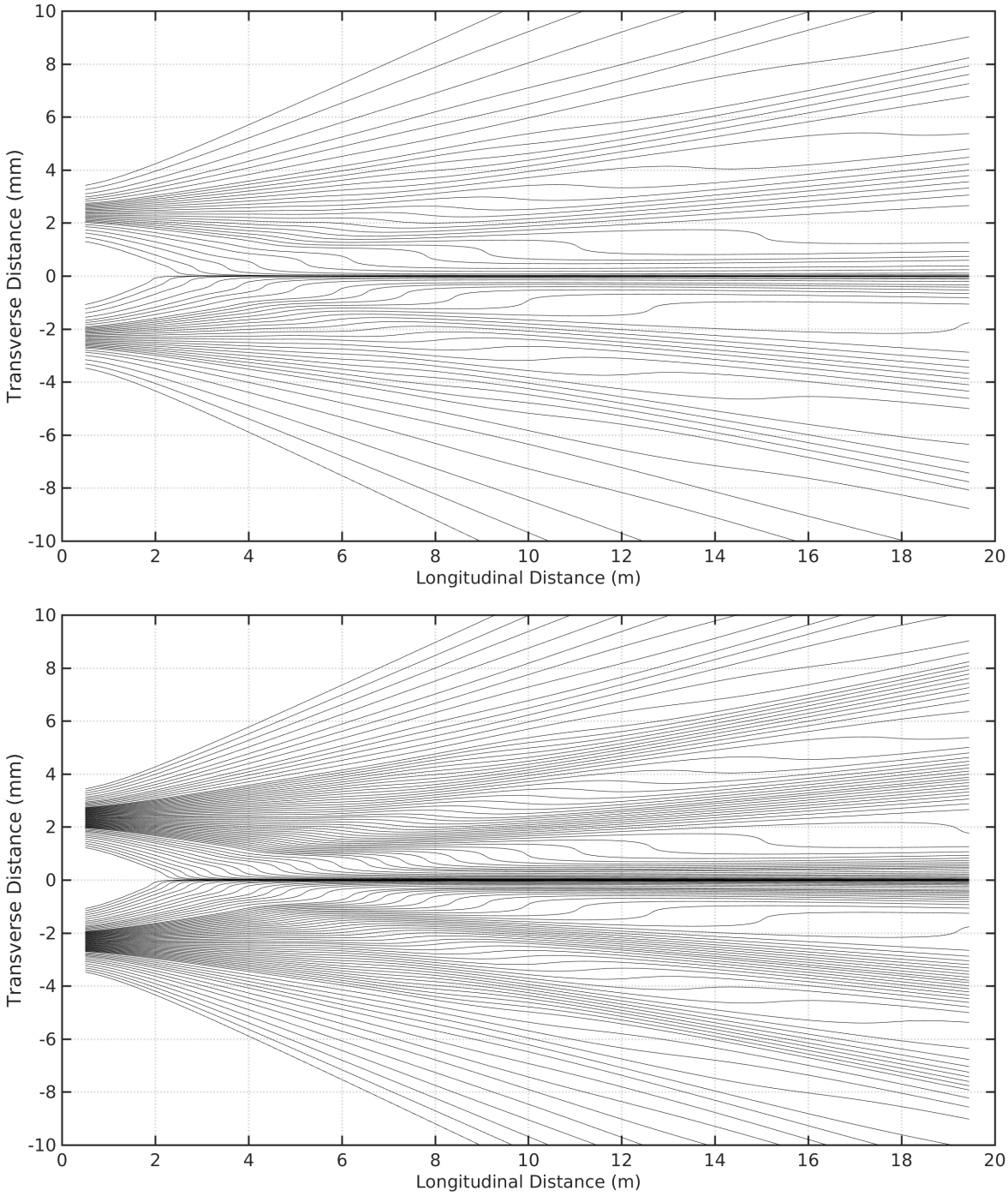

Figure 3.5: Reconstructed average trajectories of a post-selected sub-ensemble of photons for the state $|\psi_1\rangle$. Top panel. Reconstruction of a few trajectories. Bottom panel. Reconstruction of many trajectories, allowing us to see the interference pattern to form in the regions where the trajectories are concentrated.

adopted to choose the starting point was based on the intensity of the wavefunction $\psi_n(x)$ in the initial plane, in this case there is less paths coming out from the slit with lower amplitude.

Finally, from figures 3.9 and 3.12 we present a tri-dimensional graphs where the average trajectories are plotted over the probability density distribution $|\psi(x)|^2$ of the double-slit

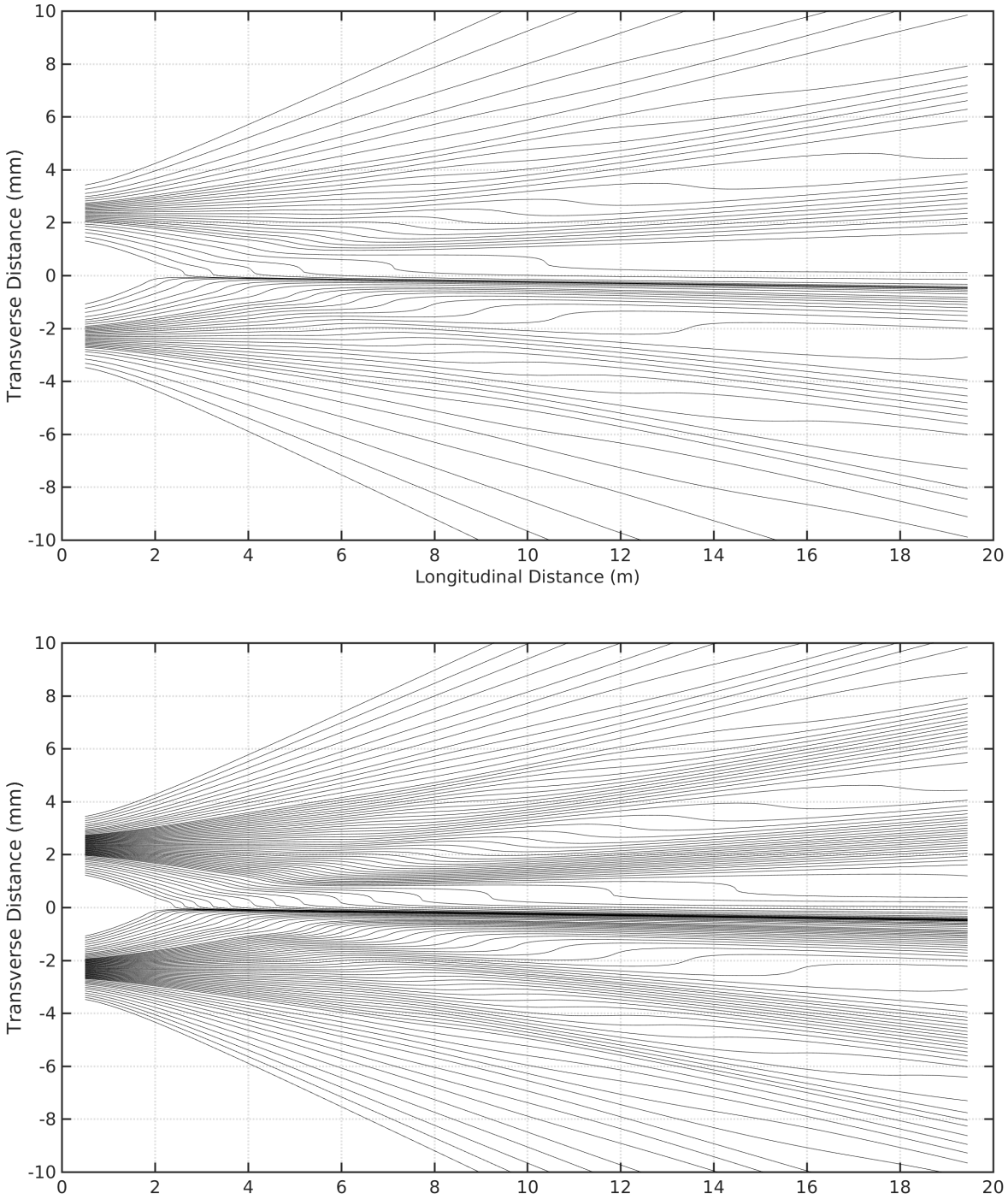

Figure 3.6: Reconstructed average trajectories of a post-selected sub-ensemble of photons for the state $|\psi_2\rangle$.

wavefunction. For states $|\psi_1\rangle$ to $|\psi_3\rangle$ these figures make clear the relationship existent between the density of average trajectories and the intensity of the wavefunction. For the state $|\psi_4\rangle$ this relationship is not that clear, may be due to an inadequate choice of starting points.

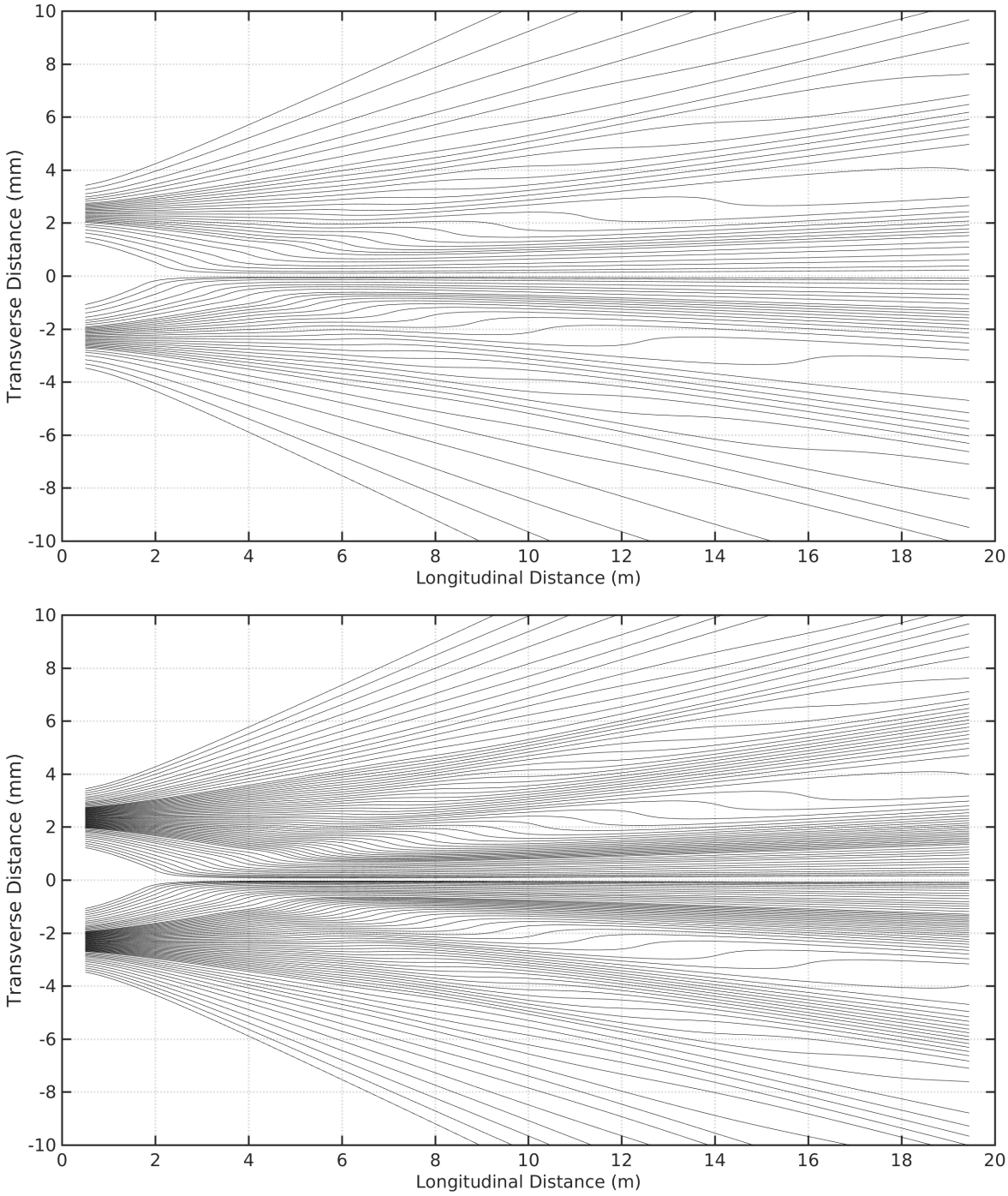

Figure 3.7: Reconstructed average trajectories of a post-selected sub-ensemble of photons for the state $|\psi_3\rangle$.

3.3 The Experiment of Kocsis *et al.*

In this section we present in details the experiment performed by Kocsis *et al.* [5] in which they measured the average trajectories of a post-selected ensemble of single photons in a double-slit-like interferometer.[7] To make the explanation more fluid, we divide it in

[7]Strictly speaking, the experiment does not use a double-slit. In fact, a 50:50 fibre beam splitter (BS) is used for splitting the photons, which are sent to the setup from two collimated fibre couplers acting as

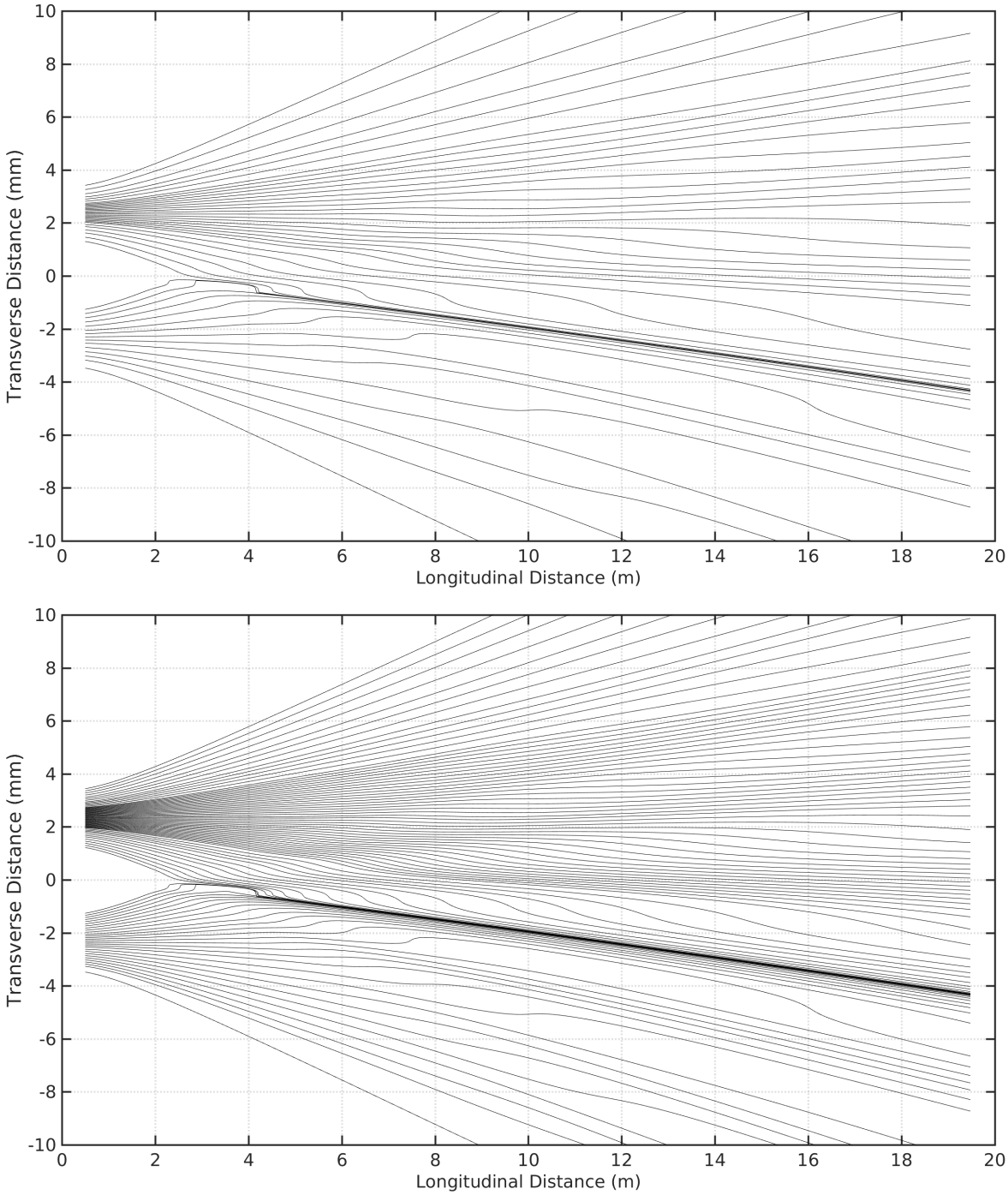

Figure 3.8: Reconstructed average trajectories of a post-selected sub-ensemble of photons for the state $|\psi_4\rangle$.

two parts: the theoretical analysis and the experiment description.

3.3.1 Theoretical Analysis

As explained in section 3.1, the core idea of reconstructing average trajectories of an ensemble of quantum particles is to use weak measurements of momentum followed by

the double-slit (see figure 3.13).

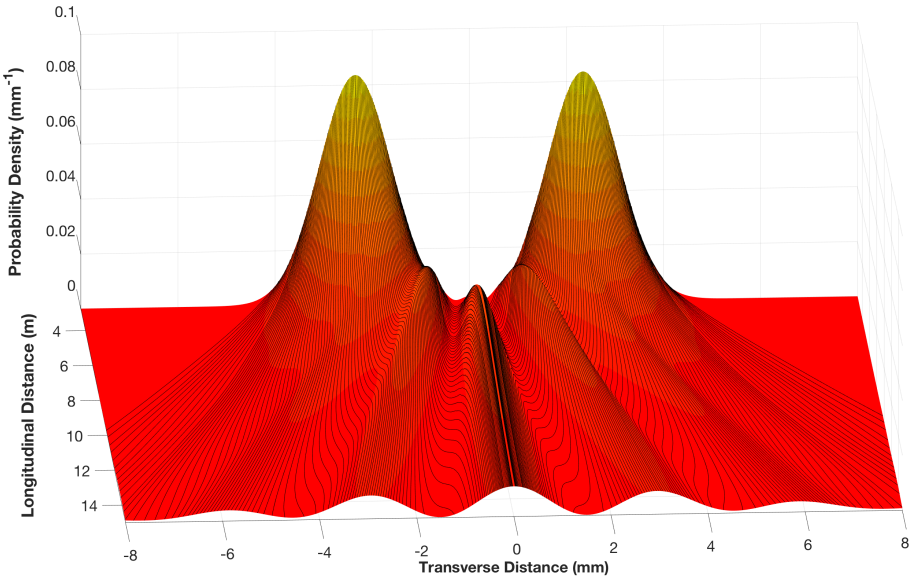

Figure 3.9: Average trajectories plotted over the probability density for the state $|\psi_1\rangle$.

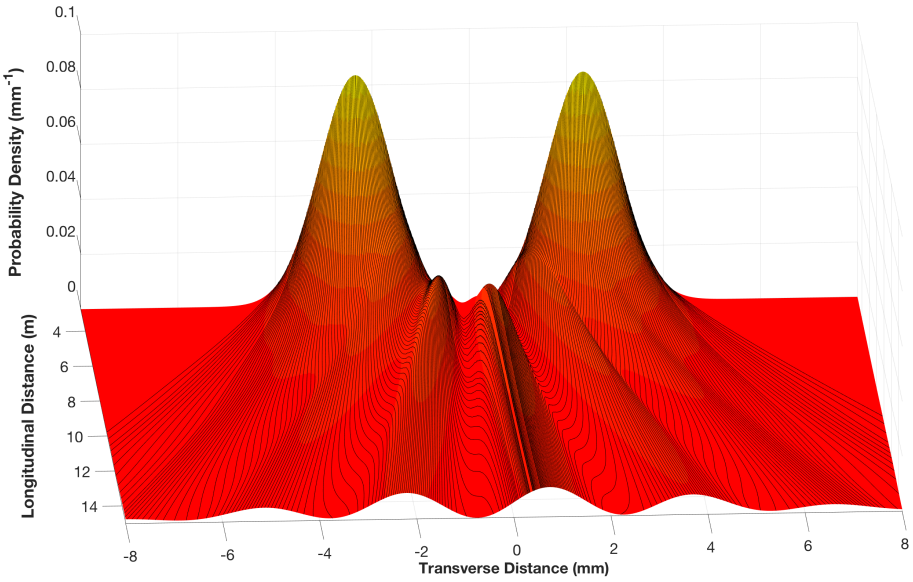

Figure 3.10: Average trajectories plotted over the probability density for the states $|\psi_2\rangle$

a post-selection in position in order to map the weak value of momentum as a function of position. Then, one can use this mapping to reconstruct the average trajectories. In the following analysis we consider that single photons are propagating in z-direction with constant k_z in the paraxial regime with their propagation restricted to plane x-z. As in the example in section 3.1, all we need here is the weak value of the transverse momentum, $(k_x)_w$. The initial state of the photons is

$$|\Psi_i\rangle = |D\rangle\,|\psi_i\rangle\,, \tag{3.18}$$

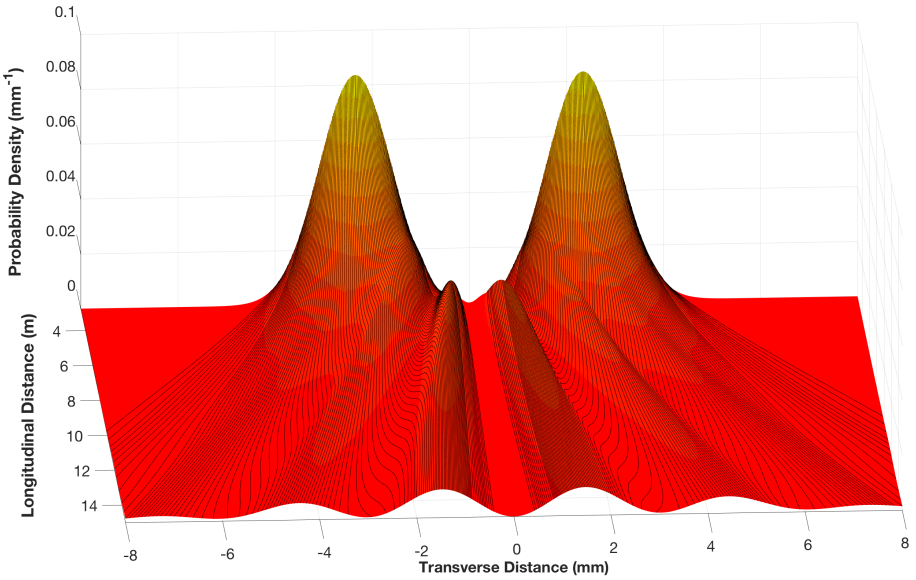

Figure 3.11: Average trajectories plotted over the probability density for the state $|\psi_3\rangle$.

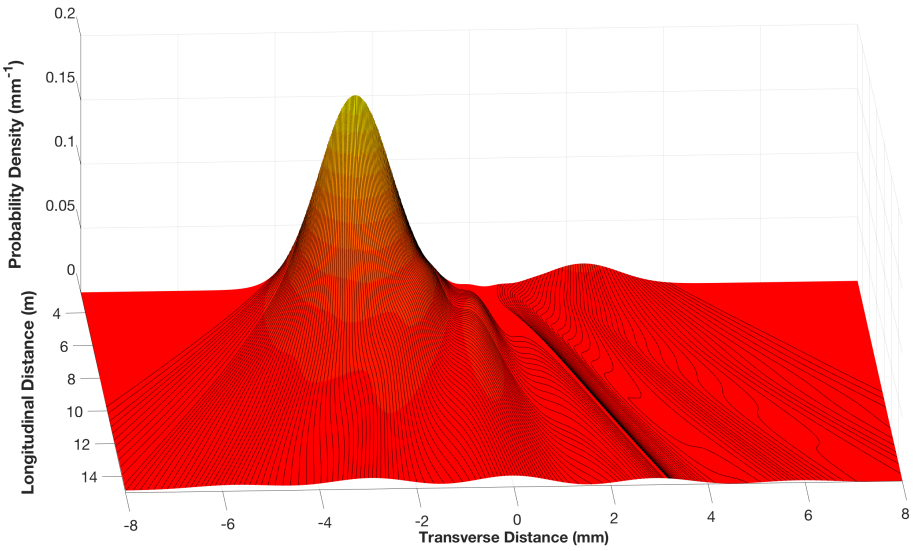

Figure 3.12: Average trajectories plotted over the probability density for the state $|\psi_4\rangle$.

where $|\psi_i\rangle$ represents the double-slit transverse spatial state [for instance, equation (3.17)] and $|D\rangle$ is the state of diagonal polarisation, written in the H-V basis as

$$|D\rangle = \frac{1}{\sqrt{2}}(|H\rangle + |V\rangle). \tag{3.19}$$

Our observable of interest here is the photon momentum in the x-direction k_x. In order to weakly measure $\hat{k}_x$, one must weakly couple it with a measuring system, which in this case will be the photon polarisation described by the operator[8]

[8] Another useful expression for this operator is $\hat{S}_1 = |D\rangle\langle A| + |A\rangle\langle D|$, where $|D\rangle$ and $|A\rangle$ are the diagonal and anti-diagonal states, respectively.

$$\hat{S}_1 = |H\rangle\langle H| - |V\rangle\langle V| \,. \tag{3.20}$$

In the experiment, a calcite is used to implement the coupling between $\hat{k}_x$ and $\hat{S}_1$, in the same fashion as in the example discussed in section 1.4. The difference is that here, instead of measuring the weak value of polarisation, one measures the weak value of momentum and uses the polarisation as the measuring system. The Hamiltonian which describes this interaction is given by

$$\hat{H}_I = g\hbar\hat{k}_x\hat{S}_1, \tag{3.21}$$

where g is the coupling parameter, which indicates the strength of the interaction. We assume that g is independent of time during the time of interaction between the systems. Using postulate 3 from section 1.1, we can use the Hamiltonian (3.21) in the evolution operator (1.2) to calculate the state of the system after this interaction, namely,

$$|\Psi\rangle = \hat{U}\,|\Psi_i\rangle = \exp(-igt\hat{k}_x\hat{S}_1)\,|\Psi_i\rangle \,. \tag{3.22}$$

Since the coupling between the polarisation and the spatial state of the photon is weak, we may approximate the operator $\hat{U}$ in first order by

$$\hat{U} = \exp(-igt\hat{k}_x\hat{S}_1) \simeq \hat{I} - igt\hat{k}_x\hat{S}_1. \tag{3.23}$$

Using this approximation for $\hat{U}$ and remembering that $|\Psi_i\rangle$ is given by equation (3.18), the global state of the system after the weak interaction takes place will be

$$|\Psi\rangle \simeq |D\rangle\,|\psi\rangle - igt\hat{k}_x\,|\psi\rangle\,|A\rangle \,, \tag{3.24}$$

where

$$|A\rangle = \frac{1}{\sqrt{2}}(|H\rangle - |V\rangle) \tag{3.25}$$

is the anti-diagonal polarisation state. Making a post-selection in a position eigenstate $|x_f\rangle$, i.e., considering only the sub-ensemble of photons that arrive at x_f in the detector, we have

$$\begin{aligned} |F\rangle \equiv \langle x_f|\Psi\rangle &\simeq \langle x_f|\psi\rangle \left(|D\rangle - igt\frac{\langle x_f|\,\hat{k}_x\,|\psi\rangle}{\langle x_f|\psi\rangle}\,|A\rangle \right) \\ &= \langle x_f|\psi\rangle \left(|D\rangle - igt(k_x)_w\,|A\rangle \right) \\ &= \frac{\langle x_f|\psi\rangle}{\sqrt{2}}\left[\left(1 - igt(k_x)_w\right)|H\rangle + \left(1 + igt(k_x)_w\right)|V\rangle \right], \end{aligned} \tag{3.26}$$

where we used the weak value definition (1.35) in the second step and rewrote the state in the H-V basis in the last step. Proceeding in the same fashion as in section 1.2, we

approximate the linear terms to an exponential, namely,

$$|F\rangle \simeq \frac{\langle x_f|\psi\rangle}{\sqrt{2}}\left[\exp\left(-igt(k_x)_w\right)|H\rangle + \exp\left(igt(k_x)_w\right)|V\rangle\right]. \tag{3.27}$$

This approximation is only valid because we are working in the weak interaction regime. From equation (3.27) we perceive that the effect of the weak measurement protocol over the polarisation state is to add a phase difference between its H and V components of

$$\phi = 2gt(k_x)_w. \tag{3.28}$$

In appendix A we show that it is possible to describe this phase difference as a function of ζ, a parameter which depends on the calcite characteristics and on the interaction between it and the photons, which can be measured in the laboratory. Thus,

$$\phi = \frac{\zeta}{k}(k_x)_w, \tag{3.29}$$

where k is the photon wave number. Equation (3.29) is important because it establishes a direct relation between $(k_x)_w$ and a measurable quantity, the phase difference ϕ between linear components of polarisation. Equation (3.27) can be rewritten using ζ as

$$|F\rangle \simeq \frac{\langle x_f|\psi\rangle}{\sqrt{2}}\left[\exp\left(\frac{-i\zeta}{2k}(k_x)_w\right)|H\rangle + \exp\left(\frac{i\zeta}{2k}(k_x)_w\right)|V\rangle\right]. \tag{3.30}$$

In order to measure ϕ, we make a strong measurement of the photon polarisation in the circular basis. The corresponding operator is given by

$$\hat{S}_3 = |R\rangle\langle R| - |L\rangle\langle L|, \tag{3.31}$$

where $|R\rangle$ and $|L\rangle$, representing the right and left-handed circularly polarised states, are written in the H-V basis as

$$|R\rangle = \frac{1}{\sqrt{2}}(|H\rangle + i|V\rangle), \tag{3.32}$$

$$|L\rangle = \frac{1}{\sqrt{2}}(|H\rangle - i|V\rangle). \tag{3.33}$$

Then, the expectation value $\langle\hat{S}_3(x_f)\rangle$ in the state $|F\rangle$, which describes the polarisation state after the post-selection in $|x_f\rangle$, will be

$$\langle\hat{S}_3(x_f)\rangle = |\langle R|F\rangle|^2 - |\langle L|F\rangle|^2. \tag{3.34}$$

This expectation value is calculated in appendix B, where we prove that

$$\langle \hat{S}_3(x_f) \rangle = \sin\left(\frac{\zeta}{k}\mathrm{Re}[(k_x)_w]\right). \tag{3.35}$$

Experimentally, $\langle \hat{S}_3(x_f) \rangle$ is obtained by

$$\langle \hat{S}_3(x_f) \rangle = \frac{I_R(x_f) - I_L(x_f)}{I_R(x_f) + I_L(x_f)}, \tag{3.36}$$

where $I_R(x_f)$ and $I_L(x_f)$ are the intensities measured in the right and left-handed circular basis at the point x_f, respectively. Thus, combining (3.35) and (3.36), we finally arrive to

$$\mathrm{Re}[(k_x)_w] = \frac{k}{2\zeta}\arcsin\left(\frac{I_R(x_f) - I_L(x_f)}{I_R(x_f) + I_L(x_f)}\right). \tag{3.37}$$

Therefore, in order to determine the real part of the weak value of the transverse momentum one needs to measure the intensities in both components of the circular polarisation basis for each transverse position x. In this way, we are able to map $\mathrm{Re}[(k_x)_w]$ for each position and, with these information, we can reconstruct the trajectories using the method discussed in section 3.1.

3.3.2 Experiment Description

State Preparation

In figure 3.13 we show the experimental setup used by Kocsis *et al.* in their work. The source of single photons was a liquid helium-cooled InGaAs quantum dot embedded in a GaAs/AlAs micropillar cavity. The continuous-wave laser used to pump the dot has a wavelength of 810 nm. By their turn, the emitted photons have a wavelength of 943 nm. These photons are coupled into a single-mode fibre which is followed by an in-fibre 50:50 beam splitter. The outputs of this fibre emerge as collimated Gaussian beams, with waist radius of (0.608 ± 0.006) mm. Then, they pass through a quarter-wave plate (QWP) and a half-wave plate (HWP), and are redirected by mirrored prisms to propagate in z-direction, with a peak-to-peak separation of (4.69 ± 0.02) mm, finally passing through a polariser, which prepares the photon with polarisation $|D\rangle$. The set of wave-plates together with the polariser are also responsible to prepare the amplitude and phase of the spatial state of the photon. Some examples of possible initial spatial states are given in equation (3.17), although in the experiment they only prepared the state $|\psi_1\rangle$.

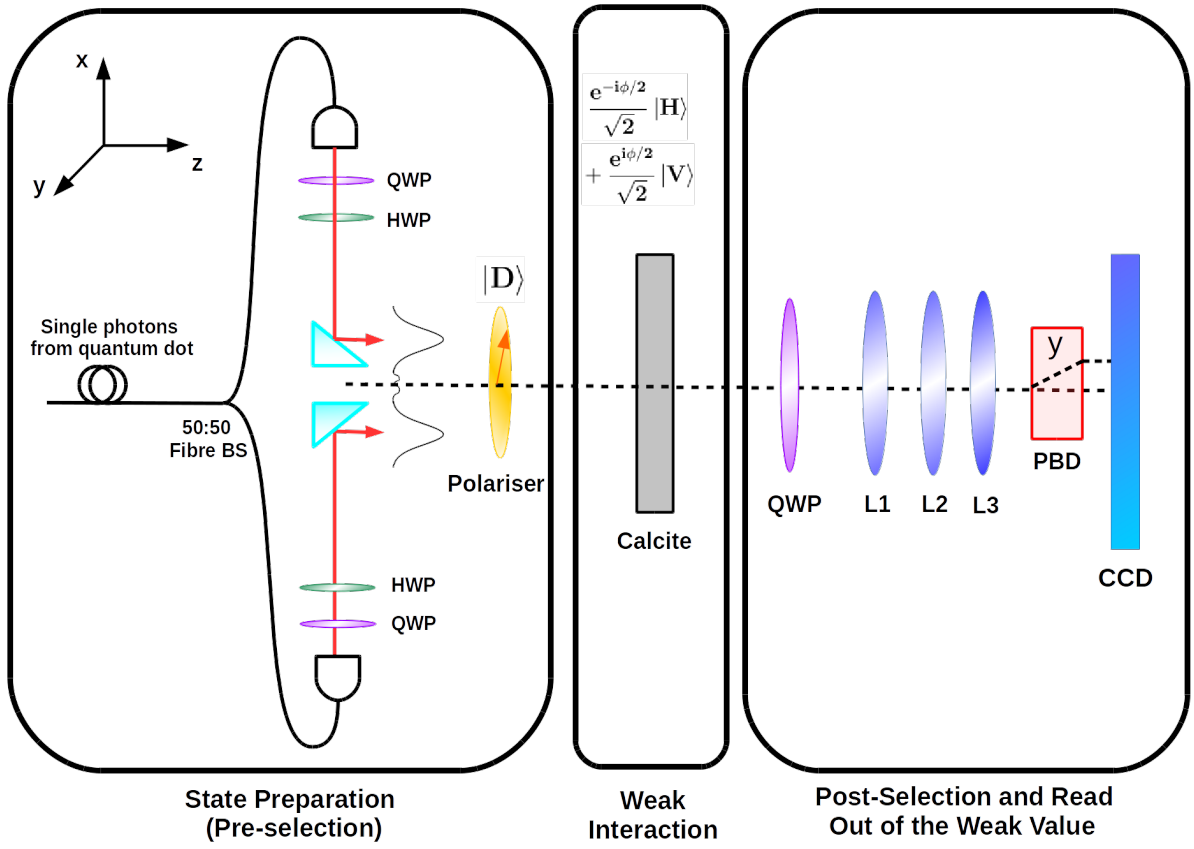

Figure 3.13: Experimental setup used by Kocsis *et al.* [5] to measure the average trajectories of a post-selected ensemble of photons in a double-slit-like interferometer.

Implementing the Weak Interaction

As the photons diffract out from the slits, they reach the calcite in different angles which are proportional to their transverse momenta k_x and k_y. The calcite is positioned with its optical axis aligned in the x-z plane, making an angle of 42° with the z-axis and has a thickness of 0.7 mm. These characteristics of the crystal are chosen to guarantee that the coupling between the spatial and polarisation states of the photon is weak. In this configuration, $|H\rangle$ is the extraordinary polarisation, which encounter a refraction index n_e dependent of the photon incident angle in x-direction, θ_x, while $|V\rangle$ is the ordinary polarisation, encountering a constant refraction index n_0. Since the incidence angle θ_x depends on the x-component of momentum k_x, the phase difference introduced by the birefringent crystal will depend on k_x. On the other hand, since the refraction index is constant for $|V\rangle$, the incidence angle in the y-direction θ_y will have no impact in the change of photon polarisation. This fact combined with the separability of components of the Gaussian allows one to ignore the y-direction in the present considerations. Therefore, the phase change induced by the birefringent crystal is proportional to k_x and one can use the former to measure the expectation value of the latter — or its weak value, as in

the present case. The photon polarisation state after it crosses the calcite is given by

$$\frac{1}{\sqrt{2}}\left(e^{i\phi_k/2}\,|H\rangle + e^{-i\phi_k/2}\,|V\rangle\right), \tag{3.38}$$

where ϕ_k is given by equation (3.28), as demonstrated in appendix A.

Post-Selection and Reading out of the weak value

A set of cylindrical lenses (L1, L2 and L3 in figure 3.13) is responsible to simulate the variation of the distance z travelled by the photons. They are placed after the calcite and images the double-slit function over different planes. This ordering of the experiment is possible because the free propagation Hamiltonian commutes with the interaction Hamiltonian and, as consequence, the moment in which the weak interaction takes place is unimportant to the final result. A QWP aligned to $-45°$ and a polarisation beam displacer (PBD) are used to project the polarisation in the circular basis, responsible to spatially separate the circularly polarised components of the beam in such a way that we are able to measure the intensities $I_R(x)$ and $I_L(x)$ separately. This beam displacer maintains the right-hand circularly polarisation undeviated, while the left-hand is deviated horizontally by 2 mm. In this way, one is able to measure both $I_R(x)$ and $I_L(x)$ in each transverse position x_f, which corresponds to make a post-selection in the state $|x_f\rangle$, allowing one to determine the real part of the weak value of momentum using equation (3.37). One should have in mind that, when the post-selection in an eigenstate of position is made, the photon is annihilated, therefore the post-selection must be the last stage in the experimental procedure. Once the $(k_x)_w$ is determined over the entire region of interest, it is possible to reconstruct the average trajectories. The photons are detected in a CCD camera with an exposure time of 15 s, which is sufficient to record the intensity pattern. About 31000 photons are detected within this time interval. The post-selection is done by the position the photons reached the CCD. The trajectories are reconstructed in the range of (2.75 ± 0.05) to (8.2 ± 0.1) m, showing the transition from the near to the far-field distribution.

Results of Kocsis *et al.*

The main results obtained by Kocsis *et al.* are presented in the figures 3.14 and 3.15. In the left panel of figure 3.14 it is shown two different graphs for four different selected planes: in the top, we have the measured intensities of the right and left-handed circular polarisations, $I_R(x)$ and $I_L(x)$, used to compute the real part of the weak value of the transverse momentum, $\mathrm{Re}[(k_x)_w]$, using equation (3.37). In the bottom, we have the calculated $\mathrm{Re}[(k_x)_w]/k$. These values were further used to reconstruct the trajectories presented in the right side of the aforementioned figure. By its turn, in figure 3.15 we have

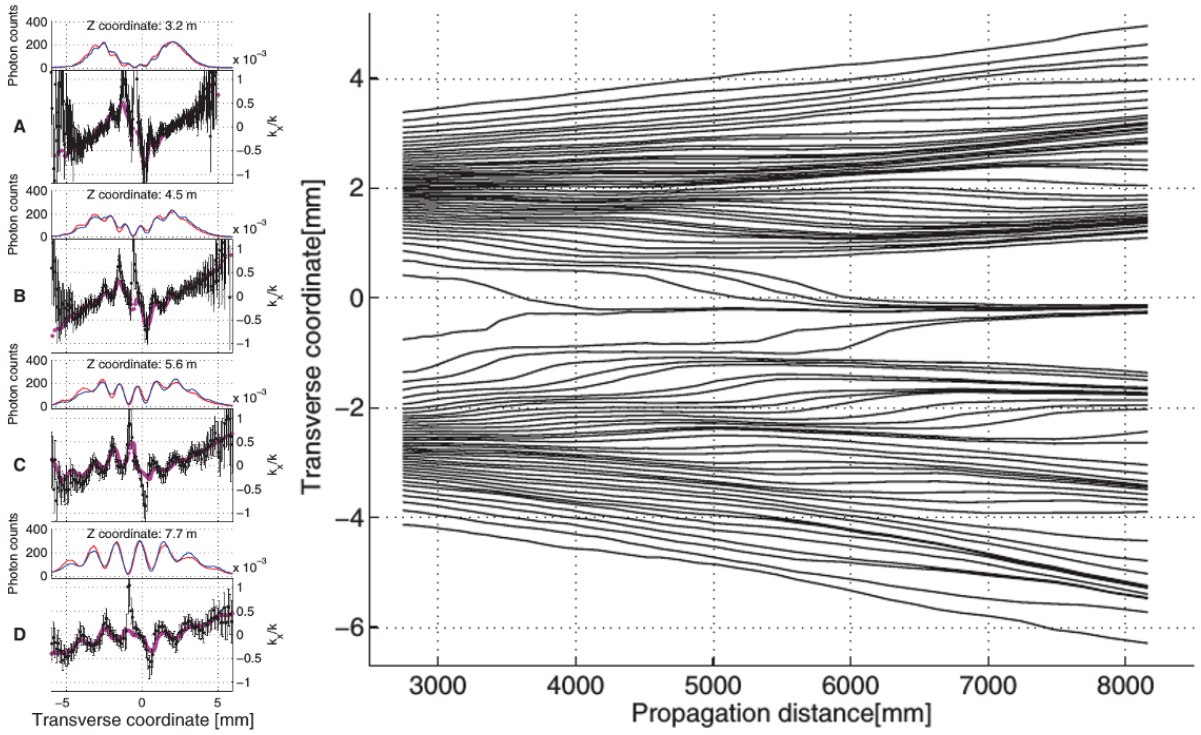

Figure 3.14: Left panel. Recorded intensities $I_R(x)$ and $I_L(x)$ (top) and calculated $\mathrm{Re}[(k_x)_w]$ (bottom) as functions of transverse position x for four selected z planes. Right panel. Reconstructed average trajectories of single photons using the information of momentum gathered for the slit state $|\psi_1\rangle$ of equation (3.17). *Figures extracted from the reference* [5].

the reconstructed average trajectories plotted over the surface of the measured probability density distribution $|\psi_1(x,z)|^2$. It is interesting to note how the trajectories accumulate over the high probability regions, also driving away from the low probability regions.

3.4 The Two Photons Scenario

Once we have presented our results and discussed the experiment of Kocsis *et al.* [5] for the case of reconstructing the average trajectories of single photons, we would like to propose a different situation where a pair of photons are sent in the interferometer. The act of adding one photon enables us to study many interesting phenomena which are impossible to study with single photons, such as two-particle interference [65]. The general state of the photon pair can be written as

$$|\Psi\rangle = c_1 |1_A, 1_B\rangle + c_2 e^{i\theta_1} |1_A, 2_B\rangle + c_3 e^{i\theta_2} |2_A, 1_B\rangle + c_4 e^{i\theta_3} |2_A, 2_B\rangle , \tag{3.39}$$

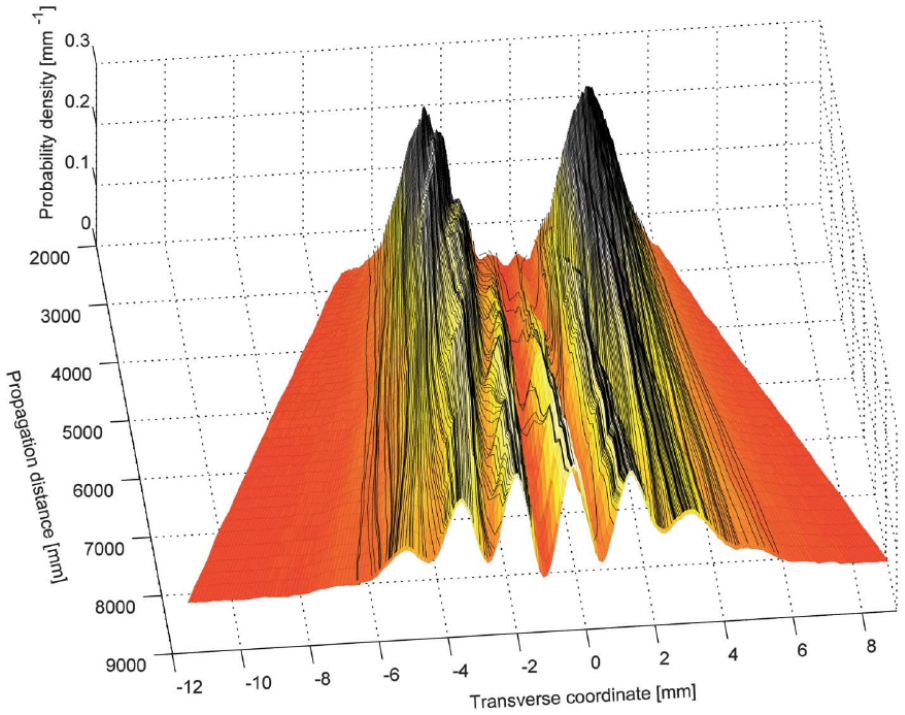

Figure 3.15: Reconstructed average trajectories of single photons plotted over the probability densities $|\psi_1(x,z)|^2$ of the photons. *Figure extracted from the reference* [5].

where c_n is the amplitude ($\sum_n c_n^2 = 1$) of the state and θ_n its the relative phase. A special case of interest occurs when the photons are entangled, for instance, in the Bell states

$$\begin{aligned} |\Phi^{\pm}\rangle &= \frac{1}{\sqrt{2}}(|1_A, 1_B\rangle \pm |2_A, 2_B\rangle), \\ |\Psi^{\pm}\rangle &= \frac{1}{\sqrt{2}}(|1_A, 2_B\rangle \pm |2_A, 1_B\rangle), \end{aligned} \tag{3.40}$$

which are examples of maximally entangled states. The states $|\Phi^{\pm}\rangle$ are correlated as the photons pass through the same slits, while the states $|\Psi^{\pm}\rangle$ are anti-correlated as the photons pass through opposed slits. These states were used to determine the de Broglie wavelength of a two-photon wave packet. The interference pattern observed in this case has doubled periodicity of what would be observed for each photon wave packet separately [66]. This has many applications, among them, in quantum litography [67].

Another interesting maximally entangled state is given by

$$|\eta\rangle = \frac{1}{2}(|1_A, 2_B\rangle + |2_A, 1_B\rangle + i\,|1_A, 1_B\rangle + i\,|2_A, 2_B\rangle), \tag{3.41}$$

which, unlike $|\Phi^{\pm}\rangle$ and $|\Psi^{\pm}\rangle$ in (3.40), does not present any which-path correlation. The entanglement of this state resides entirely in its phase [68]. We would like to trace the trajectories for all these states and compare them, since they all share the same amount of entanglement, although their which-path correlations are completely different.

The idea here is to perform a joint weak measurement in the photon pair in order to determine their trajectories in the double-slit interferometer. As explained in section 2.1 it is possible to perform these joint measurements by implementing single weak measurements in each constituent of the pair and comparing their correlations. However, in this case one needs to measure both the real and imaginary parts of the weak value for both particles. If we use the polarisation degree of freedom of the photons as the measuring system, we would need to measure it in two complementary basis, as explained in section 1.3. For instance, we could use the basis formed by the eigenstates of $\hat{S}_3$ and $\hat{S}_1$, in order to extract both the real and imaginary parts of the single weak value.

As one may see, these are only rough ideas about the problem we would like to address. However, we believe that it is an interesting case to study, despite the many issues left to investigate.

Chapter 4

Final Remarks and Perspectives

In this dissertation, we have presented a comprehensive introduction to the weak measurement protocol and the weak value. In addition, we used these ideas to analyse the problem of determining the average trajectories of a set of post-selected photons in a double-slit interferometer.

Introducing the discussion with the standard measurement process in quantum mechanics, we aimed to highlight the differences between this process and the weak measurement protocol. We derived the expression of the weak value, showing in which conditions it is valid. We also showed how one may measure both the real and imaginary parts of the weak value, with an appropriate measuring apparatus.

Once the basics ideas were laid, we moved on to show usefulness of the weak value. Acting as an amplifier which allows us to make high precision measurements or as a way of directing probing the wavefunction, we provide evidence that this new quantum variable is much more than a mere curiosity in quantum theory. We also shown that, using a generalisation named the weak value of n-th order, we could describe interactions of any strength between the measuring apparatus and the system under interest.

We briefly mentioned possible interpretations of the weak value, concentrating our efforts in establish a connection between the real part of a weak value and the conditioned average of an observable. This idea was crucial in order to analyse the process of reconstructing the average trajectories of photons in a double-slit interferometer. We based our simulations in the work of Kocsis *et al.* [5], tried to reproduce their results, and also analyse the experiment under different conditions. We succesfully reproduced the results of Kocsis *et al.* and tested some interesting new configurations.

As discussed in the last chapter, our proposal is to extend the analysis to the two-photon scenario and study the effects of the presence or absence of entanglement in the observed photon trajectories. We would like to study the similarities and differences in the cases where the entanglement resides in the modulus and in the phase of the two-photon state. We believe these results could help us to have a better understanding of the nature of two-photon state.

In addition, we would like to keep exploring weak measurements, more specifically, joint weak measurements. In order to test the difficulties of performing such measurements in the laboratory, we aim to analyse the case of measuring the joint polarisation of two particles. The usefulness of the technique to probe both pure and mixed quantum states [29, 50] compels us to have a better understand of its principles.

Appendix A

Phase Acquired during the Weak Interaction

In section 3.3, we showed that after the post-selection in a position x_f there is a phase difference ϕ between the H and V components of the photon polarisation given by equation (3.28). In this appendix, we try to rewrite the equation for ϕ in terms of parameters that can be measured in the laboratory. First of all, we note that this phase difference has its origin in the different refraction indexes perceived by the ordinary and extraordinary rays in a birefringent crystal. In these materials, the ordinary polarisation encounters a constant refraction index n_o, while the extraordinary polarisation encounters a variable index of refraction n_e which depends on the incident angle of the photon, θ [21]. Since we are working in the weak interaction regime, we expect that the phase difference ϕ induced by the crystal varies linearly with the angle θ, i.e.,

$$\phi = \zeta\theta + \phi_0, \tag{A.1}$$

where ζ is a proportionality constant and ϕ_0 is a constant phase difference which can be set to zero by an appropriate crystal alignment. Assuming that the photon propagation occurs only in the plane x-z, we know that the direction of the photons will be

$$\sin\theta = \frac{k_x}{k}, \tag{A.2}$$

where $k_x = p_x/\hbar$ and k is the photon wave-number. In this case, the photons are propagating in z-direction in the paraxial regime, therefore θ is small and we can approximate $\sin\theta \simeq \theta$. Therefore,

$$\theta \simeq \frac{k_x}{k}. \tag{A.3}$$

Substituting in equation (A.1) and remembering we are doing a weak measurement protocol, we have

$$\phi = \zeta \frac{(k_x)_w}{k}. \tag{A.4}$$

Comparing the above equation with the equation (3.28), we see that ζ is proportional to the factor gt, where g depends on the difference of the refraction index n_o and $n_e(\theta)$ and the time of interaction t, which is proportional to the calcite thickness d. Since ζ is proportional to characteristic quantities of the crystal, it can be determined in the laboratory, after one chooses the piece of calcite that will be used in the experiment.

Appendix B

Expectation Value of the Polarisation Operator $\hat{S}_3(x_f)$

In this appendix we will calculate the expectation value of $\hat{S}_3$ in the state $|F\rangle = \langle x_f|\Psi\rangle$, which describes the photon polarisation after a post-selection in the position x_f, i.e.,

$$\langle \hat{S}_3(x_f)\rangle = |\langle R|F\rangle|^2 - |\langle L|F\rangle|^2. \tag{B.1}$$

Firstly, using the decomposition of $|R\rangle$ in the H-V basis, equation (3.32), and the state $|F\rangle$ given in equation (3.30), we have

$$\begin{aligned}\langle R|F\rangle &= \frac{1}{2}\big(\langle H| - i\langle V|\big)\left[\exp\left(\frac{-i\zeta}{2k}(k_x)_w\right)|H\rangle + \exp\left(\frac{i\zeta}{2k}(k_x)_w\right)|V\rangle\right] \\ &= \frac{1}{2}\left[\exp\left(\frac{-i\zeta}{2k}(k_x)_w\right) - i\exp\left(\frac{i\zeta}{2k}(k_x)_w\right)\right].\end{aligned} \tag{B.2}$$

With this result, we are able to calculate

$$\begin{aligned}|\langle R|F\rangle|^2 = \frac{1}{4}\Bigg[&\exp\left(\frac{\zeta}{k}\mathrm{Im}[(k_x)_w]\right) + \exp\left(\frac{-\zeta}{k}\mathrm{Im}[(k_x)_w]\right) \\ &- i\exp\left(\frac{i\zeta}{k}\mathrm{Re}[(k_x)_w]\right) + i\exp\left(\frac{-i\zeta}{k}\mathrm{Re}[(k_x)_w]\right)\Bigg].\end{aligned} \tag{B.3}$$

We could use the same steps to calculate

$$\begin{aligned}|\langle L|F\rangle|^2 = \frac{1}{4}\Bigg[&\exp\left(\frac{\zeta}{k}\mathrm{Im}[(k_x)_w]\right) + \exp\left(\frac{-\zeta}{k}\mathrm{Im}[(k_x)_w]\right) \\ &- i\exp\left(\frac{-i\zeta}{k}\mathrm{Re}[(k_x)_w]\right) + i\exp\left(\frac{i\zeta}{k}\mathrm{Re}[(k_x)_w]\right)\Bigg].\end{aligned} \tag{B.4}$$

Using the two expressions above in the equation (B.1) we arrive at

$$\begin{aligned}\langle \hat{S}_3(x_f)\rangle &= \frac{1}{2}\left[i\exp\left(\frac{-i\zeta}{k}\mathrm{Re}[(k_x)_w]\right) - i\exp\left(\frac{i\zeta}{k}\mathrm{Re}[(k_x)_w]\right)\right] \\ &= \sin\left(\frac{\zeta}{k}\mathrm{Re}[(k_x)_w]\right),\end{aligned} \tag{B.5}$$

as we would like to prove.

Bibliography

[1] L. E. Ballentine. *Quantum Mechanics: A Modern Development.* *World Scientific Publishing* (2000).

[2] J. J. Sakurai and J. Napolitano. *Modern Quantum Mechanics.* *Addison-Wesley* (2011).

[3] Y. Aharonov, D. Z. Albert, A. Casher, and L. Vaidman. How the Result of a Measurement of a Component of the Spin of a Spin-1/2 Particle Can Turn Out to be 100. *Physical Review Letters* **60** 1351 (1988).

[4] H. M. Wiseman. Grounding Bohmian Mechanics in Weak Values and Bayesianism. *New Journal of Physics* **9** 165 (2007).

[5] S. Kocsis, B. Braverman, S. Ravets, M.J. Stevens, R. P. Mirin, L. K. Shalm, and A. M. Steinberg. Observing the Average Trajectories of Single Photons in a Two-Slit Interferometer. *Science* **332** 1170 (2011).

[6] O. Hosten and P. Kwiat. Observation of the Spin Hall Effect of Light via Weak Measurements. *Science* **319** 787 (2008).

[7] J. S. Lundeen, B. Sutherland, A. Patel, C. Stewart, and C. Bamber. Direct Measurement of the Quantum Wavefunction. *Nature* **474** 188 (2011).

[8] Y. Aharonov and L. Vaidman. Aharonov and Vaidman Reply. *Physical Review Letters* **62** 2327 (1989).

[9] M. Nielsen and I. Chuang. *Quantum Computation and Quantum Information.* *Cambridge University Press* (2000).

[10] M. A. Solís-Prosser. *Estudio de la Medición de Qubits y Qudits Espaciales Codificados en Fotones Individuales y Aplicaciones.* Master Dissertation, Universidad de Concepción, (2011).

[11] R. L. Jaffe. *Supplementary Notes on Dirac Notation, Quantum States, etc.* 2007.

[12] J. B. Marion. *Classical Dynamics of Particles and Systems.* *Elsevier Science* (2013).

[13] I. M. Duck, P. M. Stevenson, and E. C. G. Sudarshan. The Sense in which a "Weak Measurement" of a Spin-1/2 Particle's Spin Component Yields a Value 100. *Physical Review D* **40** 2112 (1989).

[14] J. von Neumann. *Mathematical Foundations of Quantum Mechanics.* *Princeton University Press* (1955).

[15] Y. Aharonov, D. Z. Albert, A. Casher, and L. Vaidman. Surprising Quantum Effects. *Physics Letters A* **124** 199 (1987).

[16] J. S. Lundeen and K. J. Resch. Practical Measurement of Joint Weak Values and Their Connection to the Annihilation Operator. *Physics Letters A* **334** 337 (2005).

[17] N. W. M. Ritchie, J. G. Story, and R. G. Hulet. Realization of a Measurement of a "Weak Value". *Physical Review Letters* **66** 1107 (1991).

[18] A. D. Parks, D. W. Cullin, and D. C. Stoudt. Observation and Measurement of an Optical Aharonov–Albert–Vaidman Effect. *Proceedings of the Royal Society of London A: Mathematical, Physical and Engineering Sciences* **454** 2997 (1998).

[19] J. M. Knight and L. Vaidman. Weak Measurement of Photon Polarization. *Physics Letters A* **143** 357 (1990).

[20] R. C. Silva. *O Gato de Cheshire Quântico como um Fenômeno de Interferência.* Master's Thesis, UFMG (2015).

[21] E. Hecht. *Optics.* *Addison-Wesley* (2002).

[22] J. Dressel, M. Malik, F. M. Miatto, A. N. Jordan, and R. W. Boyd. Colloquium: Understanding Quantum Weak Values: Basics and Applications. *Reviews of Modern Optics* **86** 307 (2014).

[23] A. J. Leggett. Comment on "How the Result of a Measurement of a Component of the Spin of a Spin-*1/2* Particle Can Turn Out to be 100". *Physical Review Letters* **62** 2325 (1989).

[24] A. Peres. Quantum Measurements with Postselection. *Physical Review Letters* **62** 2326 (1989).

[25] Y. Aharonov and L. Vaidman. Properties of a Quantum System During the Time Interval Between Two Measurements. *Physical Review A* **41** 11 (1990).

[26] P. B. Dixon, D. J. Starling, A. N. Jordan, and J. C. Howell. Ultrasensitive Beam Deflection Measurement via Interferometric Weak Value Amplification. *Physical Review Letters* **102** 173601 (2009).

[27] J. Z. Salvail, M. Agnew, A. S. Johnson, E. Bolduc, J. Leach, and R. W. Boyd. Full Characterization of Polarization States of Light via Direct Measurement. *Nature Photonics* **7** 316 (2013).

[28] M. Malik, M. Mirhosseini, M. P. J. Lavery, J. Leach, M. J. Padgett, and R. W. Boyd. Direct Measurement of a 27-Dimensional Orbital-Angular-Momentum State Vector. *Nature Communications* **5** 3115 (2014).

[29] G. S. Thekkadath, L. Giner, Y. Chalich, M. J. Horton, J. Banker, and J. S. Lundeen. Direct Measurement of the Density Matrix of a Quantum System. *Physical Review Letters* **117** 120401 (2016).

[30] J. S. Lundeen. and C. Bamber. Procedure for Direct Measurement of General Quantum States Using Weak Measurement. *Physical Review Letters* **108** 070402 (2012).

[31] J. S. Lundeen and A. M. Steinberg. Experimental Joint Weak Measurement on a Photon Pair as a Probe of Hardy's Paradox. *Physical Review Letters* **102** 020404 (2009).

[32] K. Yokota and T. Yamamoto and M. Koashi and N. Imoto. Direct Observation of Hardy's Paradox by Joint Weak Measurement with an Entangled Photon Pair. *New Journal of Physics* **11** 033011 (2009).

[33] Y. Aharonov, S. Popescu, and J. Tollaksen. A Time-Symmetric Formulation of Quantum Mechanics. *Physics Today* **63** 27 (2010).

[34] N. D. Mermin. Consistent Treatments of Quantum Mechanics. *Physics Today* **64** 8 (2011).

[35] Y. Aharonov, E. Cohen, A. C. Elitzur. Foundations and Applications of Weak Quantum Measurements. *Physical Review A* **89** 052105 (2014).

[36] R. Corrêa, M. F. Santos, C. H. Monken, and P. L. Saldanha. 'Quantum Cheshire Cat' as Simple Quantum Interference. *New Journal of Physics* **17** 053042 (2015).

[37] C. H. Bennett, G. Brassard, C. Crépeau, R. Jozsa, A. Peres, and W. K. Wootters. Teleporting an Unknown Quantum State via Dual Classical and Einstein-Podolsky-Rosen Channels. *Physical Review Letters* **70** 1895 (1993).

[38] D. Bouwmeester, J. Pan, K. Mattle, M. Eibl, H. Weinfurter, and A. Zeilinger. Experimental Quantum Teleportation. *Nature* **390** 575 (1997).

[39] M. Żukowski, A. Zeilinger, M. A. Horne, and A. K. Ekert. "Event-ready-detectors" Bell experiment via Entanglement Swapping. *Physical Review Letters* **71** 4287 (1993).

[40] C. H. Bennett and S. J. Wiesner. Communication via One- and Two-Particle Operators on Einstein-Podolsky-Rosen States. *Physical Review Letters* **69** 2881 (1992).

[41] J. F. Clauser, M. A. Horne, A. Shimony, and R. A. Holt. Proposed Experiment to Test Local Hidden-Variable Theories. *Physical Review Letters* **23** 880 (1969).

[42] J. C. Howell, R. S. Bennink, S. J. Bentley, and R. W. Boyd. Realization of the Einstein-Podolsky-Rosen Paradox Using Momentum- and Position-Entangled Photons from Spontaneous Parametric Down Conversion. *Physical Review Letters* **92** 210403 (2004).

[43] D. Dehlinger and M. W. Mitchell. Entangled Photons, Nonlocality, and Bell Inequalities in the Undergraduate Laboratory. *American Journal of Physics* **70** 903 (2002).

[44] L. T. Neves. *Estados Emaranhados de Qubits e Qudits Criados com Pares de Fótons Produzidos na Conversão Paramétrica Descendente.* PhD Thesis, Departamento de Física, UFMG, (2006).

[45] L. Neves, G. Lima, E. J. S. Fonseca, L. Davidovich, and S. Pádua. Characterizing Entanglement in Qubits Created with Spatially Correlated Twin Photons. *Physical Review A* **76** 032314 (2007).

[46] K. J. Resch. Practical Weak Measurement of Multiparticle Observables. *Journal of Optics B: Quantum and Semiclassical Optics* **6** 482 (2004).

[47] K. J. Resch and A. M. Steinberg. Extracting Joint Weak Values with Local, Single-Particle Measurements. *Physical Review Letters* **92** 130402 (2004).

[48] K. Mølmer. Counterfactual Statements and Weak Measurements: an Experimental Proposal. *Physics Letters A* **292** 151 (2001).

[49] Y. Aharonov, A. Botero, S. Popescu, B. Reznik, and J. Tollaksen. Revisiting Hardy's paradox: Counterfactual Statements, Real Measurements, Entanglement and Weak Values. *Physics Letters A* **301** 130 (2002).

[50] A. N. Jordan. Viewpoint: Mapping Out the State of a Quantum System. *Physics* **9** 104 (2016).

[51] R. Mir, J. S. Lundeen, M. W. Mitchell, A. M. Steinberg, J. L. Garretson, and H. M. Wiseman. A Double-Slit 'Which-Way' Experiment on the Complementarity–Uncertainty Debate. *New Journal of Physics* **9** 287 (2007).

[52] A. Palacios-Laloy, F. Mallet, F. Nguyen, P. Bertet, D. Vion, D. Esteve, and A. N. Korotkov. Experimental Violation of a Bell's Inequality in Time with Weak Measurement. *Nature Physics* **6** 442 (2010).

[53] A. G. Kofman, S. Ashhab, and F. Nori. Nonperturbative Theory of Weak Pre-and Post-Selected Measurements. *Physics Reports* **520** 43 (2012).

[54] G. J. Pryde, J. L. O'Brien, A. G. White, T. C. Ralph, and H. M. Wiseman. Measurement of Quantum Weak Values of Photon Polarization. *Physical Review Letters* **94** 220405 (2005).

[55] K. J. Resch. Amplifying a Tiny Optical Effect. *Science* **319** 733 (2008).

[56] M. Onoda, S. Murakami, and N. Nagaosa. Hall Effect of Light. *Physical Review Letters* **93** 083901 (2004).

[57] J. B. Altepeter and E. R. Jeffrey and P. G. Kwiat. Photonic State Tomography. *Advances In Atomic, Molecular, and Optical Physics* **52** 105 (2005).

[58] S. Wu. State Tomography via Weak Measurements. *Scientific Reports* **3** 1193 (2013).

[59] L. Hardy. Quantum Mechanics, Local Realistic Theories, and Lorentz-Invariant Realistic Theories. *Physical Review Letters* **68** 2981 (1992).

[60] T. Denkmayr, H. Geppert, S. Sponar, H. Lemmel, A. Matzkin, J. Tollaksen, and Y. Hasegawa. Observation of a Quantum Cheshire Cat in a Matter-Wave Interferometer Experiment. *Nature Communications* **5** 4492 (2014).

[61] Y. Aharonov, S. Popescu, D. Rohrlich, and P. Skrzypczyk. Quantum Cheshire Cats. *New Journal of Physics* **15** 113015 (2013).

[62] J. Dressel,and S. Agarwal, and A. N. Jordan. Contextual Values of Observables in Quantum Measurements. *Physical Review Letters* **104** 240401 (2010).

[63] S. H. Strogatz. *Nonlinear Dynamics and Chaos: With Applications to Physics, Biology, Chemistry, and Engineering.* *Westview Press* (2014).

[64] B. E. A. Saleh and M. C. Teich. *Fundamentals of Photonics.* *Wiley* (2007).

[65] D. M. Greenberger, A. M. Horne, and A. Zeilinger. Multiparticle Interferometry and the Superposition Principle. *Physics Today* **46** 22 (1993).

[66] E. J. S. Fonseca, C. H. Monken, and S. Pádua. Measurement of the de Broglie Wavelength of a Multiphoton Wave Packet. *Physical Review Letters* **82** 2868 (1999).

[67] M. D'Angelo, M. V. Chekhova, and Y. Shih. Two-Photon Diffraction and Quantum Lithography. *Physical Review Letters* **79** 043817 (2009).

[68] W. H. Peeters, J. J. Renema, and M. P. van Exter. Engineering of Two-Photon Spatial Quantum Correlations Behind a Double Slit. *Physical Review A* **79** 043817 (2009).